The Pennsylvania State University

The Graduate School

College of Earth and Mineral Sciences

THERMAL MATURITY OF GAS SHALES IN THE

APPALACHIAN PLATEAU OF PENNSYLVANIA

A Thesis in

Geosciences

by

Mitchell A. Modlich

Submitted in Partial Fulfillment
of the Requirements
for the Degree of

Master of Science

December 2014

The thesis of Mitchell A. Modlich was reviewed and approved* by the following:

Rudy Slingerland
Professor of Geology
Thesis Adviser

Michael Arthur
Professor of Geosciences

Kevin Furlong
Professor of Geosciences

Demian Saffer
Professor of Geosciences
Associate Head for Graduate Programs and Research

*Signatures are on file in the Graduate School.

ABSTRACT

Ongoing shale gas exploration and production in the western Appalachian Basin of Pennsylvania (WPAB) necessitates a better understanding of the thermal evolution of the basin to constrain uncertainty in risk assessments. Anomalies of thermal maturity in southwestern and west-central Pennsylvania along the Allegheny Front are hypothesized to be associated with hot brines driven through Upper Devonian aquifers from the foreland to the east. To test this hypothesis, a total of 402 1-D vertical heat diffusion experiments are conducted in 9 locations to investigate the effects of heating by fluid flow on organic-rich shales in the WPAB. Model simulations are constrained by compiled datasets of maximum reflectance of coal vitrinite, random reflectance of dispersed marine vitrinite in shales, and apatite fission-track ages. Modeling results indicate that the salient or promontory in maturity in Carboniferous and Devonian strata in northern Somerset and southern Cambria Counties is reproduced by an increase in temperatures of 40 – 50 ℃ above those expected solely by heat conduction for at least one myr. from 260 – 259 Ma following the end of the Alleghanian Orogeny. These results show that an increase in the thermal gradient caused by hot fluids for a geologically plausible amount of time can explain the anomalous variations in thermal maturity in western Pennsylvania.

TABLE OF CONTENTS

LIST OF TABLES

LIST OF FIGURES

ACKNOWLEDGEMENTS

INTRODUCTION

The recent commercial interest in shale gas plays in the Marcellus and Utica/Point Pleasant Formations in the Appalachian Basin (Fig. 1) of Pennsylvania, Ohio, and West Virginia necessitates a better understanding of the thermal evolution of the basin and its unconventional reservoirs. Among other factors, it is the thermal evolution of black shales that determines where different phases of hydrocarbons (oil/wet gas/dry gas) are located. Thus the spatial pattern of time-temperature histories at various locations in the Appalachian Basin is an important economic factor in the exploration and production activities of oil and gas producers. At present, the location of the wet gas boundary in western Pennsylvania is only roughly defined; indicators of thermal maturity vary spatially throughout western Pennsylvania, and are often inconsistent.

This investigation uses one-dimensional numerical simulations of heat conduction in geological strata as a tool to better understand the mapped trends of paleo-temperature indicators in the Appalachian plateau in Pennsylvania. Here I explore the hypothesis that the migration of hot fluids from deeper levels within the hinterland and eastern foreland play a greater role than previously recognized in determining the level of maturity of organic-rich shales in the Appalachian Basin of Pennsylvania. I test the hypothesis by compiling vitrinite reflectance and apatite fission track data and conducting 402 1-D vertical heat diffusion experiments with, and without, lateral heat flow from basinal

brines. Results show that an increase in the thermal gradient for the duration of one myr at the end of the Alleghanian Orogeny will reproduce anomalously high vitrinite reflectance data in the Carboniferous in southwestern Pennsylvania.
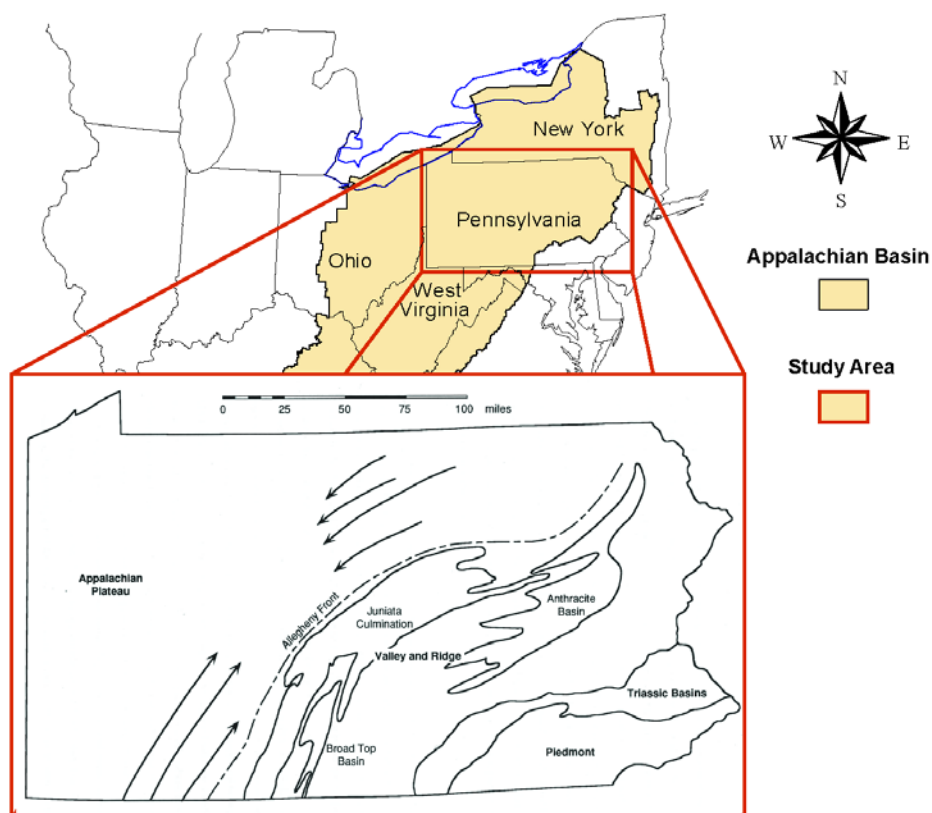
Figure 1. The Appalachian Basin, USA. The study area is outlined in red, with a focus on the Appalachian Plateau region to the west and north of the Allegheny Front. To the east lies the highly deformed Valley and Ridge Province, the Anthracite Basin, the Mesozoic rift basin (labeled "Triassic Basins" in figure), and the Piedmont. The arrows represent anticlinal axes (modified after Blackmer et al., 1994; Milici and Swezey, 2006)

Statement of the Problem

In a typical foreland basin the thickest accumulation of sediments occurs adjacent to the crustal load in the hinterland and tapers towards the foreland. Likewise, burial depths are greatest in the hinterland and decrease towards the foreland. Consequently, thermal maturity indicators typically show a similar pattern in which maturity isolines parallel the strike of the orogen. It is interesting then, that existing maps of thermal maturity indicators in Paleozoic strata of Pennsylvania show a complex variability at the county to sub-county scale in western Pennsylvania (Figs. 2-6). The most prominent variability is observed in maps of vitrinite reflectance of Carboniferous coal seams. A salient of elevated iso-reflectance is centered in southwestern Pennsylvania over Somerset and Cambria Counties, and extends into Westmoreland and Indiana Counties as well (Figs. 2-4). Westward and northward of this salient, the reflectance contours follow patterns that would be expected for a foreland basin. A salient is also seen in maps of vitrinite reflectance from Devonian-aged shales (Figs. 5 and 6) although it lies across most of southwestern Pennsylvania from Butler County in western PA to Somerset County adjacent to the Allegheny structural front. This Devonian feature is not as well defined because of the paucity of data in Somerset, Westmoreland, and Fayette Counties. Another deviation from the expected strike-parallel maturity isolines is the area of lower maturity in northern Cambria County (Figs. 5 and 6).

Given the scale of these anomalies, it is difficult to explain them as functions of

variations in overburden thickness or basal heat flow. Sedimentation along strike in the basin is not expected to differ greatly enough to produce such variations in overburden thickess, and there is no indication that middle to late Paleozoic accommodation space was locally greater due to say, grabens or local thrusts. Basal heat flow varies regionally, but because the Paleozoic Appalachian Basin lies on stable continental crust of Grenvillian age, significant local variation in heat flow is not expected (Turcotte and Schubert, 2002). Measurements of present-day heat flow do not show large variation across the Appalachian plateau of Pennsylvania (Blackwell and Richards, 2004; Blackwell et al., 2011). What then, could have caused the thermal perturbation necessary to produce these patterns? Two possibilities are: 1) the features are an artifact of contouring scarce data; or 2) hot brines migrated westward along preferred local pathways from deeper in the basin.

Here I test the hypothesis that the thermal maturity anomalies observed along strike at the county scale are caused by localized flow of hot brines out of the deeper Appalachian Basin to the east. This possibility is suggested by the correspondence between the isorank anomalies and variations in isoliths of Upper Devonian sandstone as can be seen in Smith (1983).
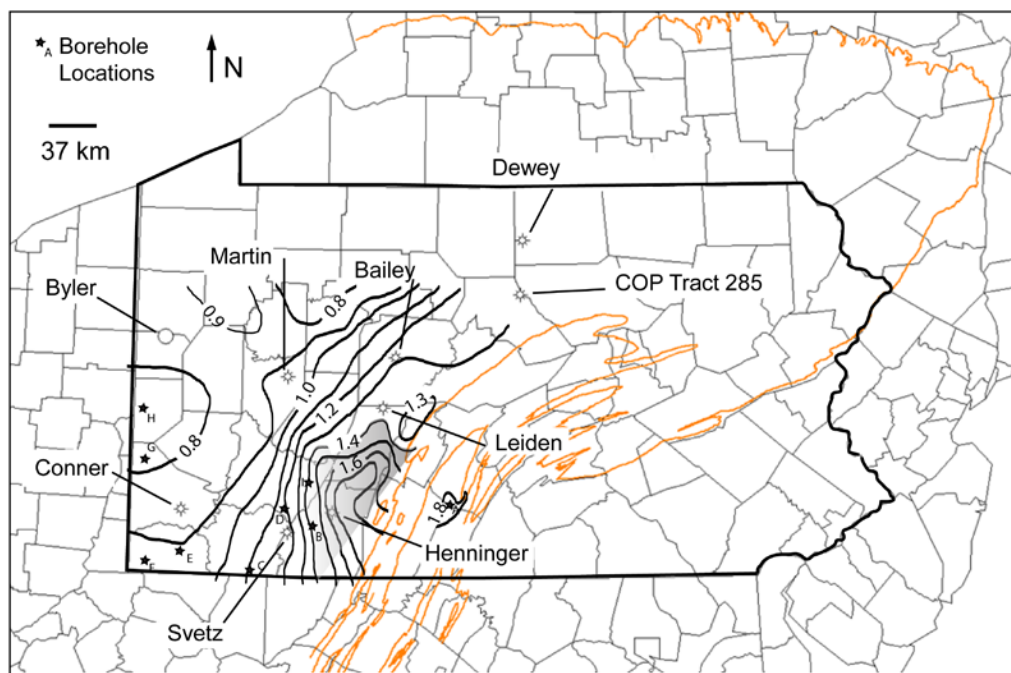
Figure 2. Pennsylvanian Iso-reflectance Contours (%$R_{o\ max}$) in southwestern Pennsylvania (modified after Zhang and Davis, 1993). Gray indicates region of anomalously high vitrinite reflectance. Names and locations of wells modeled in this study are shown. Boreholes of Zhang and Davis (1993) are marked by stars. The orange outline represents the Devonian outcrop belt.
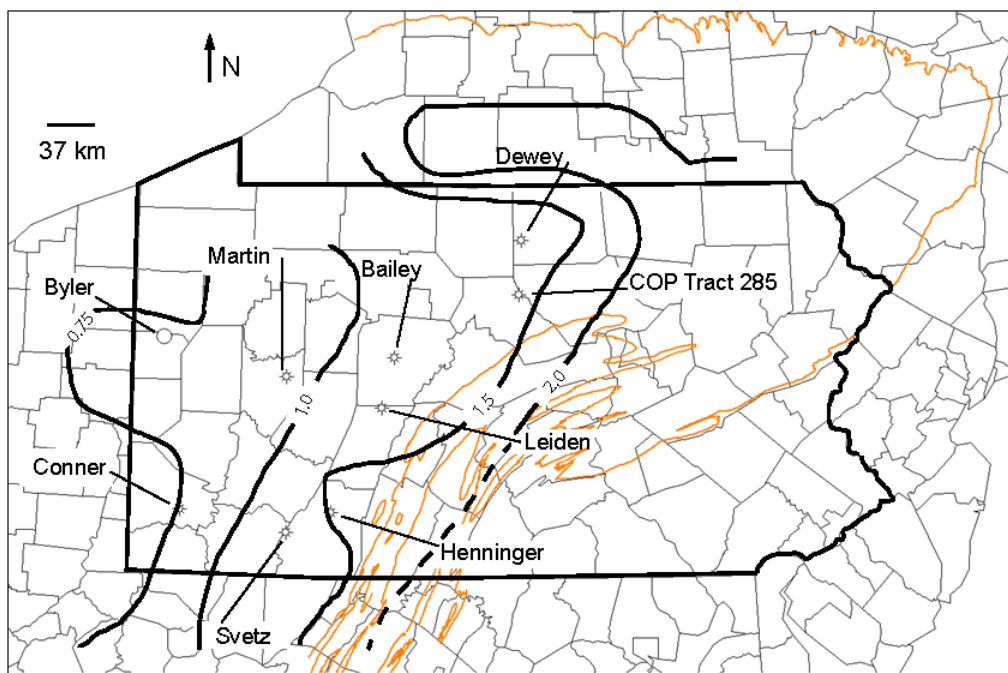
Figure 3. Pennsylvanian Iso-reflectance Contours (%$R_{o\ max}$), Central Appalachian Basin (modified after Hulver, 1997). Note the salient of higher maturity extending to the northwest near the Henninger well.
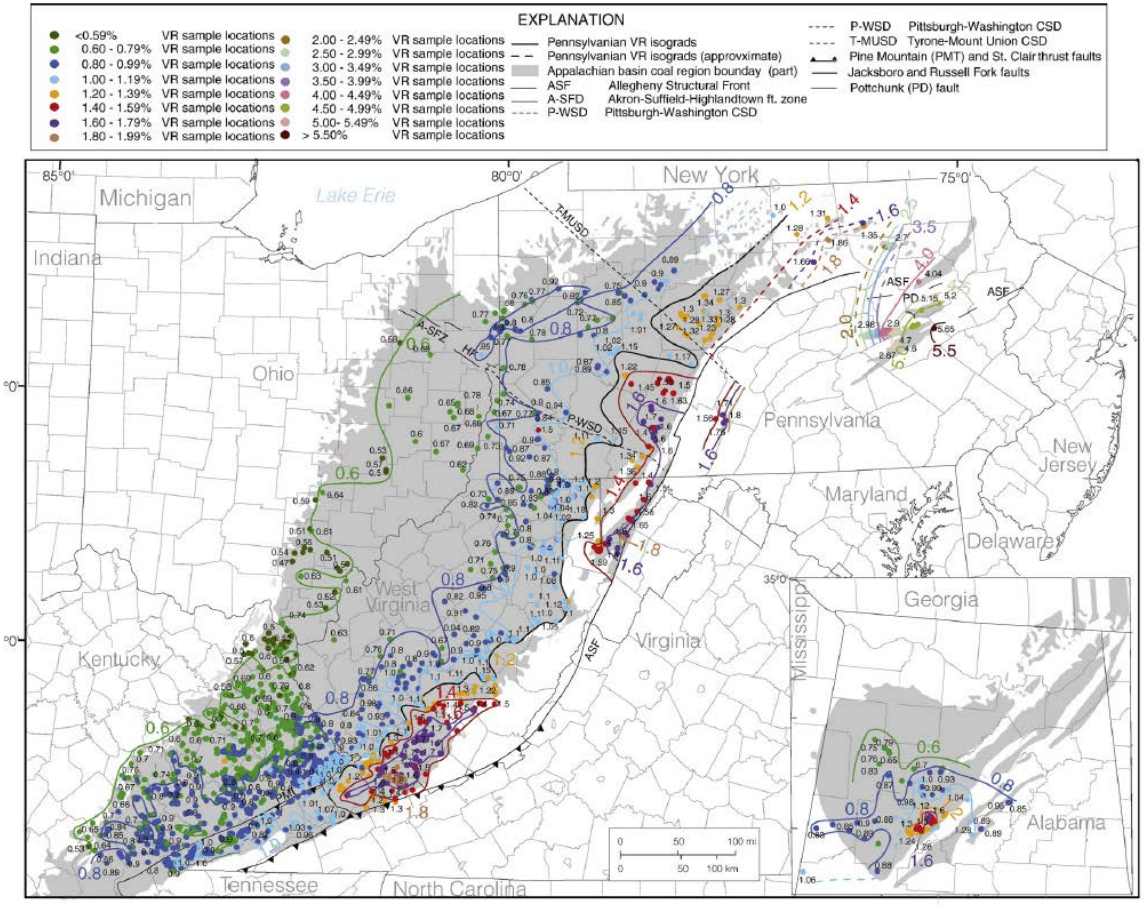
Figure 4. Pennsylvanian Iso-reflectance Contours (%R$_o$), Central Appalachian Basin (Ruppert et al., 2010). Salients and recesses of iso-reflectance are apparent.
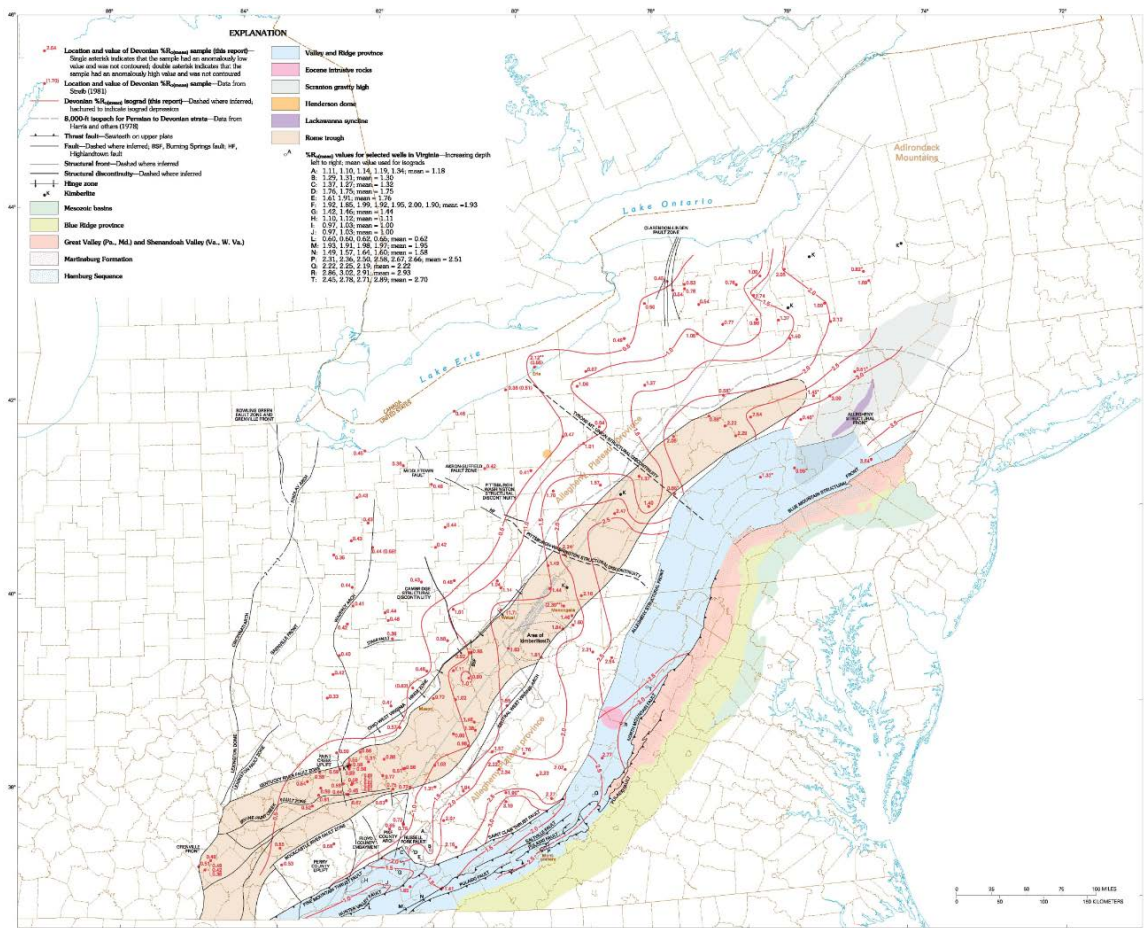
Figure 5. Devonian Iso-reflectance Contours (%R$_{o\ rand}$), Central Appalachian Basin (From Repetski et al., 2008). Deviations of iso-reflectance contours are apparent and suggested to lie along northwest-trending lineaments.
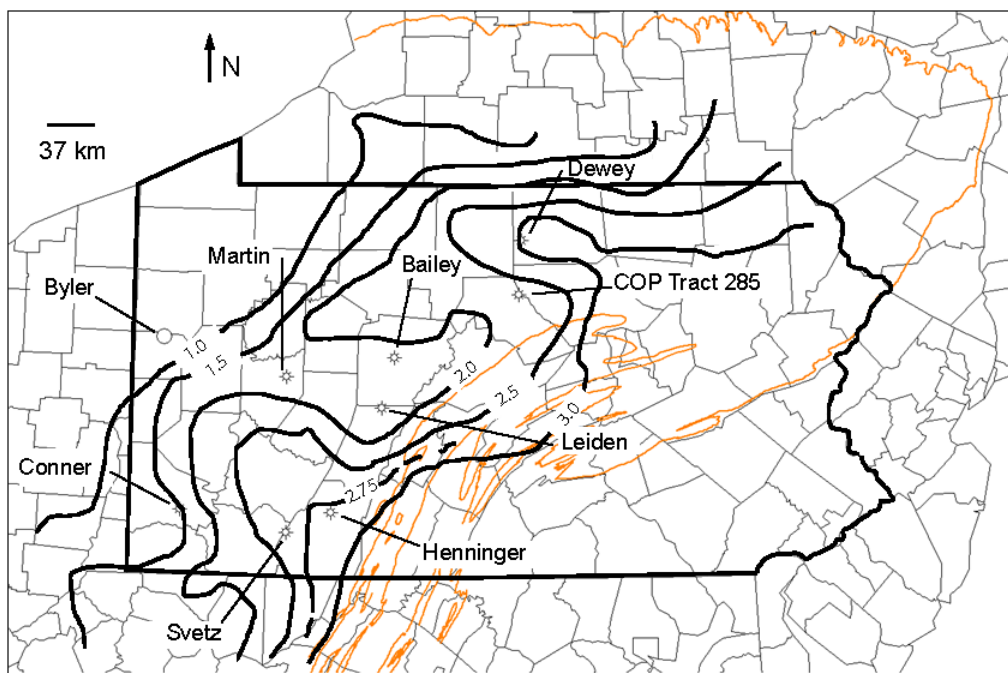
Figure 6. Devonian Iso-reflectance Contours (%$R_{o\ rand}$), Central Appalachian Basin (From Wrightstone, 2009). Two iso-reflectance salients are suggested in the WPAB, one centered on the Henninger well and one on the Dewey well.

Background

Basin History

The region of Pennsylvania with gas shale potential lies north and west of the Allegheny Front. For simplicity this will be called the western Pennsylvania Appalachian Basin (WPAB). In this region the basement consists of Precambrian crystalline rocks of the Grenville Terrane. Above this basement lies a sequence of Paleozoic strata deposited as a consequence of three separate major orogenic events (Figs. 7-9). Following rifting of the supercontinent Rodinia, a marine transgression proceeded westward across Grenvillian-age crystalline rocks in Pennsylvania. This resulted in a passive margin succession of sandstone and shale, followed by a Cambro-Ordovician carbonate bank, the whole of which varies from 10,000 ft (3.05 km) thick at its eastern edge to 2,000 ft (0.6 km) at the PA/Ohio border. In the Middle to Late Ordovician a collision of an island arc system and the continent of Laurentia resulted in the Taconian Orogeny. A northeast-southwest-trending foreland basin developed along the former passive margin into which clastics shed from the island arc accumulated as a black shale and organic-rich carbonate called the Utica Fm. in New York State, the Point Pleasant Fm. in Ohio, and the Antes Shale in Pennsylvania. This unit is 250-500 ft (0.1 – 0.2 km) thick in the WPAB. This was succeeded by a thick coarsening- and shoaling-upwards sequence of turbidites, coastal sandstones, and fluvial to near-shore mudstones, sandstones, and conglomerates. A period of relative quiescence in the Silurian Period allowed the accumulation of

Figure 7. Precambrian through Silurian Stratigraphic Correlation Chart, Western Pennsylvania Appalachian Basin (WPAB) (Carter, 2007).

Figure 8. Devonian through Permian Stratigraphic Correlation Chart, WPAB. Note the delta succession of the Upper Devonian (Carter, 2007).
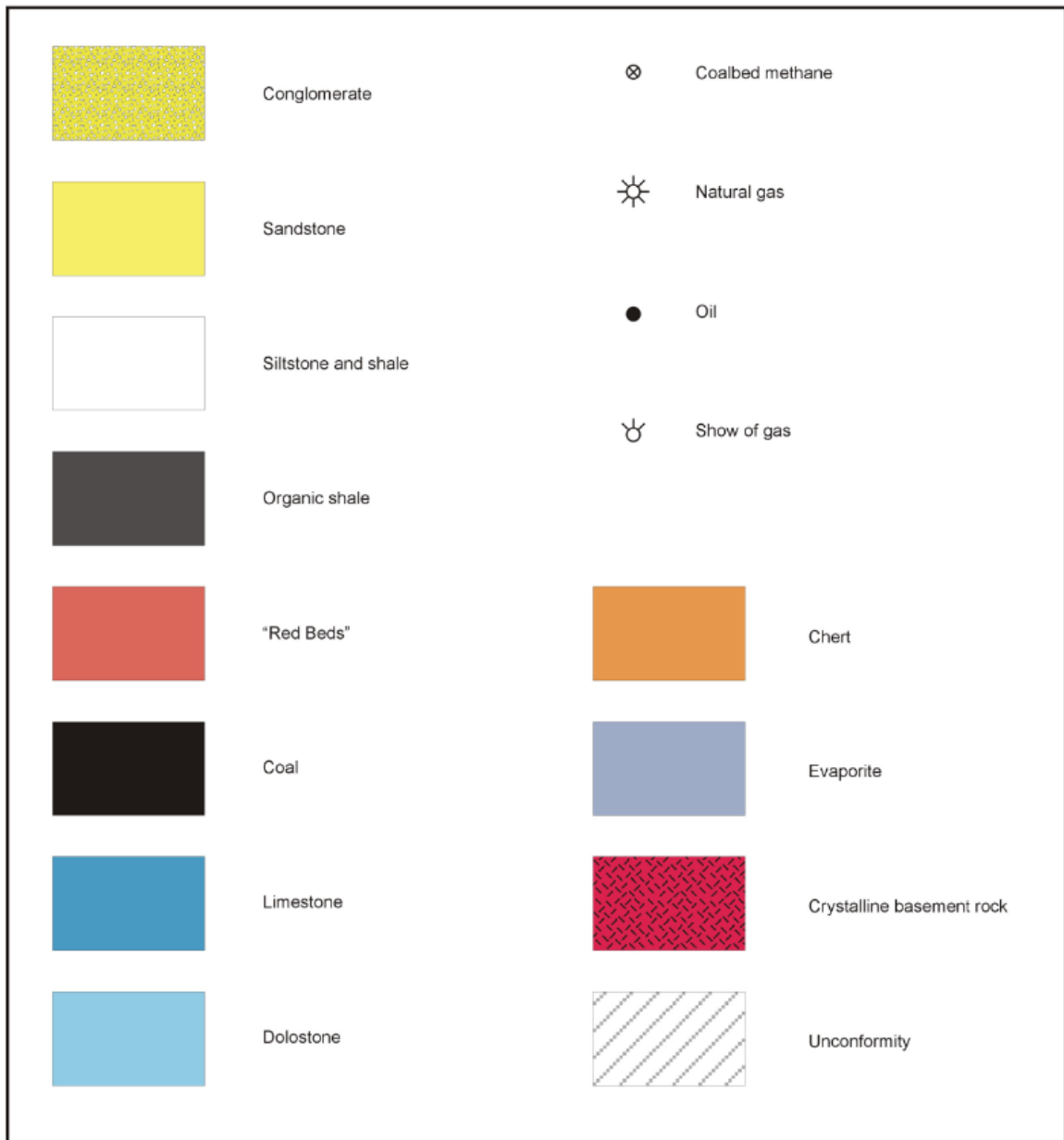
Figure 9. Legend for Stratigraphic Correlation Chart, WPAB (Carter, 2007).

predominately carbonate and salt. These vary in thickness from 1,500 ft (0.5 km) to 2,000 ft (0.6 km) across the WPAB. The salt is important due to its role as a detachment surface in the tectonic evolution of the basin, and for its high thermal conductivity relative to other rock types. The Acadian Orogeny commenced in the Middle Devonian due to a collision between Laurentia and another lesser continental plate. Thrust sheets thickened the crust along the present-day US Eastern seaboard, and this elevated topography was the main source for the roughly 5,000 - 8,000 ft (1.5 – 2.4 km) of siliciclastic rocks that were deposited during the Middle Devonian to the Mississippian Periods in the WPAB. Among these rocks are at least three potentially economically feasible black shales—the Marcellus, Burket/Geneseo, and Rhinestreet Fms.

The climactic compressional deformation event in the central Appalachian Mountains was the Pennsylvanian-Permian Alleghenian Orogeny brought about by the convergence of Laurentia and the Moroccan shoulder of Africa. During this time, the Pennsylvania foreland basin received as much as 10,000 – 25,000 ft (3.1 – 7.6 km) of sediment from the orogenic highlands to the east. In central Pennsylvania these rocks are defined as the Pottsville Gp. through Conemaugh Gp. (Fig. 8). In southwestern Pennsylvania the sequence is capped by the Permian Dunkard Gp.

During the Permian the whole eastern half of the orogen was subjected to folding and thrusting, and, to a lesser extent, metamorphism and plutonism. Flexural modeling by Beaumont et al. (1987, 1988) and Quinlan and Beaumont (1984), and a fluid inclusion

study by Orkan and Voight (1985) indicates that sediments in the foreland basin of Pennsylvania became buried at this time under as much as 25,000 feet of additional sediments and possibly thrusts. The loads necessary to flex the stiff Grenvillian crust are given in Figure 10, along with resulting sediment thicknesses in the basin. This loading of crustal material created the burial and heat necessary for the Ordovician and Devonian black shales to generate and mature hydrocarbons.
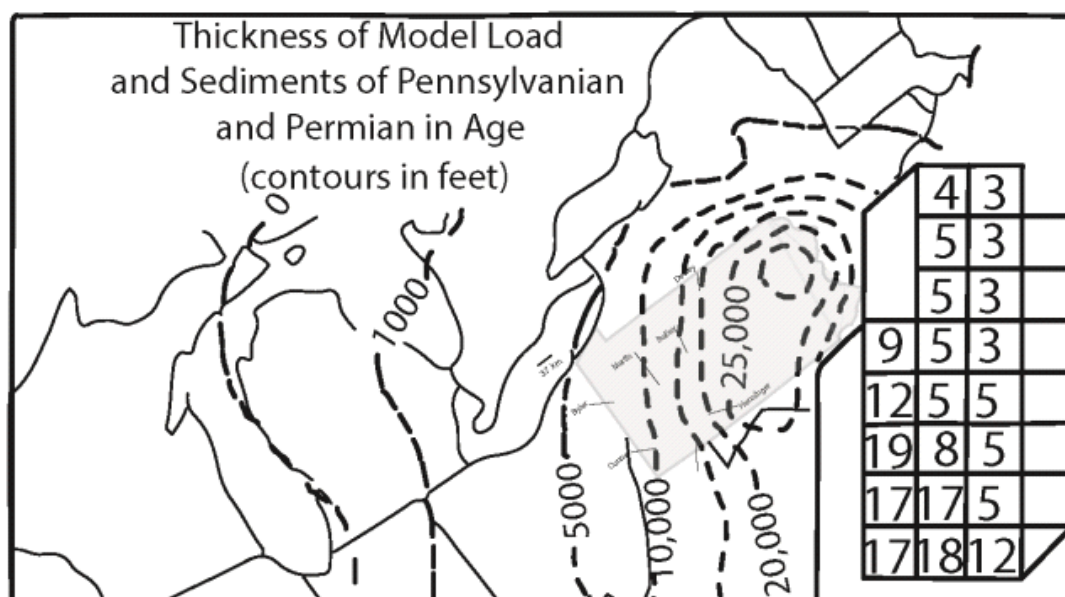
Figure 10. Thickness of model load and sediments of Pennsylvanian and Permian in age resulting from the Alleghanian Orogeny. The boxed numbers represent the crustal loads (km) required to produce the currently observed stratigraphic thicknesses. 10,000 ft = 3.05 km (modified after Beaumont et al., 1987).

According to Miller and Kent (1988) the Alleghanian Orogeny ended approximately 260 Ma ago. This is the date of apparent re-magnetization ages of

components in carbonate and red-bed units in the Appalachian orogenic belt. The apparent remagnetization ages are thought to indicate the timing of fluid flow related to thrust-sheet emplacement during the Alleghanian Orogeny.

The Late Permian and Early Triassic post-orogenic history of the Appalachian Basin is uncertain because there are no preserved deposits of that age. It is clear however, that by the Carnian or late Ladinian (230-225 Ma) sediments had begun accumulating in basins along reactivated strike-slip and thrust faults (Manspeizer and Cousminer, 1988; Traverse, 1987), recording the initial breakup of Pangaea. The unconformity below these sediments cuts across the same Cambro-Ordovician rocks that presently outcrop outside the basin, indicating that the present level of erosion must have been reached at least by the Carnian. Rupture occurred roughly along the present continental shelf edge, and seafloor spreading began between late Early to Middle Jurassic (190-175 Ma) (Klitgord and Schouten, 1986).

Basin Fluid Flow

The migration of pore fluids on a basin-wide scale has been widely invoked to explain Mississippi Valley-type ore deposits in the mid-continent (Garven, 1995; Garven and Freeze, 1984a; Garven and Freeze, 1984b; Garven et al., 1993; Harrison et al., 2004), Copper-Uranium (Cu-U) deposits in Pennsylvania (Smith, 1983), anthracitization of coal in Pennsylvania (Harrison et al., 2004), and clay mineral diagenesis in the Appalachian Basin (Osborn et al., 2012). Two different mechanisms for basin-wide or continental

scale fluid flow have been proposed: gravity-driven fluid flow (Garven and Freeze, 1984a; Garven and Freeze, 1984b; Garven et al., 1993) and flow due to tectonic compression or a "squeegee" effect (Oliver, 1986).

Garven and Freeze (1984a; 1984b) used numerical modeling techniques to solve equations related to fluid flow, heat and mass transport, and geochemical mass transfer. They proposed that a gravity-driven fluid flow system could result in the creation of ore deposits in sedimentary basins. Their 2-D model simulations show that this is possible, and that discharge rates of fluids through deep basin aquifers would be on the order of 1 - 10 m^3 m^{-2} yr^{-1}. Deep basin, gravity-driven fluid flow theoretically could take place over several hundred kilometers and raise temperatures as high as 130 °C at a depth of one km at the basin margin.

Garven and others then used their model to infer that Mississippi Valley type ores in the mid-continent are the result of deep basin brines driven out of the Appalachian Basin (Garven et al., 1993). They assumed that the driving head arose from elevated topography in the east and possibly compaction of pores (Garven et al., 1993). A gravity-driven groundwater flow system will lower temperatures in recharge areas and raise temperatures in discharge areas of the basin beyond the effect of conductive heat processes. Heat will be extracted from deeper parts of the basin and transferred to more distal basin areas. Their modeling indicates the temperature in a discharge area (on the basin margin) can be increased by up to 30 °C above that expected by only conductive

heating (Garven and Freeze, 1984b). According to those authors, stratigraphic pinchouts, basement arches, or topographic variations can significantly alter the temperature gradients regionally. Peak temperatures will lag up to 10^6 years after the initiation of the gravity-driven flow system. The highest transient thermal gradients could last up to 5 x 10^5 years (Garven et al., 1993).

Oliver (1986) proposed that tectonic compression during Orogeny or mountain-building would have a "squeegee" effect on deep basin brines. The fluids would be squeezed by the compressive forces of thrust sheets from the proximal to the distal part of the basin resulting in geologic phenomena such as mineral transport, faulting, hydrocarbon migration, and paleo-magnetic effects. Ge and Garven (1992) modeled deep basin fluid flow by compression and determined that flow rates would be an order of magnitude less than gravity-driven flow (0.1 – 1 m yr^{-1}), and that increased flow would dissipate after 10^3 to 10^4 years. Additionally, fluid flow velocities would be greater near the area of compressive loading relative to distal basin areas. The volume of fluid is low compared to gravity-driven flow systems, but repeated thrusting events could flush fluids through the basin (Ge and Garven, 1992).

Other studies have examined the link between migrating brine fluids and other unique geochemical occurrences. Smith (1983) examined Cu-U redbed occurrences in the Upper Devonian Catskill Formation near the anthracite region in eastern Pennsylvania. Migrating, metal-bearing fluids from the east were proposed as the source

of these Cu-U deposits (Smith, 1983). It is also noted by Repetski et al. (2008) that unusual patterns in thermal maturity in the Devonian might be at least partially explained by hot fluid migration further to the west.

The hypothesis pursued in this study is that the same fluid flow that produced the proximal (Cu-U deposits) and distal (Mississippi Valley type ores) could have altered thermal gradients in the Appalachian Plateau of Pennsylvania. During and following the Alleghanian Orogeny, fluids could be forced deep into the basin, where they would be heated and forced into shallower rock units (Fig. 11). How might the organic-rich, potentially hydrocarbon bearing rocks be affected by a perturbation in thermal gradient lasting on the order of one million years?
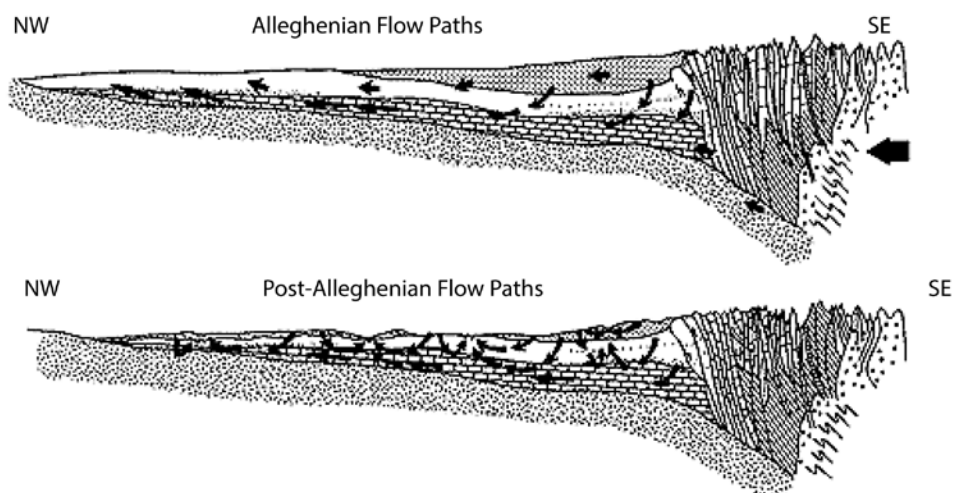
Figure 11. Possible fluid flow pathways associated with the Alleghanian Orogeny. (modified after Garven et al., 1993).

Previous Thermal Maturity Studies in the Appalachian Basin in Pennsylvania and the Surrounding Region

The thermal and depositional history of the Appalachian Basin has been investigated with a basin-wide geodynamic flexural model (Beaumont et al., 1987, 1988; Quinlan and Beaumont, 1984), and basin to regional scale investigations of coal rank and paleo-temperature indicators (Blackmer et al., 1994; Cercone et al., 1996; Chyi et al., 1987; Gerlach and Cercone, 1993; Hulver, 1997; Johnsson, 1986; Reed et al., 2005; Rowan, 2006; Rowan et al., 2004; Zhang and Davis, 1993). However, few of these studies investigated the entire WPAB.

Chyi et al. (1987) and Zhang and Davis (1993) studied coal maturation patterns in southwestern Pennsylvania. The former study determined that the Pittsburgh Coal would have to be buried under an additional 1.5 km of overburden relative to the present surface, while the latter determined that western Pennsylvania experienced between 2.5 – 4.0 km of burial in the Permian. Both of these studies utilize the Lopatin-Waples-TTI method of vitrinite reflectance modeling described in the methodology section of this thesis. Blackmer et al. (1994) focused on the "unroofing" history of the Appalachian plateau in Pennsylvania using apatite fission-track thermochronology. Their results indicate that cooling of the basin began immediately after the Alleghanian Orogeny. Cercone et al. (1996) performed an in-depth study of coal and black shale thermal conductivity in western Pennsylvania and concluded that high insulating rock formations

could produce the maturation levels of the Pennsylvanian coals. Hulver (1997) focused on the denudation or erosion history of the entire Appalachian Basin. Using the chemical kinetic method of vitrinite maturation described in the methodology section of this thesis, he concludes that the near-surface coals in Pennsylvania experienced temperatures from 115 ºC near the border with Ohio to 180 ºC along the Allegheny structural front. Additionally, he made estimates of additional sediment burial resulting from the Alleghanian Orogeny. His estimates from correlations of depth, coal moisture content, and coal volatile matter indicate that burial depths were up to 4.3 km along the Allegheny structural front.

In 2006 the USGS published a study that used 2-D burial and thermal models in the distal portion of the Appalachian Basin, through Ohio, southwestern Pennsylvania, and West Virginia (Rowan, 2006; Rowan et al., 2004). These models do not include the Middle Devonian interval, nor do they provide much information on the major shale gas play areas of southwest and north-central Pennsylvania.

Paleo-temperature Indicators and Thermal Maturity

Numerous methods have been proposed for estimating the thermal maturity of rocks in a basin. The term *thermal maturity* is meant to indicate the degree of heating of a petroleum source rock in the process of transforming kerogen into hydrocarbons. As a rock unit is subjected to greater amounts of heat due to burial, subsidence, and other potential factors, the organic material chemically reacts. These reactions produce a

progressive series of products including hydrocarbons such as oil and gas. It is generally acknowledged that the integration of multiple types of maturation data increases the confidence in regional interpretations over any single data type (Beardsmore and Cull, 2001). Additionally, each type of data has its advantages and disadvantages. Thermal maturity in the western Pennsylvania Appalachian Basin has been evaluated using coal rank, vitrinite reflectance, conodont analysis, fluid inclusions, and fission-track thermochronology.

Coal Rank

Coal rank is a measure of thermal maturity that assesses the degree to which the organic matter has progressed along the coalification series. Coalification begins with peat, and with increasing coal metamorphism peat becomes lignite, then bituminous coal, then anthracite. There are different sub-classifications of bituminous coal and anthracite: high-volatile, medium-volatile, and low-volatile bituminous, and semi to meta-anthracite. These ranks are determined by their geochemical and physical properties, including weight percent carbon, volatile matter, and moisture content, and calorific value (Ruppert et al., 2010). Coal rank has given way to vitrinite reflectance as a preferred maturation indicator in both coal and hydrocarbon exploration (Ruppert et al., 2010). Figure 12 shows the distribution of coals in Pennsylvania. Note that the area of low-volatile bituminous coal coincides with the highest area of mapped maturity of vitrinite reflectance in Pennsylvanian coals (compare with Figs. 2 - 4).
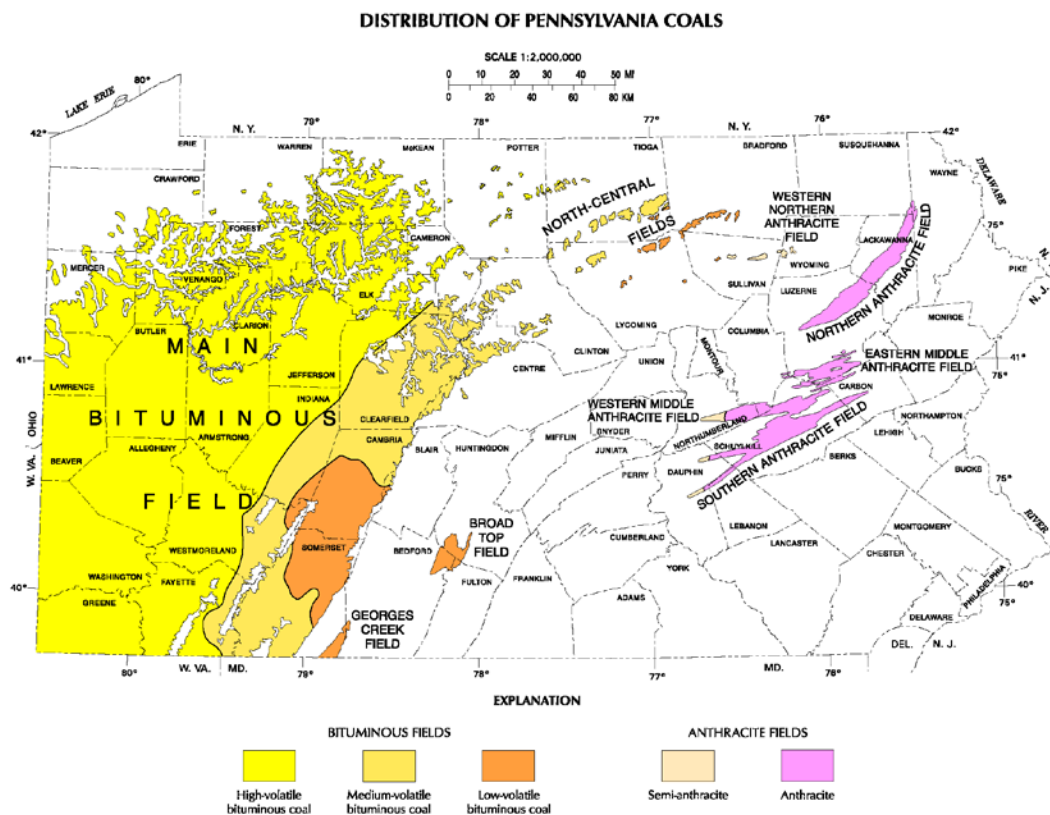
Figure 12. Coal fields of Pennsylvania (Edmunds, 2002). Note the lower rank (high-volatile bituminous) in the west and the anomalously high rank (low-volatile bituminous) in Somerset and Cambria Counties.

Vitrinite Reflectance

Vitrinite reflectance (R_o) is a useful measure of thermal maturity, and is commonly used in the petroleum industry to determine locations that will contain the desired phase. It has also been used extensively in the coal industry to assess a coal's rank or maturity. The magnitude of vitrinite reflectance is controlled more by temperature than time, as

shown by its modeling with a power law expression. The evolution of vitrinite reflectance is not significantly affected by fluid chemistry and other diagenetic parameters (Huang, 1996).

Vitrinite reflectance measurements are subject to issues that affect their interpretation, such as errors from drilling (Dow, 1977), reflectance anisotropy (Levine and Davis, 1989), and suppressed or lowered values of marine-sourced vitrinite relative to coal or terrigenous vitrinite. Additionally, measurements of vitrinite may not be consistent among different operators due to differences in sample preparation and techniques of measurement.

A recent study shows the spread of values reported by 19 different operators (Araujo et al., 2014). There is more than a 0.3% difference in the range of reflectance values for 2 samples. Ryder et al. (2013) suggested that low vitrinite reflectance values measured in previous studies in low maturity Devonian shales could have resulted from the inadvertent inclusion of solid bitumen reflectance values. In addition, their data suggested that the northern part of their study area has higher thermal maturity than previously reported by Repetski et al. (2008).

The correlation between vitrinite and hydrocarbon generation is shown in Figure 13. Hydrocarbons mature according to the original composition of organic matter (liptinitic or humic, or a combination of both types) and the degree to which the organic matter has been altered by heating.

Conodont Alteration Index (CAI)

The conodont alteration index (CAI) (Epstein et al., 1977; Harris et al., 1978) is another paleo-temperature indicator that has been used in the Appalachian plateau, although due to its poor resolution (Beardsmore and Cull, 2001) of maximum paleo-temperature ($\pm$ 20-50 ℃), it is generally of limited use. The USGS has mapped the thermal maturity patterns (Repetski et al., 2002; Repetski et al., 2008) in the Ordovician and Devonian rocks of the Appalachian Basin using both vitrinite reflectance and CAI, but there is a need for more data both laterally and vertically, and for those data to be examined more carefully to ensure the observed spatial variations are not spurious (Ryder et al., 2013).
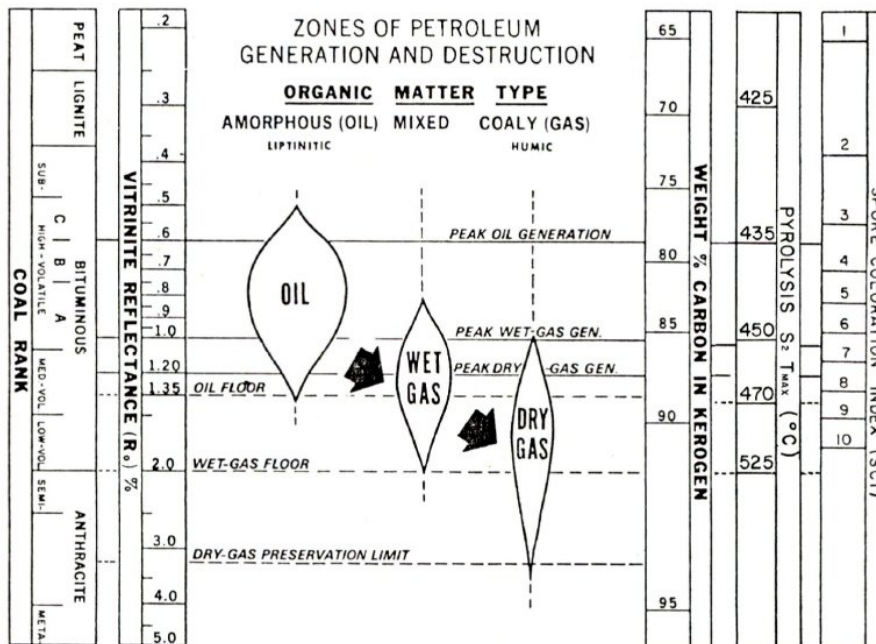
Figure 13. Correlations between Maturation Indices (Dow, 1977). Vitrinite Reflectance here is mean random reflectance (%R$_{o\ rand}$). Hydrocarbon generation zones are approximate.

Fluid Inclusions

Small amounts of fluid and vapor are trapped during the original growth of a mineral crystal, or when fractures in a rock heal in the presence of a fluid. These trapped fluids are known as fluid inclusions. When reheated in a laboratory, the vapor and fluid phases of the inclusion revert to a single phase at the homogenization temperature, T_h. This temperature represents the minimum temperature at which the inclusion formed (Roedder, 1984). Orkan and Voight (1985) measured fluid inclusions in the Valley and Ridge Province of Pennsylvania. Their data indicates homogenization temperatures in Devonian samples vary from 70 ºC to 290 ºC. Pennsylvanian-aged rocks in the Anthracite region have homogenization temperatures of 212 ºC.

Apatite Fission Track Thermochronology

Fission track thermochronology is the only known paleo-temperature indicator that gives information on the timing of thermal events. After the maximum paleo-temperature has been determined by making assumptions about burial history, fission track thermochronology can be used to determine the age of cooling to a certain temperature. Fission tracks are preserved in the crystal lattices of certain minerals (including apatite). These tracks are caused mainly by Uranium-238 undergoing fission and producing a track of damage through the crystal structure of the mineral. These tracks begin to heal or "anneal" following their formation. New tracks will continue to be created (as long as U-238 is present) at a rate that is dependent upon the amount of the radioactive isotope

present in the mineral. Once the mineral crystal cools to below a certain temperature, the fission tracks will stop annealing. The time at which this happens is the apparent fission track age (Beardsmore and Cull, 2001).

An important limitation of fission track thermochronology is that apparent fission track age may not be a precise date of cooling. If there has been re-heating above 75 C, the apparent age could be an average between the latest and an earlier episode of cooling (Hulver, 1997).

DATA AND METHODOLOGY

This work integrates Vitrinite Reflectance (%R_o) and Apatite Fission Track Thermochronology from previous studies to model the burial and thermal history in the study area.

Vitrinite Reflectance (%R_o) and Coal Rank

Vitrinite reflectance is commonly used to predict the thermal maturity of marine shales and coal seams. For model calibration, vitrinite reflectance values from coal samples are preferred over reflectance values from marine organic carbon. Here, Pennsylvanian-aged vitrinite and coal rank parameters have been used to support the sparse, marine-influenced vitrinite samples from Devonian shales.

Pennsylvanian Coal Measures

Coal rank data including maximum vitrinite reflectance are compiled in Ruppert et al. (2010) from the Penn State Coal Bank (Glick and Davis, 1991), Chyi et al. (1987), Zhang and Davis (1993), and other unpublished sources. In this study, the nearest coal reflectance measurements as reported in Ruppert et al. (2010) are used for calibration of well models. In the absence of a nearby coal seam, the reflectance is inferred from analysis of the reflectance isolines as drawn by (Ruppert et al., 2010).

Pre-Pennsylvanian Marine-Influenced Vitrinite

The Pennsylvania Petroleum Source Rock Geochemistry Database (PPSRG) (Laughrey et al., n.d.) contains geochemical data sampled from several wells throughout Pennsylvania. All data in the PPSRG database are presented as an open-file report compiled over several decades by different Pennsylvania Geological Survey researchers (K. Carter, pers. comm.). Therefore, consistency in collection and measurement techniques cannot be verified. The data are provided in an "as is" state. I searched the database for wells in the study area that contain an unusually complete suite of vitrinite reflectance data distributed throughout the Paleozoic strata. Four were selected to compare with the modeling predictions of this study (Fig. 14): Dewey, COP Tract 285, Svetz, and Martin. It should be noted that the database does not differentiate between mean maximum reflectance ($\%R_{o\ max}$) or mean random reflectance ($\%R_{o\ rand}$). For this study, the assumption has been made that the samples are of $\%R_{o\ rand}$ due to that

method's common usage for dispersed vitrinite samples. These data provide the best

control available on the reflectance gradient with depth.
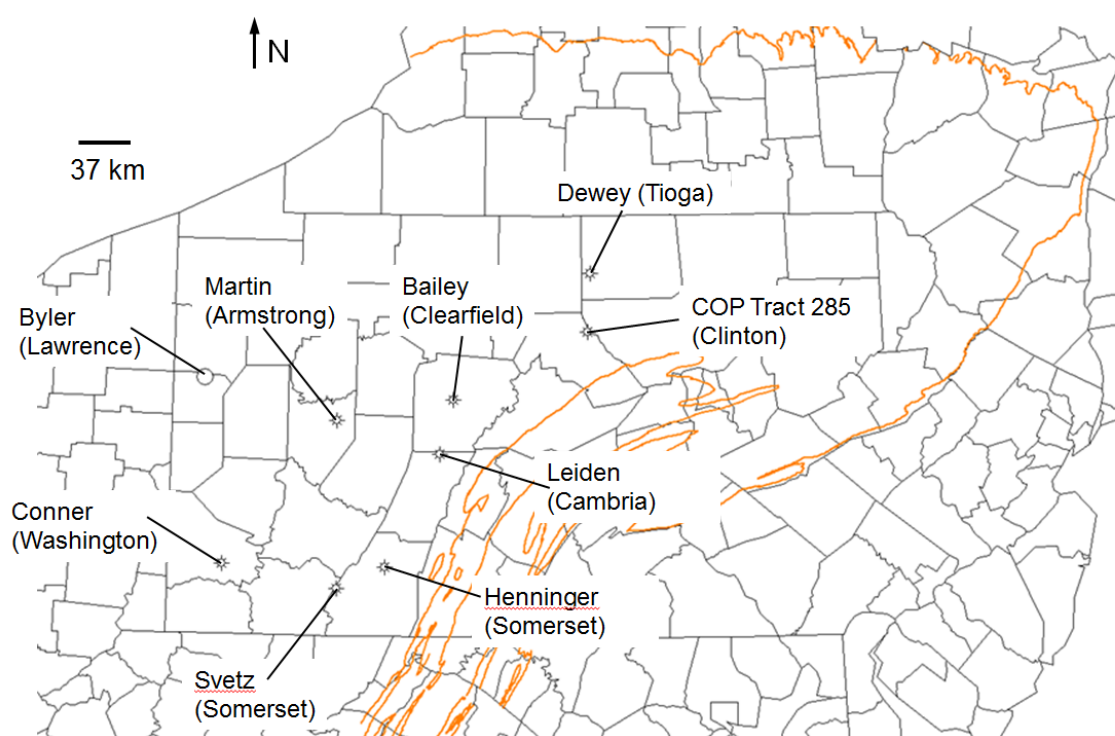
Figure 14. Locations of well models used in this study.

Apatite Fission Track Data

Fission track data from Roden and Miller (1989) and Blackmer et al. (1994) have been used here to calibrate the erosion or unroofing history in the Appalachian plateau. These data were obtained throughout the Paleozoic section, from the Ordovician to the Pennsylvanian. Roden and Miller (1989) and Blackmer et al. (1994) used fission track data to define the unroofing history of the present-day Appalachian Plateau in western PA (Figs. 15 and 16). Fission track samples were collected from Ordovician to Pennsylvanian strata. Blackmer et al. (1994) focused on the Appalachian plateau, while Roden and Miller (1989) focused on the Valley and Ridge province. The data are sometimes in disagreement, and this is interpreted by us as analytical error.
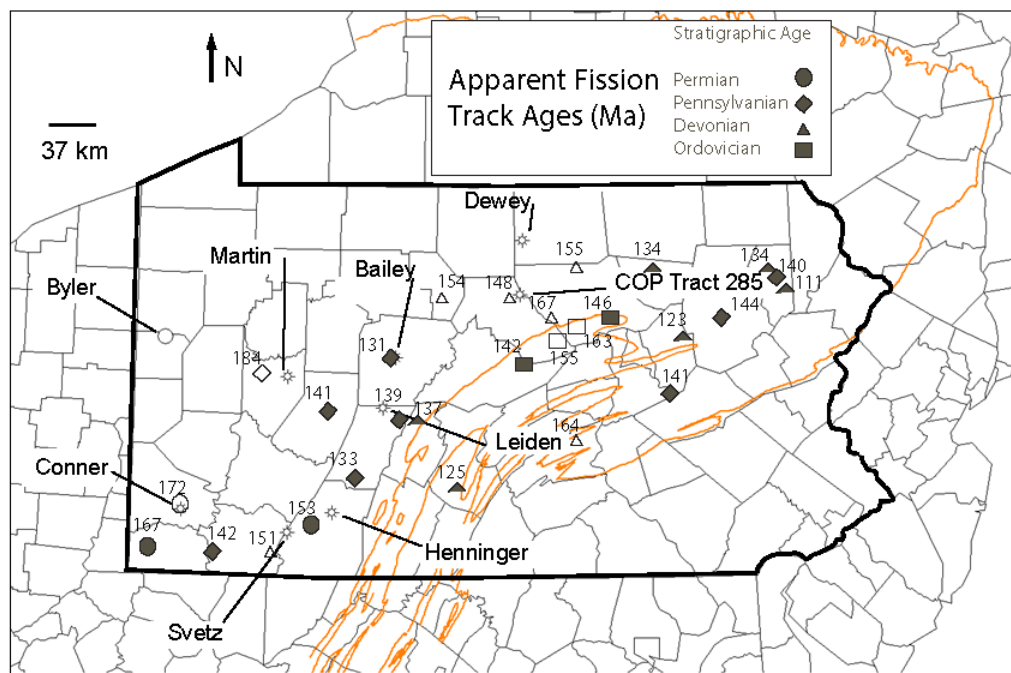
Figure 15. Fission-track sample locations (modified after Blackmer et al., 1994).
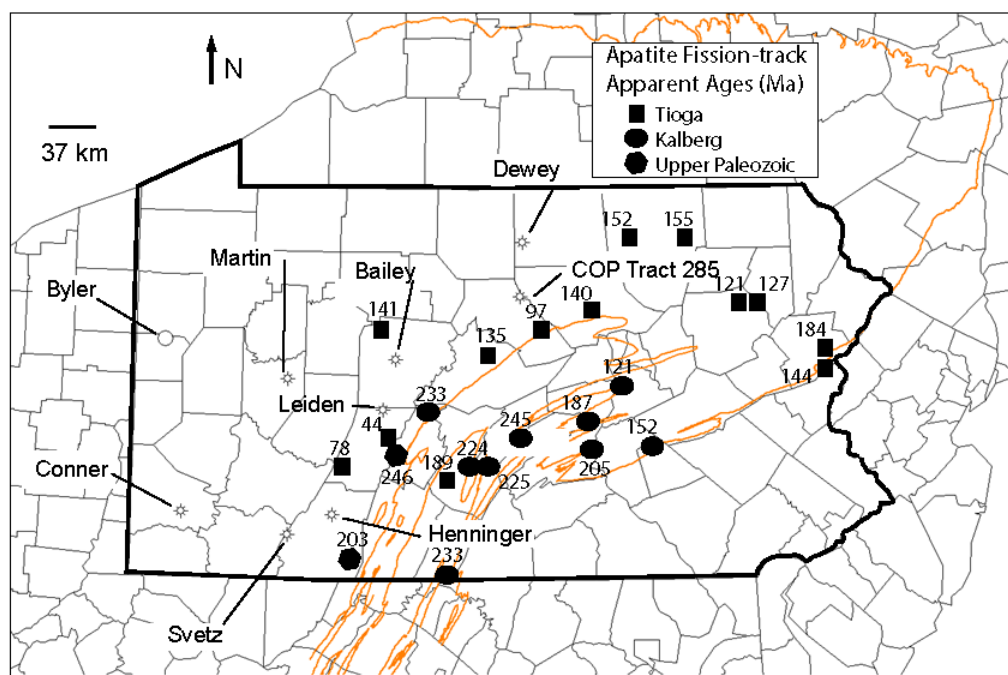
Figure 16. Fission-track sample locations (modified after Roden and Miller, 1989).

Thermal Modeling

To test the hypothesis that advection of hot brines could have caused the thermal maturity anomalies defined above, I attempt to match the maturity data in nine wells (Fig. 14) by solving the 1-D heat flow equation with and without lateral advection of heat. On continental crust the most important thermal processes are known to be conductive heat transport and radiogenic heat production (Turcotte and Schubert, 2002). Combining the

law of conservation of energy with Fourier's Law (Equation 1), which describes the relationship between heat flux (flow per unit area) and the thermal gradient at a point in a material,

$$q = -k \, \frac{dT}{dz}$$ (1)

where:

q = heat flux

k = thermal conductivity

T = temperature (°C)

z = depth (km)

yields (in one-dimension) the transient heat conduction equation,

$$\left(\frac{1}{\alpha}\right) \frac{\partial T}{\partial t} = \frac{\partial^2 T}{\partial z^2} + \frac{A}{k}$$ (2)

where:

α = thermal diffusivity ($m^2 \, s^{-1}$)

T = temperature (°C)

t = time (m.y.)

z = depth (km)

A = heat production ($\mu W \, m^{-2}$)

k = thermal conductivity ($W \, m^{-1} \, K^{-1}$)

One-dimensional modeling was chosen for this study because a two-dimensional model was deemed unwarranted given the sparse availability of calibration data across the basin and with depth.

Solution of the Heat Conduction Equation

Numerical solutions were obtained using the FORTRAN code, TQTec (K. Furlong, pers. comm.). TQTec implements a finite-difference scheme to solve for temperature as a function of depth and time. It can simulate episodes of burial, erosion, and tectonic thrusting, although thrusting is not considered here.

Model Input Parameters

Boreholes were chosen for 1-D modeling based on availability of paleo-temperature data for calibration, location, and availability of petrophysical and lithologic data. The stratigraphic section from the Grenvillian basement to the Permian was divided into grossly lithologically similar units using geophysical well logs, lithologic logs of well cuttings, and the interpretations of workers from the Pennsylvania Geological Survey in the well database PAIRIS. These units were then assigned absolute ages based on the Stratigraphic Correlation Chart of Pennsylvania (Berg et al., 1983) and GSA geologic time scale (Walker et al., 2013).

Ground Surface Heat Flow throughout Model Duration

Modeling results of this study indicate heat flow values vary between 67 to 90 mW m^{-2}. An average value for heat flow may be generally assumed for the study area, because in the absence of suspected perturbations due to fluid flow, one can assume that time-dependent effects of heat flow can be neglected for Grenvillian crust due to its antiquity (Turcotte and Schubert, 2002). A global compilation of heat flow measurements shows that the present-day heat flow range is 61.0 ± 30.2 mW m^{-2} for Paleozoic sedimentary and metamorphic rocks on continental crust, and the mean heat flow for all continental crust is 65 mW m^{-2} (Pollack et al., 1993; Turcotte and Schubert, 2002). Heat fluxes in the range of 50 to 100 mW m^{-2} are likely realistic values in sedimentary basins (Garven and Freeze, 1984b).

Recent heat flow values calculated from corrected bottom hole temperature measurements in the Appalachian plateau of Pennsylvania indicate that heat flow there ranges from approximately 55 to 75 mW m^{-2} (Blackwell and Richards, 2004; Blackwell et al., 2011). Likewise, Cercone et al. (1996) suggested that the range of present-day heat flow in the Appalachian plateau of western Pennsylvania is 54 to 84 mW m^{-2}. Previous modeling studies of the Appalachian Basin (Blackmer et al., 1994; Rowan, 2006; Rowan et al., 2004; Zhang and Davis, 1993) used lower heat flow values than the 67 to 90 mW m^{-2} proposed in this study. This could be because their thermal maturity (e.g. vitrinite reflectance) models may have overestimated maturity (Blackmer et al., 1994; Zhang and

Davis, 1993), or because the studies were focused on the distal, cooler part of the basin (Rowan, 2006; Rowan et al., 2004).

Surface Temperature

The temperature at the surface has been set to an average of 20 ℃ following previous studies (Barker, 2000; Cercone et al., 1996; Hulver, 1997; Wygrala, 1989), although average temperatures in the Carboniferous through Triassic Periods for the WPAB were 25 – 30 ℃ according to Wygrala (1989). The average surface temperature is presently approximately 10 ℃, but the temperature during maximum burial of the sediments should have a significantly greater influence on thermal maturation. Thus, 20 ℃ is considered an acceptable assumption for surface temperature in the model.

Burial History

The history of burial and erosion for each location in the study area is the parameter with the greatest degree of uncertainty in this model, yet constraining it is important due to its significant impact on paleo-temperature indicators. Burial estimates used in this study have been guided by previous research (Beaumont et al., 1987; Hulver, 1997; Zhang and Davis, 1993). In addition, critically-tapered wedge theory (Dahlen and Suppe, 1988) is incorporated to further constrain amounts of Alleghanian burial throughout the Appalachian plateau region in Pennsylvania. Slingerland and Furlong (1989) proposed that the basic topography of an accretionary mountain range at steady state can be determined as a function of the critical taper of the accretionary wedge (Fig. 17). They

suggested that at the end of the Alleghanian Orogeny, the Early Permian Appalachian mountains were similar to the current central Andean topography. Their estimates of average relief range from 3.5 – 4.5 km, with a mountain belt width of 250 – 300 km.

The maximum burial of a given horizon in the wedge should be consistent with the wedge model, increasing at a linear rate towards the hinterland. Calibrated amounts of subsequently eroded overburden from the Alleghanian Orogeny varies from well to well, and increases with distance from the Allegheny structural front.
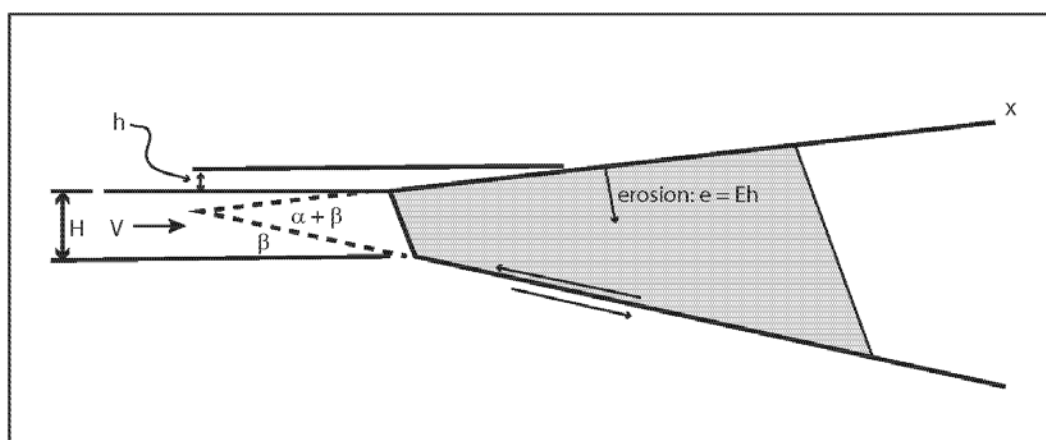
Figure 17. Critically tapered wedge (modified after Dahlen and Suppe, 1988).

Erosion History

Maximum burial of strata in western PA is assumed to have occurred at the peak of the Alleghanian Orogeny in the mid-Permian. Subsequently, the strata are assumed to have been exhumed, but the history of this exhumation is poorly known, particularly in the crucial interval between the end of the Alleghanian Orogeny and the initiation of

continental rifting and opening of the Atlantic. Zhang and Davis (1993) used data of post-rift Mesozoic and Cenozoic sedimentary deposits of the U.S. middle Atlantic continental margin (Poag and Sevon, 1989) to estimate an unroofing history, whereas Blackmer (1994) and Hulver (1997) each used apatite fission-track modeling at different locations within the Appalachian Basin. Blackmer generalized her results into several regional unroofing histories. This study is guided by Blackmer's unroofing rates, as well as Hulver's site specific and regional denudation histories, because they include Late Permian and early Triassic erosion.

Blackmer's results indicate a slow and steady unroofing rate in the western and broadtop/plateau regions of approximately 10 m Myr $^{-1}$ from 240 to 20 Ma, followed by more rapid unroofing of 50 m Myr $^{-1}$ from 20 Ma to present. Hulver's model indicates moderate denudation of 8 to 12 m Myr $^{-1}$ from 260 Ma to 150 Ma, followed by 2 to 4 m Myr $^{-1}$ from 150 Ma to 50 Ma, then 32 Myr $^{-1}$ from 50 Ma to present. Likewise, Zhang and Davis show moderate erosion from 260 Ma to 160 Ma, slower erosion from 160 to 20 Ma, and again rapid erosion from 20 Ma to present for the Appalachian plateau in southwestern Pennsylvania.

This author has taken the approach of varying erosion rates to match apatite fission-track data to nearby 1-D borehole models. Erosion rates were varied from 260 Ma to 160 Ma in the western plateau, and from 260 Ma to 200 Ma in the north-central plateau. This is done under the assumption that reheating of the basin on a regional scale

did not occur following the end of the Alleghanian Orogeny. This initial period of erosion is followed by a slow, steady erosion until 20 Ma, when rapid erosion from falling base level related to a drop in global sea level (Hulver, 1997) occurred. It is interesting to note that the current global erosion rates are, on average, 12 ± 1.3 m Myr^{-1} for rock outcrops, and 218 ± 35 m Myr^{-1} for drainage basins (terrestrial areas where the rocks are covered by soil) (Portenga and Bierman, 2011). However, these data are heavily skewed to the right. The median current global erosion rates are 5.4 m myr-1 for outcrops, and 54 m myr-1 for drainage basins. Thus the modeled erosion rates (Blackmer et al., 1994; Hulver, 1997) are low compared to present-day global averages.

Thermal Conductivity

The thermal conductivities of rocks were assigned by examining geophysical logs and lithologic logs of the modeled wells and assigning a median value from Table 1. The proportion of each lithology was determined in two wells with good lithologic logs (Dewey and Henninger), and a geometric average of thermal conductivity was assigned to each burial unit. Other wells were assigned thermal conductivities based on these analyses.

Table 1. Thermal Conductivity Ranges (data from Cercone et al., 1996; Blackwell and Steele, 1989; and Beardsmore and Cull, 2001).

Lithology	Thermal Conductivity (W m^{-1} K^{-1})
Coal	< 0.5
Black Shale	0.9
Shale	1.2 - 3
Siltstone	1.8 – 4.5
Limestone	2.5 – 3.1
Sandstone	2.5 – 4.2
Dolomite	3.75 – 6.3
Salt	4.8 – 6.05

Fluid Flow Modeling

As noted earlier, the advection of heat to shallower levels in the foreland by gravity-driven and tectonically-driven groundwater flows might occur for durations on the order of 10^6 years (Garven et al., 1993; Ge and Garven, 1992). Because the flow rates and heat losses along the flow paths are not the point of this study, I have chosen to model the addition of advective heat in western PA as a conductive heat flow boundary. If hotter fluid is more or less continuously supplied to a specific stratigraphic level for a specified time, then its thermal effect on higher strata can be simulated either by adding a heat source, or by lowering the thermal conductivities of units from the surface to the hypothesized flow path. This has the effect of raising the thermal gradient above and

below the location of the fluid boundary (Fig. 18). Below the fluid flow heat boundary,

the increase in thermal gradient would approach the slope of line A in Fig. 18, however it

will decay at some unknown rate. This is represented by line B. For rocks far below the

hypothesized heat boundary, the modeled results will be inaccurate. However, for this

study the organic-rich shales of the Middle and Upper Devonian straddle the

hypothesized source of advective heat closely enough (< 1 km above or below) that this

modeling approach is assumed to be valid.
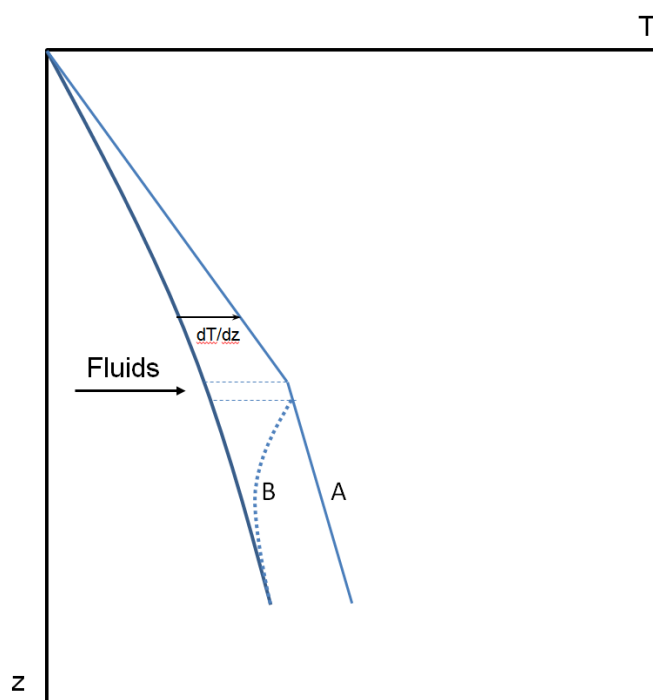
Figure 18. Diagram of Fluid Flow Modeling Concept. T is temperature, and z is depth. The dark blue line is the original thermal gradient before perturbation. The light blue line is the transient thermal gradient during periods of advection by fluid flow. Below the fluid boundary, Line A represents the theoretical maximum of the thermal gradient, and Line B represents the decay of the thermal gradient (unknown) with depth.

Vitrinite Reflectance Models

The heat flow model computes a time-temperature history for the different stratal packages. Therefore an additional model must be defined that converts time-temperature history to vitrinite reflectance and vice versa. Two types of vitrinite models based on a given temperature history are used in this study: the Lopatin-Waples-TTI method and the chemical kinetic method. Initially, the Lopatin-Waples-TTI method was used, following on previous work in the basin (Blackmer et al., 1994; Zhang and Davis, 1993). But the chemical kinetic approach was ultimately favored.

Lopatin-Waples TTI Method

An empirical method was first proposed by Lopatin (1971) who introduced the Time-Temperature Index (TTI), a cumulative thermal maturation scale that is based on the assumption that maturation has both a linear relationship with time and an exponential relationship with temperature, based on chemical reaction rates (Waples, 1980). Waples used the following equation to describe the relationship between TTI, temperature, and time:

$$\text{TTI} = \sum_{nmin}^{nmax}(\Delta T_n)(r^n) \tag{3}$$

where *nmin* and *nmax* are the minimum and maximum temperature intervals, ΔT_n is the change in time in Myr required to increase the temperature by 10 ºC, and *r* is the factor by which maturation increases exponentially for each temperature interval. Based on the generalization from the Arrhenius equation that chemical reaction rates double for every 10 ºC increase in temperature, i.e., $r = 2$.

Some previous researchers used the Lopatin-Waples-TTI method in the study area (Blackmer et al., 1994; Evans, 1995; Zhang and Davis, 1993), while more recent studies (Hulver, 1997; Reed et al., 2005) have used the chemical kinetic method. The shortcomings of the TTI method (e.g. poor calibration) (Tissot et al., 1987) have led to its decreased use in recent modeling studies in favor of methods that model the kinetics of the chemical reactions involved in the maturation of vitrinite.

Chemical Kinetic Method

The chemical kinetic method as described by Burnham and Sweeney (1989) assumes that the time-temperature dependence of maturation is described by the Arrhenius equation

$$k = A\, e^{(\frac{-E}{R\,T})} \tag{4}$$

where k is the rate constant (s^{-1}), A is the frequency factor (s^{-1}), E is the activation energy ($kJ\ mol^{-1}$), R is the universal gas constant ($J\ mol^{-1}\ K^{-1}$), and T is temperature (K). Reactions involving the elimination of water, carbon dioxide, methane, and heavier

hydrocarbons are modeled with distributions of activation energies. Vitrinite reflectance is calculated by using correlations between reflectance and elemental composition. Their chemical kinetic model was developed into a popular form known as EASY%R_o (Sweeney and Burnham, 1990).

The EASY%R_o model applies to values of mean random reflectance of 0.3-4.5%. The model was originally calibrated with mean maximum reflectance of vitrinite (%$R_{o\ max}$) from coal, but was later optimized using mean random reflectance (%$R_{o\ rand}$) (Burnham and Sweeney, 1989; Sweeney and Burnham, 1990). Figure 19 illustrates how the Waples (1980) method greatly overestimates reflectance at low heating rates at TTI values greater than approximately 30. While the EASY%R_o model remains popular, another chemical kinetic model, SIMPLE-R_o, was used for this study because the SIMPLE-R_o model provided a more effective way to implement the chemical kinetic method with the large temperature output files from TQTec.
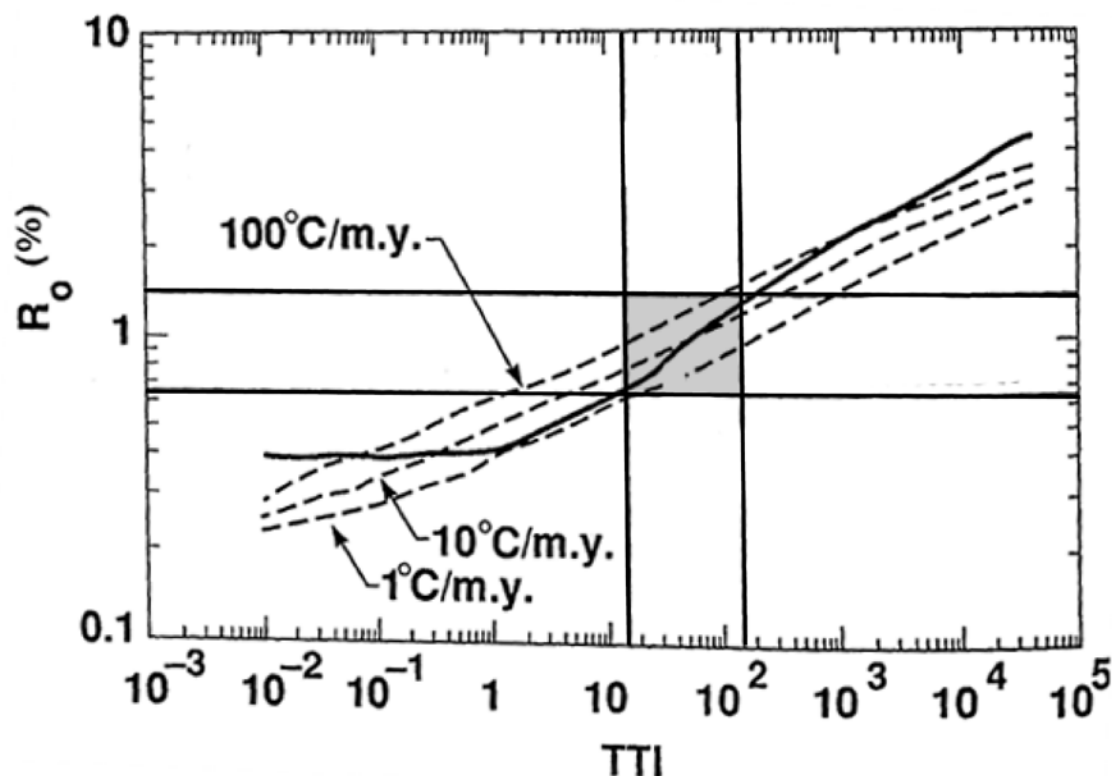
Figure 19. Comparison of time-temperature index (TTI) vs R_o at different heating rates of the chemical kinetic model EASY%Ro (Sweeney and Burnham, 1990) and Waples (1980) method. (modified after Sweeney and Burnham, 1990). Note how the Waples model (solid black curve) overestimates R_o at higher TTI values as compared to the EASY%R_o model (dashed curves) at the geological heating rate of 1°C/m.y. The grey box represents the approximate oil window in TTI and %$R_{o\ rand}$.

The SIMPLE-R_o model (Suzuki et al., 1993) is a simplified chemical kinetic model that yields results similar to EASY%R_o (Fig. 20). SIMPLE-R_o is based on the assumption that of the 20 reactions modeled in EASY%R_o, only a few of them operate at any given time. The other reactions are thought not to be important, either because of the

low concentrations of reactive sites for a certain reaction, or because of their higher

activation energies (Suzuki et al., 1993). This model assumes one reaction is occurring,

and that reaction has an apparent activation energy that increases slowly along with the

increase of R_o.
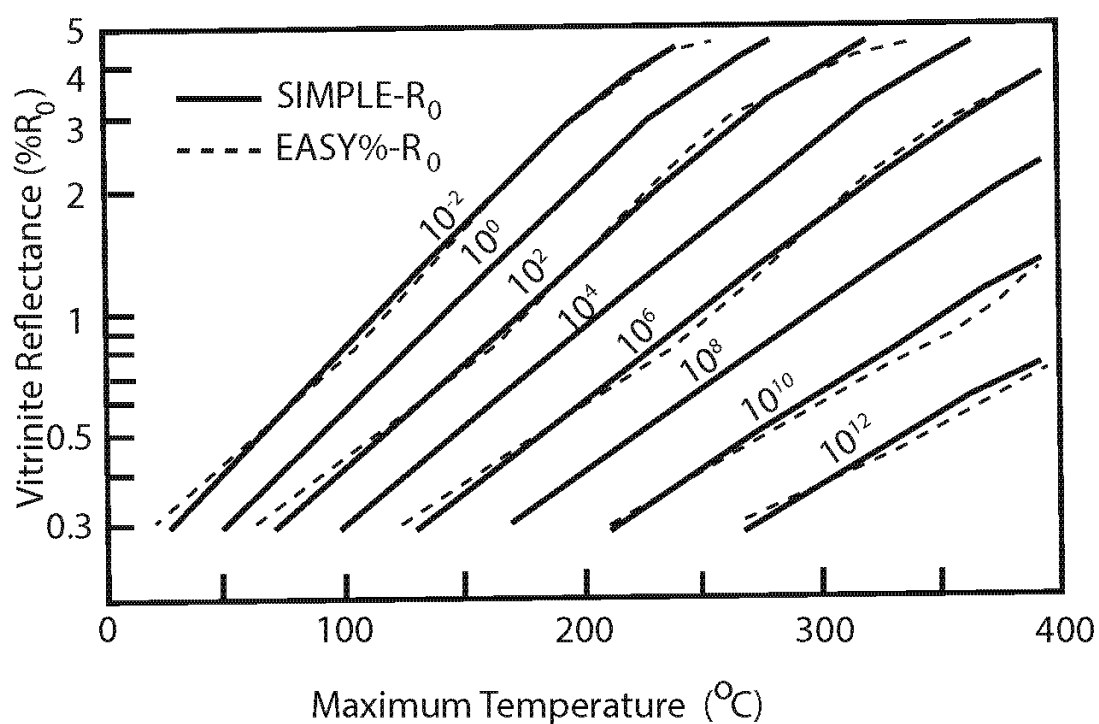
Figure 20. Comparison of the chemical kinetic models EASY%R_o and SIMPLE-R_o at constant rates of heating (modified after Suzuki et al., 1993). Note the close match of the SIMPLE-Ro model to the EASY%Ro model at lower rates of heating (10^{-2} to 10^2 °C myr^{-1}).

In the present study both mean random and mean maximum reflectance values are

used. Ting (1978) showed that mean maximum reflectance is greater than mean random

reflectance by a factor of 1.07. To correct for this disparity the relationship (Equation 5) established by Zhang and Davis (1993) has been used to convert measurements made on whole rock, dispersed vitrinite into maximum reflectance, the standard measurement for in situ coal samples:

$$R_{o\ max} = 1.2005 \times R_{o\ rand} - 0.0903 \tag{5}$$

Equation (5) is based on data with a range from approximately 0.6 to 1.7 %$R_{o\ rand}$. Previous researchers (England and Bustin, 1986; Hoover and Davis, 1980; Koch and Günther, 1995; O'Hara et al., 1990; Ting, 1978; Zhang and Davis, 1993) have published similar relationships. In one study, the linear trend was shown to be approximately accurate from 1 to 4% $R_{o\ rand}$ (Koch and Günther, 1995). Above 4%, the relationship is no longer linear. Figure 21 illustrates these relationships.
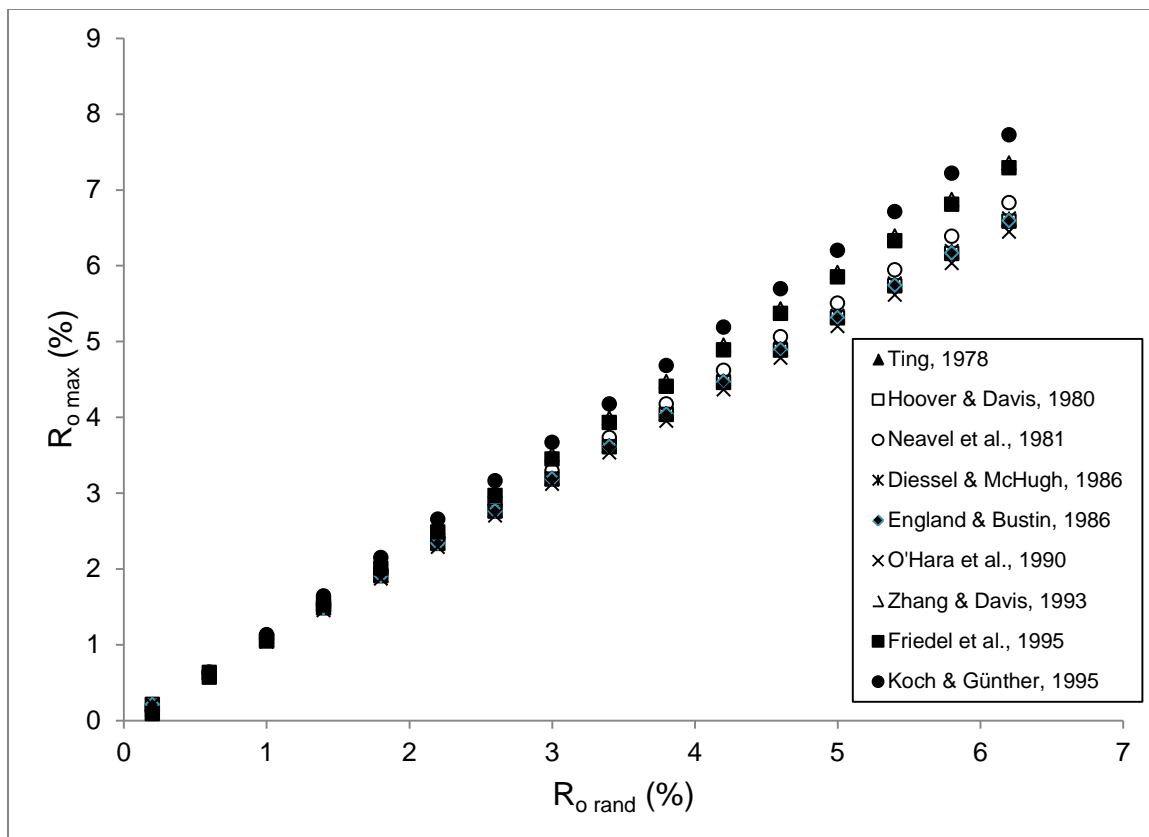
Figure 21. Mean Maximum Vitrinite Reflectance vs. Mean Random Vitrinite Reflectance.

Although there is significant variability of $R_{o\ max}$ with increasing $R_{o\ rand}$, within the range of values that correlates with petroleum generation and preservation (approx. 0.6 - 3.0 %$R_{o\ rand}$), the discrepancy between correlations will likely be within typical ranges of data uncertainty. The Zhang & Davis (1993) correlation is used in this study, because it was calibrated with samples from southwestern Pennsylvania.

The chemical kinetic vitrinite models described previously are calibrated with vitrinite reflectance data measured as %$R_{o\ rand}$. Consequently, in this study the time-temperature history from the heat conduction model was used as input to the SIMPLE-R_o model. Output from the SIMPLE-R_o model was then converted to %$R_{o\ max}$ using the Zhang and Davis (1993) conversion. Additionally, the compiled data of dispersed vitrinite samples have been converted and displayed as %$R_{o\ max}$. Figure 22 compares sample data before and after conversion to %$R_{o\ max}$.
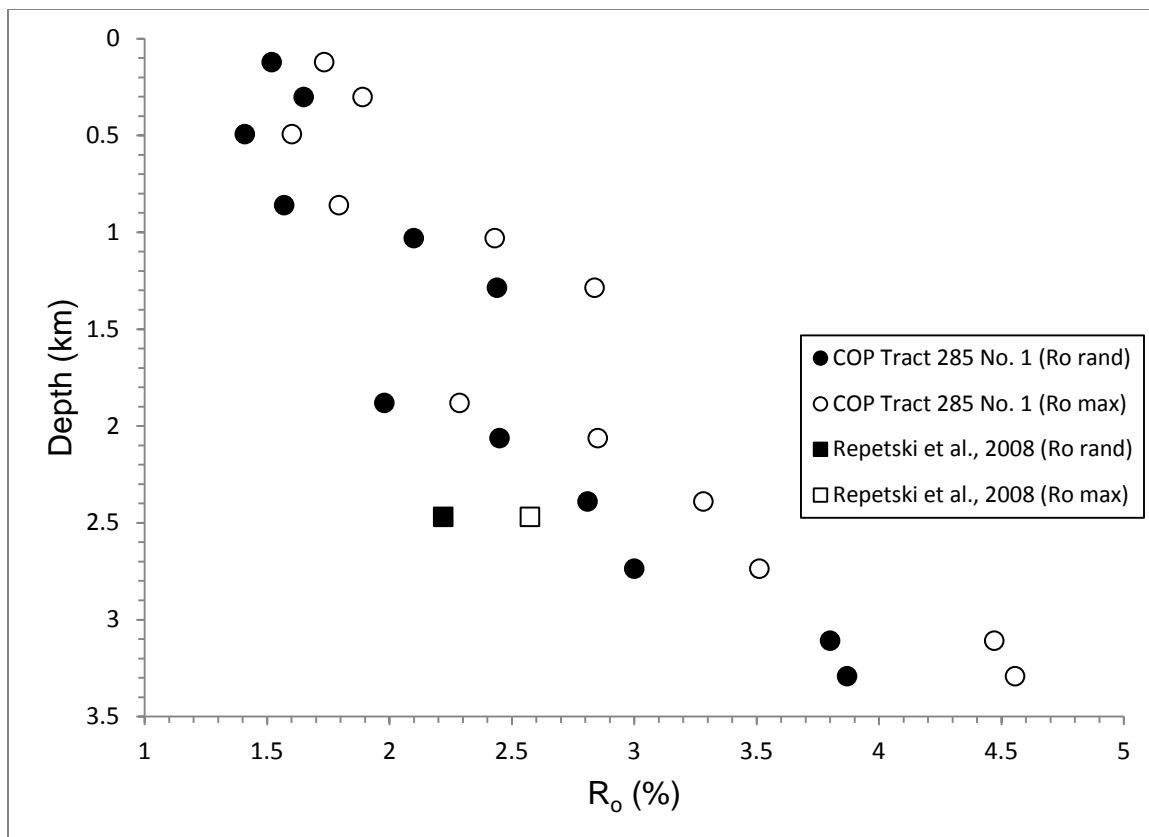
Figure 22. Comparison of random and maximum vitrinite reflectance (R_o) with depth. COP Tract 285 No. 1 data is from PPSRG.

Apatite Fission Track Model

The apatite fission track model used here is based on a number of studies and uses the FORTRAN code FTage of Legg (2010). The model creates 20 fission tracks per time step. The distribution of lengths of these modeled fission tracks is based on data of Green et al. (Green et al., 1986). Fission tracks are subsequently annealed based on the time-temperature history of the conduction model simulation. If temperatures in the model fall below that required for annealing of fission tracks, those tracks are preserved. The age at which the fission tracks are preserved is known as the retention age. The retention age is corrected based on the length distribution and operator bias. This age is reported along with its corresponding temperature for each modeled point in the simulation.

Model Calibration

Each model is calibrated to the available data within and near the well being modeled. For this study, the coal reflectance is relied on heavily, as well as the reflectance gradients of vertically-sampled wells for four model locations (Dewey No. 1 (Tioga County), COP Tract 285 No. 1 (Clinton County), Svetz No. 1 (Somerset County), Martin No. 1 (Armstrong County). These were used to initially calibrate amounts of burial and heat flow before the remaining five well models were evaluated. Successive iterations of model runs were performed until the data matched reflectance gradients and coal reflectance data. Additionally, histories of erosion were adjusted to match apatite fission-

track ages.

Initially, the Lopatin-Waples-TTI method was used to predict vitrinite reflectance. Surface temperatures of 10 – 12 ºC, surface heat flow of 50 – 60 mW m^{-2}, Alleghanian burial, and erosion histories were based on Zhang and Davis (1993). The Svetz No. 1 well in Somerset County was the first well modeled due to its extensively sampled R$_o$ data, extensive suite of geophysical and lithologic logs, proximity to coal reflectance data including vertically sampled reflectance gradients of Zhang and Davis (Zhang and Davis, 1993), and proximal location to the thermal anomaly (Figs. 2 – 6) in southwestern Pennsylvania. Burial amounts from the Alleghanian (presently eroded) were increased or decreased to match coal reflectance data near the present-day surface, and surface heat flow amounts were likewise adjusted to match the reflectance gradient with depth. Thermal conductivities of the existing stratigraphic section were not changed throughout the modeling process unless some error was discovered in previous determinations of conductivities. The thermal conductivity of the Alleghanian burial was changed incrementally in the range of 2.0 – 2.2 W m^{-1} K^{-1} based on values of Zhang and Davis (1993) to understand its effect on maturation. Ultimately a value of 2.1 W m^{-1} K^{-1} was set as the assumed value for these (mostly) Permian-aged sediments. These rocks are assumed to be similar to the preserved Dunkard Group, a sequence primarily consisting of siltstones, shales, sandstones, and minor coals. In subsequent iterations, Alleghanian burial amount and surface heat flow were the main parameters to be adjusted.

Later, the chemical kinetic method was explored (Burnham and Sweeney, 1989; Suzuki et al., 1993; Sweeney and Burnham, 1990) due to its popular use in current basin modeling studies. For a given time-temperature history, thermal maturation tends to be lower with the chemical kinetic method than the Lopatin-Waples-TTI method. As a result, higher heat flow values and amounts of burial were required to match maturity data. The chemical kinetic method was ultimately preferred, although either method could have been used in this study to compare the relative effects on thermal maturation by advection from hot fluids. Surface temperature was increased to 20 °C after further analysis of paleoclimate in the Paleozoic. Different erosion histories (Blackmer et al., 1994; Hulver, 1997; Zhang and Davis, 1993) were simulated, and the predictions of FTage were used to match apatite fission track data. Following these experiments, erosion rates were set for three intervals for model simplicity.

The first erosion period (260 – 160 Ma) was adjusted to match apparent fission track age data. The second period (160 – 20 Ma) was set to $5 - 10$ m myr^{-1}, consistent with the determinations of previous studies. The erosion rate of the third period (20 Ma – present) was much higher (generally $40 - 80$ m myr^{-1}), and served as a placeholder for excess sediments not eroded in the previous two periods (high erosion rates from 50 - 20 Ma to present are consistent with previous studies). The erosion rates become irrelevant regarding thermal maturation by 200 Ma due to the reduction in temperature by exhumation across the WPAB. Erosion rates after 200 Ma do affect the apparent fission

track age predictions, however.

Following these adjustments, well models were added to the study beginning with the peripheral areas of the WPAB (Tioga County, Washington County, Armstrong County, Lawrence County) assumed to be less affected by heating by fluid flow than areas more proximal to the Allegheny Front. After these models were calibrated, models along the Allegheny Front were investigated with and without the effect of heating by fluid flow.

MODELING RESULTS

A total of 402 1-D thermal diffusion models were run for the 9 locations indicated in Figure 14 (see Appendix to obtain access to all model parameters and predictions). All models use a surface temperature of 20º C, a basement thermal conductivity of 2.6 W m^{-1} K^{-1}, and a value for radiogenic heat production from sediments of 1.000 µW m^{-2}. Each model simulated heat flow from 450 Ma to present. The initial temperature profile was prescribed as 20º C (surface temperature). For the first 10-15 million years, depending upon location in the basin, the models were allowed to adjust their temperatures, after which burial units were added according to the estimates of the absolute ages of preserved sediments. Four wells (Dewey, COP Tract 285, Martin, Svetz) contain vertical profiles of vitrinite reflectance as well as near-surface coal reflectance data. These wells

were used to calibrate predicted heat flow values and amounts of Alleghanian maximum burial. Temperatures in the remaining five wells (Byler, Conner, Henninger, Leiden, Bailey) were matched to time-temperature histories required by near-surface coal reflectance data and reflectance data from Devonian strata collected by the USGS. The USGS data are consistently, and sometimes significantly lower than model predictions. This may be representative of mud contamination or caving in the borehole, natural variations in vitrinite, statistical errors, or technical errors. Model predictions are fit to match a logarithmic regression line of coal reflectance data and vertical profiles of reflectance from dispersed vitrinite where available. Modeled apatite fission-track ages were honored as much as possible by varying the rate of erosion following the end of burial at 260 Ma. For each well, maximum reflectance of vitrinite ($\%R_{o\ max}$) is reported and plotted versus depth. The random reflectance of vitrinite ($\%R_{o\ rand}$) is also reported in the text for correlation to thermal maturity of potential hydrocarbons in the Marcellus Fm. and various Upper Devonian black shale units where present.

Well Models

Tioga County – Dewey No. 1 (API 37117200570000)

The Dewey No. 1 well model begins in the Lower Silurian Irondequoit Dolomite and ends in the Upper Devonian Catskill Fm. (Table 2). A heat flow of 68 mW m^{-2} and Alleghanian maximum burial of 4.5 km above the Catskill Fm. produces the best fit to

the data (Fig. 23). An erosion rate of 27 m myr^{-1} (Fig. 24) from 260 Ma to 160 Ma yields a modeled fission-track age of 154 Ma in the Catskill Fm.. This is in agreement with nearby fission-track data (~150 Ma) of Blackmer et al. (1994) (Fig. 15). Coal reflectance data come from the nearby Bloss coal seam of the Allegheny Gp., but this unit is not preserved in the Dewey well. The Allegheny Gp. is projected to an estimated height of 0.3 km above the well based on current topography. A modeled reflectance value of 1.24% $R_{o\ max}$ at 0.3 km above the current surface (projected Allegheny Gp.) compares with estimated coal reflectance data from the contouring of Ruppert et al. (2010) equal to 1.2% $R_{o\ max}$. Modeled $R_{o\ max}$ values of the Upper Devonian black shales (Sonyea, Middlesex, Burket) are 2.31 – 2.40%, and the modeled $R_{o\ max}$ value of the Marcellus Formation is 2.70%. Converting to $R_{o\ rand}$ using Equation 4 gives values of 2.00 – 2.07% and 2.33%, respectively. These values indicate that all prospective black shales at this location lie firmly in the mature, dry gas window, consistent with known production in the area. The contoured value of 2.0% in the Marcellus Fm. of Repetski et al. (2008) is low compared to the modeled predictions and measured data of the PPSRG database, but is still within the dry gas zone.

Clinton County – COP Tract 285 (API 37035202760000)

The model of time-temperature history in the COP Tract 285 No. 1 well is defined for the stratigraphic interval from the Lower Silurian Rose Hill Fm. to the Lower Mississippian Burgoon Sandstone (Table 5). An Alleghanian maximum burial amount of 4.9 km and a

heat flow of 67 mW m^{-2} give the best fit (Fig. 26) to the measured reflectance data. An erosion rate of 32 m myr^{-1} from 260 Ma – 160 Ma (Fig. 27) yields a modeled fission-track age of 149 Ma in the Catskill Fm.. This is also in agreement with the observed data of Blackmer et al. (1994) (Fig. 15). Like the Dewey well, the Allegheny Gp. is projected to 0.3 km above the current surface. There are no coal reflectance measurements available in Clinton County, but based on analysis of Ruppert et al. (2010), maximum reflectance in this area is estimated to be approximately 1.3%. The modeled reflectance in the Allegheny Gp. is 1.28%. Cuttings from this well measured by Repetski et al. (2008) in the Marcellus Fm. give a reflectance of 2.57% after conversion from random reflectance to maximum reflectance. Model Run 14 follows a logarithmic trend that very closely matches the observed reflectance data of the Pennsylvania Source Rock Database. The modeled maximum reflectance in the Burket Member is 3.09%, and the maximum reflectance in the Marcellus Fm. determined from the curve of Model Run 14 is 3.45%. This corresponds to a random reflectance of 2.65% in the Burket and 2.95% in the Marcellus. Thus, according to the model these shales are also in the mature, dry gas zone.

Armstrong County - Martin No. 1 (API 37005212010000)

Model simulations in this well include the Lower Silurian dolomites of the Clinton Gp. through the Middle Pennsylvanian Allegheny Gp. (Table 8). In Fig. 29 two model runs (26 and 27) are plotted along with data from the PPSRG database, coal data from the

Lower Kittanning seam in the Allegheny Gp. (0.95%), and a local sample of cuttings in the Marcellus Fm. (1.79%) from Repetski et al. (2008). The two model runs shown here test different scenarios for heat flow and burial during the Alleghanian Orogeny.

Model Run 26 (Fig. 29) provides the best fit to the vertical profile of reflectance data. For this run Alleghanian maximum burial depth is 3.1 km and the basal heat flow is 90 mW m^{-2}. The erosion rate from 260 – 160 Ma is 16 m myr^{-1} (Fig. 30) which corresponds to a modeled fission-track age of 178 Ma in the Allegheny Gp. The values from Model Run 26 are maximum reflectance of 0.94% in the Allegheny Gp., an estimated 2.13% - 2.34% in the Upper Devonian black shales from the Rhinestreet through the Burket, and 2.49% in the Marcellus Fm. These correspond to 1.85% - 2.02% random reflectance in the Upper Devonian shales and 2.15% in the Marcellus Fm., which likely puts all of these units in the mature, dry gas zone.

Model Run 27 does not fit the observed maturity data, but it uses an amount of Alleghanian maximum burial (3.8 km) that seems more reasonable based on other locations in the basin. Heat flow was set to 67 mW m^{-2} based on calibrations of the previously discussed well models in Tioga and Clinton counties. An erosion rate of 18.5 m myr^{-1} (Fig. 32) provides a reasonable fit of modeled fission-track age (180 Ma) in the Allegheny Gp. to the observed data of Blackmer et al. (1994) (Fig. 15) of 184 Ma. The modeled values of maximum reflectance for units of interest are 0.87% in the Allegheny Gp., 1.63 – 1.76% for the Upper Devonian black shales, and 1.84% in the Marcellus Fm.

Converted back to random reflectance, these are 1.43 – 1.54% for the Upper Devonian black shales, and 1.61% for the Marcellus Fm. This model puts all prospective shales in the dry gas generating zone, with some production of wet gas possible.

Somerset County – Svetz No. 1 (API 37111200450000)

The Svetz No. 1 well model simulates heat flow in the interval between the Lower Silurian Rochester Member of the Mifflintown Fm. and the Upper Mississippian Mauch Chunk Fm. (Table 11). Multiple samples of vitrinite reflectance from drill cuttings (PPSRG database) begin in the near-surface and end at 3.15 km depth. The first four samples have a much higher reflectance gradient with depth than the remaining samples (Fig. 34). The coal reflectance data from the nearby (approx. 7 km to the north) Lower Kittanning seam in the Allegheny Gp. is 1.15%. A point (3.21%) in the Marcellus Fm. is estimated from reflectance contours of Repetski et al. (2008). The Allegheny Gp. is estimated to be 0.1 km above the current surface at this location based on analysis of surficial geologic maps, current topography, and estimated thickness of units from a geologic cross section (Ryder et al., 2012).

Model Run 71 best fits the data with 4.6 km of Alleghanian maximum burial and a heat flow of 72 mW m^{-2}. The erosion rate from 260 – 160 Ma is 27 m myr^{-1} (Fig. 35). This yields a modeled fission-track age of 163 Ma in the Allegheny Gp. The observed age in the Allegheny Gp. is 153 Ma (Blackmer et al. 1994) (Fig. 15). The modeled reflectance curve is a good match to the PA Source Rock data below 0.5 km depth. With

these parameters, reflectance in the Allegheny Gp. (projected) is 1.32%. The upper

Devonian Burket shale has a modeled maximum reflectance of 3.43%, and the Marcellus

Fm. has a maximum reflectance of 3.67% based on the modeled reflectance curve. This

corresponds to a random reflectance of 2.93% for the Burket and 3.13%, which puts both

units in the gas window in this model.

Washington County – Conner N271 (API 37125200700000)

The Conner No. 1 well has the most remaining Permian rock section of all the boreholes

included in this study. The modeled well begins in the Lower Silurian Rose Hill Fm. and

ends in the Lower Permian Dunkard Gp. (Table 14). The actual well penetrates only as

far as the Lower Devonian Helderberg Gp., so a 0.8 km package of limestones, dolomites

and evaporites has been added to the model (Table 15) to simulate the higher thermal

conductivity of the Silurian section as observed in other wells in this study.

Model Run 14 has a maximum burial from the Alleghanian of 4.0 km and heat

flow at 67 mW m^{-2} based on the calibrated Dewey and COP Tract 285 well models. The

erosion rate from 260 – 160 Ma is 18.5 m myr^{-1} (Fig. 39). This gives a modeled fission-

track age of 172 Ma in the Monongahela Gp., which matches the 172 Ma in the

Monongahela Gp. determined by Blackmer et al. (1994) (Fig. 15). Observed data used to

calibrate this well are coal reflectance from the Pittsburgh seam at the bottom of the

Monongahela Gp., and a reflectance measurement from cuttings in the Marcellus Fm. in

this well (Fig. 37). Since there are only two observed data points in this well, the linear

reflectance gradient with depth (Fig. 38) (< 0.6 km depth) is compared to boreholes E (Fayette County) and G (northern Washington County) of Zhang and Davis (1993) (Fig. 2). The slope (%Ro/depth) of Model Run 14 is 0.39. The slopes for boreholes E and G are 0.3477 and 0.3093, respectively. Measurements of maximum reflectance are 0.90% from Ruppert et al. (2010) for the Pittsburgh seam and 1.70% in the Marcellus Fm. The modeled reflectance values (Fig. 37) are 0.87% in the Pittsburgh Coal, 1.84% in the Rhinestreet Shale, 2.01% in the Geneseo Member of the Genesee Fm. (both estimated from the modeled reflectance curve), and 2.18% in the Marcellus Fm. For the prospective black shales, these correspond to random reflectance values of 1.61% in the Rhinestreet, 1.75% in the Geneseo, and 1.89% in the Marcellus. The model indicates these shales are likely in the dry gas generating zone with the possibility of production of wet gas.

Lawrence County – Byler No. 24 (API 37073201830000)

The Byler No. 24 well model begins in the Upper Silurian Salina Gp. and ends in the Middle Pennsylvanian Pottsville Gp. (Table 17). This well lies in the most distal part of the basin for the focus of this study. Measured reflectance data used for calibration and comparison are nearby (approx. 7 km east) coal reflectance data (Ruppert et al., 2010) from the Lower Kittanning Coal in the Allegheny Gp., two reflectance samples from cuttings in a well in Mercer County (30 km north) and a sample from the Marcellus Fm. from a well in northern Lawrence County (Repetski et al., 2008). The Allegheny Gp. is

estimated to be 0.05 km above the current surface at this location based on analysis of surficial geologic maps, current topography, and estimated thickness of units from the geologic cross section of Ryder et al. (2012).

Model Run 47 has a heat flow of 68 mW m^{-2} and an Alleghanian maximum burial amount of 3.1 km. The erosion rate from 260 – 160 Ma is 16.5 m myr-1 (Fig. 43). This amount of erosion yields a modeled fission-track age of 198 Ma. There are no nearby fission-track samples, but Hulver's (1997) basin-wide compiled dataset suggests this age is reasonable. The linear reflectance gradient with depth (Fig. 42) (< 0.6 km depth) is compared to borehole G (northern Washington County) of Zhang and Davis (1993) (Fig. 2). The slope (%Ro / depth) of Model Run 14 is 0.3311, and the slope for borehole G is 0.3093. Measured maximum reflectance values are 0.75% in the Lower Kittanning seam and 0.41% in the Marcellus Fm. The modeled reflectance values (Fig. 41) are 0.76% in the Allegheny Gp., 1.09% in the Dunkirk Shale, 1.18% in the Rhinestreet Shale, 1.22% in the Geneseo Member, and 1.25% in the Marcellus Fm. Converting these values to random reflectance gives 0.98% in the Dunkirk, 1.06% in the Rhinestreet, 1.09% in the Geneseo, and 1.12% in the Marcellus. From this model, all of these units are in the wet gas generating zone with a possibility of oil production as well.

Somerset County – Henninger No. 1 (API 37111200270000)

The Henninger No. 1 well model starts in the Upper Pennsylvanian Conemaugh Gp. and ends in the Lower Silurian Rose Hill Fm. (Table 20). The actual well penetrates only as

far as the Lower Devonian Ridgeley Sandstone, so a package of limestones, dolomites, and evaporites was added (Table 21) to simulate these lower conductivity units as described previously. The Henninger well lies in the highest maturity area of the western Plateau according to coal reflectance studies. This well was chosen for the modeling of heating by fluid flow. The only measured reflectance data near this well model is in the Lower Kittanning Coal (1.72%) of the Allegheny Gp. A point in the Marcellus Fm. (3.21%) is estimated from reflectance contours of Repetski et al. (2008). The reflectance gradient (Fig. 46) from borehole B of Zhang and Davis (1993) (Fig. 2) is also used to validate the model. Several scenarios were modeled to test the hypothesis of heating by fluid flow of the rocks in this part of the basin.

Model Run 81 has an amount of Alleghanian maximum burial of 4.8 km and a heat flow of 83 mW m^{-2}. The erosion rate from 260 – 160 Ma is 27 m myr-1(Fig. 47), which yields a modeled fission-track age of 134 Ma in the Allegheny Gp. This is in agreement with the measured fission-track age of 133 Ma in the Allegheny Gp. in southern Cambria County by Blackmer et al. (1994) (Fig. 15). The linear reflectance gradient with depth (Fig. 46) (< 0.6 km depth) is compared to borehole B (central Somerset County) of Zhang and Davis (1993) (Fig. 2). The slope (%Ro / depth) of Model Run 81 is 0.7621, and the slope for borehole B is 0.6898. The modeled maximum reflectance values (Fig. 45) are 1.75% in the Lower Kittannning Coal, 4.53% in the Burket Member of the Genesee Fm., and 4.97% in the Marcellus Fm. These correspond

to random reflectance values of 3.85% and 4.22% in the Marcellus Fm. This model suggests the prospective shales here are over mature, outside of the dry gas generating zone, with little preservation of dry gas.

Model Runs 83, 85, 86, 93, and 95 test the hypothesis of heating by fluid flow. They each use a heat flow of 72 mW m^{-2} based on the Svetz well 35 km to the southwest. 4.8 km of Alleghanian maximum burial is also used in these models. Model Run 83 is the base or control model, and Model Runs 85, 86, 93, and 95 test heating by fluid flow. Model Run 85 has an increased thermal gradient for 1 myr. from 260 Ma – 259 Ma, while Model Run 86 has an increased thermal gradient for 100,000 years from 260 – 259.9 Ma. Model Run 93 increases the thermal gradient for 20 myr. From 280 – 260 Ma, and Model Run 95 increases the thermal gradient for 30 myr. From 290 – 260 Ma. These increased thermal gradients were achieved by reducing the thermal conductivities of the burial units from the Upper Devonian Scherr Fm. upward through the Alleghanian maximum burial unit by 27% for the aforementioned periods of time for Model Runs 85 and 86. Thermal conductivities were reduced by 24% for Model Run 93 and 22% for Model Run 95. The erosion rate for each of these models is 28 m myr^{-1} (Fig. 49), which results in a modeled fission-track age of 160 Ma in the Allegheny Gp. This is closer to the measured fission-track age of 153 Ma in the Allegheny Gp. by Blackmer et al. (1994) (Fig. 15) in western Somerset County. The modeled fission-track age is not changed by the increase thermal gradients in Model Runs 85, 86, 93, and 95. Model Run 86 does not

provide a long enough duration of increased thermal gradient to have the desired effect on thermal maturity. The linear reflectance gradients with depth of Model Runs 83, 85, 93, and 95 (Fig. 46) (< 0.6 km depth) are compared to borehole B (central Somerset County) of Zhang and Davis (1993) (Fig. 2). The slope (%Ro / depth) of Model Run 85 is 0.7572, and the slope for borehole B is 0.6898. For Model Run 85, the modeled maximum reflectance values (Fig. 45) are 1.71% in the Lower Kittanning Coal, 4.26% in the Burket Member of the Genessee Fm., and 4.60% in the Marcellus Fm. These correspond to random reflectance values of 3.62% in the Burket and 3.91% in the Marcellus. Model Run 93 yields similar results to Model Run 85, while Model Run 95 predicts slightly lower values. According to these models, the Devonian shales are both very mature and potentially lie beyond the zone of dry gas generation. It is possible that some dry gas may be preserved, however.

Cambria County – Leiden No. 1 (API 37021200030000)

The Leiden No. 1 well model begins in the Lower Silurian Rose Hill Fm. and ends in the Middle Pennsylvanian Allegheny Gp. (Table 23). The actual well penetrates only as far as the Lower Devonian Oriskany Sandstone, so a package of limestones, dolomites, and evaporites have been added (Table 24) as described for previous well models. The Leiden well lies in an area of lower maturity relative to areas 10-20 km to the north and south in Clearfield and southern Cambria Counties. There is a measured maximum reflectance value (1.17%) in the Lower Freeport Coal in the Allegheny Gp.

approximately 8 km to the west of the Leiden well. Additionally there is a reflectance measurement (1.71%) by Repetski et al. (2008) from cuttings in the Marcellus Fm. 8 km to the west of this well.

Model Run 14 has an Alleghanian maximum burial amount of 4.7 km and a heat flow of 67 mW m^{-2}. The erosion rate is set at 27 mW m^{-2} from 260 – 160 Ma (Fig. 56) to be consistent with other well models with similar amounts of Alleghanian maximum burial, and the modeled fission-track age 165 Ma. This contrasts with the measured fission-track age of Blackmer et al. (1994) (Fig. 15) of 139 Ma in the Allegheny Gp. in eastern Cambria County. The linear reflectance gradient with depth (Fig. 59) (< 0.6 km depth) is compared to borehole D (eastern Westmoreland County) of Zhang and Davis (1993) (Fig. 2), since each of these wells lies in an area of similar coal reflectance (~1.2%). The slope of borehole B is 0.6309, while the slope of Model Run 14 is 0.4852. Modeled maximum reflectance values (Fig. 55) are 1.20% in the Allegheny Gp., 2.22% in the Burket Member of the Genesee Fm., and 2.41% in the Marcellus Fm. For the prospective shales, these values in random reflectance are 1.92% for the Burket, and 2.08% in the Marcellus. The model indicates these shales are dry gas generating zone.

Clearfield County – Bailey No. 1 (API 37033203820000)

The Bailey No. 1 well lies in an area of slightly higher maturity than northern Cambria County as indicated by coal vitrinite reflectance (~1.3%). The well model begins in the Lower Silurian Rose Hill Fm. and ends in the Middle Pennsylvanian Pottsville Gp.

(Table 26). The actual well penetrates only as far as the Lower Devonian Oriskany Sandstone, so a package of lower conductivity representing limestones, dolomites, and evaporites has been added (Table 27). Measured reflectance data (1.30%) is from the Lower Kittanning Coal in the Allegheny Gp. A sample point in the Marcellus Fm. is estimated (1.71%) from reflectance contours of Repetski et al. (2008). The Allegheny Gp. is projected to be 0.1 km above the current surface based on thicknesses of nearby wells.

Model Run 14 has 4.6 km of Alleghanian maximum burial and a heat flow of 78 mW m^{-2}. The erosion rate is 26 m myr^{-1} from 260 – 160 Ma (Fig. 60). This gives a modeled fission-track age of 165 Ma in the Allegheny Gp. This is in contrast to the measured fission-track age of 131 Ma in the Allegheny Gp. by Blackmer et al. (1994) (Fig. 15). The linear reflectance gradient with depth (Fig. 59) (< 0.7 km depth) is compared to borehole D (eastern Westmoreland County) of Zhang and Davis (1993) (Fig. 2). The slope (%Ro / depth) of Model Run 14 is 0.5845, and the slope for borehole D is 0.6309. Modeled maximum reflectance (Fig. 58) is 1.27% in the Allegheny Gp., 2.85% in the Burket Member of the Genesee Fm., and 3.11% in the Marcellus Fm. These correspond to random reflectance values of 2.45% in the Burket and 2.67% in the Marcellus. These prospective shales are in the dry gas generating zone.

Table 2. Well Stratigraphy, Dewey No. 1Well.

Group or Formation	Top (ft)	Top (m)	Thickness (m)
Catskill	0	0	150
Lock Haven	492	150	568
Brallier	2355	718	608
Sonyea	4350	1326	33
Middlesex	4457	1358	42
Genesee	4596	1401	37
Burket	4719	1438	14
Tully	4765	1452	23
Hamilton	4839	1475	192
Marcellus	5470	1667	47
Selinsgrove	5625	1715	5
Needmore	5643	1720	1
Ridgeley	5646	1721	8
Shriver	5671	1729	10
Mandata	5704	1739	1
New Scotland	5708	1740	17
Keyser	5765	1757	39
Salina	5894	1796	404
Wills Creek	7220	2201	125
Bloomsburg	7629	2325	90
McKenzie	7923	2415	34
Rochester	8036	2449	20
Keefer	8101	2469	11
Rose Hill	8136	2480	8
Irondequoit	8162	2488	143
Tuscarora	8630	2630	

Table 3. Model Inputs, Dewey No. 1 Well.

Burial #	Burial Units	Thickness (m)	Deposited From (Ma)	Deposited To (Ma)	Burial Depth (km)	Thermal Conductivity, k (W m^{-1} K^{-1})
1	Catskill	150	368	360	0.15	2.505
2	Lock Haven	568	376	368	0.60	2.362
3	Brallier	608	378	376	0.60	1.844
4	Sonyea/Middlesex/Genesee/Burket	126	383	378	0.15	1.073
5	Tully/Hamilton/Marcellus/Selinsgrove	262	392	383	0.25	1.752
6	eedmore/Ridgeley/Shriver/Mandata/New Scotland/Keys	77	421	392	0.10	2.633
7	Salina	404	423	421	0.40	4.911
8	Wills Creek/Bloomsburg	214	426	423	0.20	4.229
9	McKenzie/Rochester/Keefer	65	434	426	0.05	2.171
10	Rose Hill/Irondequoit	151	440	434	0.15	2.220
				Total	2.65	

Table 4. Present-Day Sample Depth and Formation, Dewey No. 1 Well. Modeled temperatures in TQTec were sampled at these points at 10^4 year intervals. See Figs. 25 and 26 for modeled basin history.

Depth (km)	Unit
-0.45	Permian
-0.3	Allegheny (projected)
0	Catskill
0.4	Lock Haven
0.8	Brallier
0.95	Brallier
1.2	Brallier
1.4	Genesee
1.6	Hamilton
2.5	Irondequoit
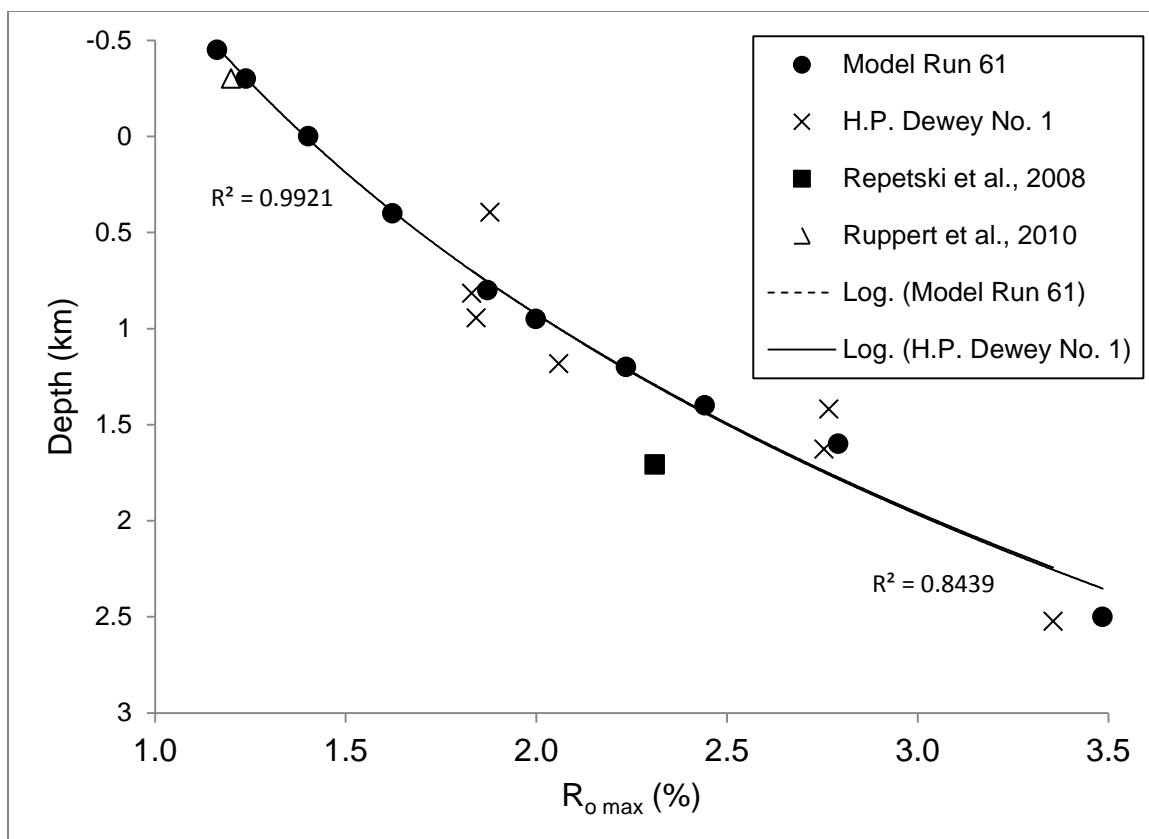
Figure 23. Observed and modeled maximum vitrinite reflectance in the BP Production North America Inc. Dewey No. 1 Well. "H.P. Dewey No. 1" data are observed values from PPSRG database. Model Run 61 of this well model provides best fit to logarithmic regression line of PPSRG data.
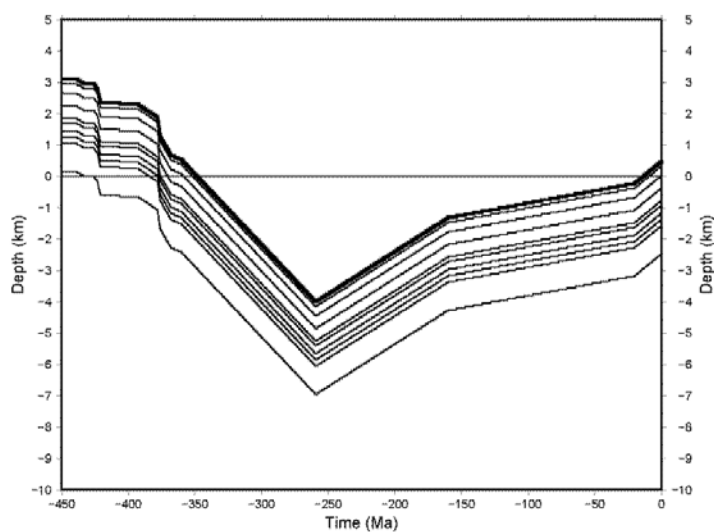
Figure 24. Burial History, Run 61, Dewey No. 1 Well. Lines indicate points monitored throughout model simulation, with the bold line indicating the youngest monitored unit. Refer to Table 4 for list of monitored points.
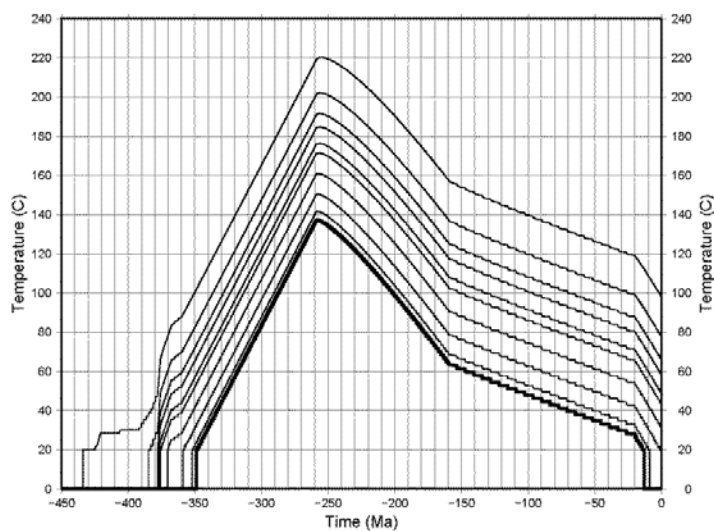
Figure 25. Temperature History, Run 61, Dewey No. 1 Well. Lines indicate points monitored throughout model simulation, with the bold line indicating the youngest monitored unit. Refer to Table 4 for list of monitored points.

Table 5. Well Stratigraphy, COP Tract 285 No. 1 Well.

Group or Formation	Top (ft)	Top (m)	Thickness (m)
Burgoon	0	0	91
Huntley Mountain	300	91	152
Catskill	800	244	338
Lock Haven	1910	582	876
Brallier	4785	1458	583
Harrell	6698	2042	110
Burket	7060	2152	27
Tully	7150	2179	49
Hamilton	7310	2228	232
Marcellus	8070	2460	37
Selinsgrove LS	8190	2496	13
Ridgeley	8232	2509	17
Shriver Chert	8289	2526	22
Mandata Shale	8360	2548	5
Corriganville LS	8375	2553	17
Keyser	8430	2569	47
Salina	8585	2617	292
Wills Creek	9542	2908	124
Bloomsburg	9950	3033	73
McKenzie	10190	3106	32
Keefer	10295	3138	34
Rose Hill	10407	3172	209
Tuscarora	11092	3381	89
Juniata	11385	3470	

Table 6. Model Inputs, COP Tract 285 No. 1Well.

Burial #	Burial Units	Thickness (m)	Deposited From (Ma)	Deposited To (Ma)	Burial Depth (km)	Thermal Conductivity, k (W m^{-1} K^{-1})
1	Burgoon/Huntley Mountain	244	360	347	0.25	2.734
2	Catskill	338	376	360	0.35	2.505
3	Lock Haven	876	378	376	0.9	2.362
4	Brallier	583	380	378	0.6	1.844
5	Harrell/Burket	138	383	380	0.15	1.9
6	Tully/Hamilton/Marcellus/Selinsgrove	330	407	383	0.35	1.752
7	Ridgeley/Shriver/Mandata/Corriganville/Keyser	108	421	409	0.1	2.633
8	Salina	292	423	421	0.3	4.911
9	Wills Creek/Bloomsburg	198	426	423	0.20	4.229
10	McKenzie/Keefer	66	434	426	0.05	2.171
11	Rose Hill	209	440	434	0.20	2
				Total	3.25	

Table 7. Present-Day Sample Depth and Formation, COP Tract 285 No. 1 Well. Modeled temperatures in TQTec were sampled at these points at 10^4 year intervals. See Figs. 28 and 29 for modeled basin history.

Depth (km)	Unit
-0.3	Allegheny (projected)
0.3	Catskill
0.85	Lock Haven
1.05	Lock Haven
1.3	Lock Haven
1.9	Brallier
2.05	Harrell
2.4	Hamilton
2.75	Salina
3.3	Rose Hill
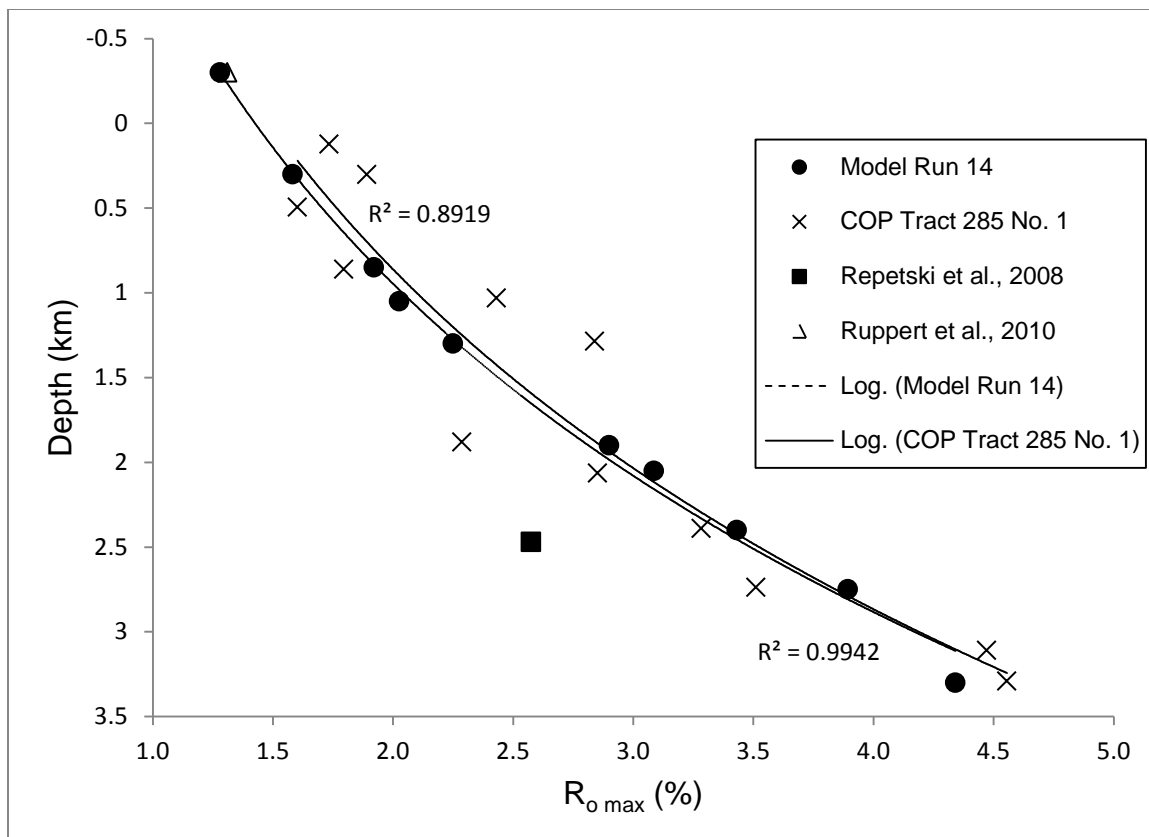
Figure 26. Observed and modeled maximum vitrinite reflectance in the Anadarko E&P Onshore LLC COP Tract 285 No. 1 Well. "COP Tract 285 No. 1" data are observed values from PPSRG database. Model Run 14 of this well model provides best fit to logarithmic regression line of PPSRG data.
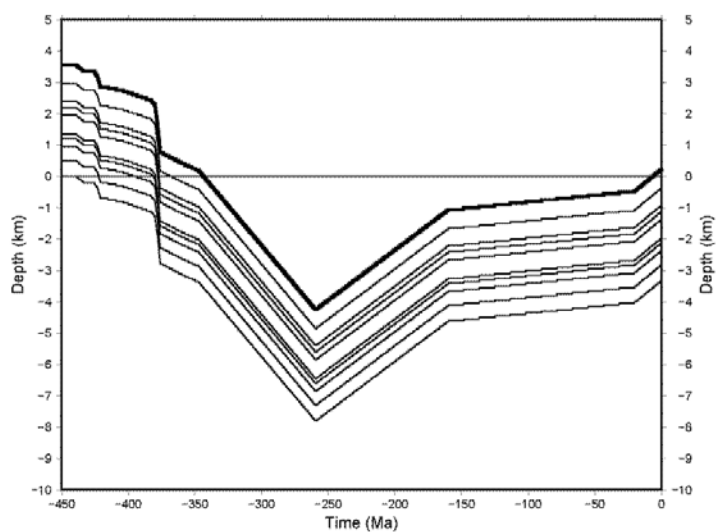
Figure 27. Burial History, Run 14, COP Tract 285 No. 1 Well. Lines indicate points monitored throughout model simulation, with the bold line indicating the youngest monitored unit. Refer to Table 7 for list of monitored points.
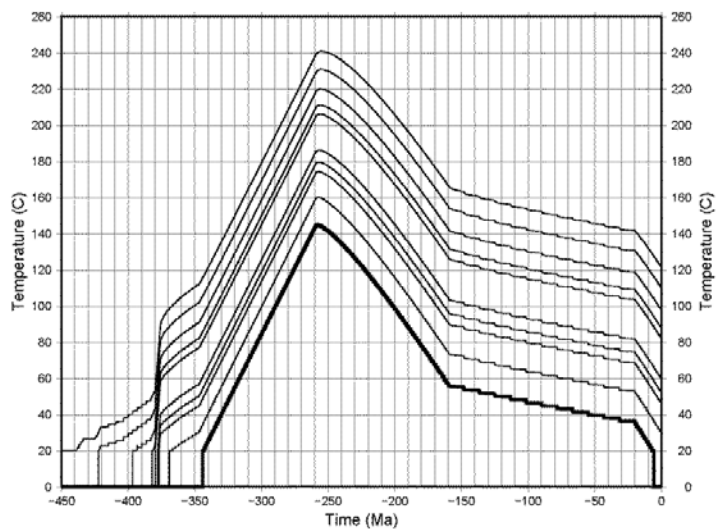
Figure 28. Temperature History, Run 14, COP Tract 285 No. 1 Well. Lines indicate points monitored throughout model simulation, with the bold line indicating the youngest monitored unit. Refer to Table 7 for list of monitored points.

Table 8. Well Stratigraphy, Martin No. 1 Well.

Group or Formation	Top (ft)	Top (m)	Thickness (m)
Allegheny	0	0	23
Vanport Limestone	77	23	2
Clarion Coal	83	25	1
Pottsville	85	26	48
Mauch Chunk	242	74	3
Loyalhanna	251	77	5
Burgoon	268	82	89
Patton Shale	560	171	46
Shenango	710	216	34
Cuyahoga	820	250	35
Murrysville	935	285	17
Oswayo	990	302	15
Venango	1038	316	187
Chadakoin	1650	503	140
Bradford	2110	643	390
Brallier	3390	1033	574
Rhinestreet	5273	1607	80
Sonyea	5537	1688	59
Middlesex	5730	1747	27
Genesee	5818	1773	32
Burket	5923	1805	6
Tully	5942	1811	28
Hamilton	6034	1839	91
Marcellus	6334	1931	16
Onondaga	6388	1947	6
Huntersville	6408	1953	22
Bois Blanc	6480	1975	8
Springvale SS	6506	1983	1
Licking Creek	6510	1984	18
Mandata Shale	6568	2002	2
Corriganville	6575	2004	5
Keyser	6591	2009	34
Bass Islands	6704	2043	5
Salina	6722	2049	615
Lockport Dolomite	8740	2664	42
Rochester	8878	2706	22
Irondequoit Dolomite	8951	2728	1
Rose Hill	8954	2729	48
Dayton Dolomite	9110	2777	18
Reynales Dolomite	9168	2794	23
Tuscarora	9244	2818	

Table 9. Model Inputs, Martin No. 1 Well.

Burial #	Burial Units	Thickness (m)	Deposited From (Ma)	Deposited To (Ma)	Burial Depth (km)	Thermal Conductivity, k (W m^{-1} K^{-1})
1	Allegheny/Vanport/Clarion/Pottsville	74	323	307	0.1	1.89
2	Mauch Chunk/Loyalhanna/Burgoon	97	352	331	0.1	2.6
3	Patton/Shenango/Cuyahoga/Murrysville	131	359	352	0.15	2.6
4	Oswayo/Venango	201	363	359	0.2	2.077
5	Chadakoin	140	365	363	0.15	2.077
6	Bradford	390	369	365	0.4	2.26
7	Brallier/Rhinestreet	654	378	369	0.65	1.9
8	Sonyea/Middlesex/Genesee/Burket	123	383	378	0.1	1.073
9	Tully/Hamilton/Marcellus/Onondaga/Huntersville/Bois Blanc/Springvale	173	410	383	0.15	1.752
10	Licking Creek/Mandata/Corriganville/Bass Islands	65	421	410	0.05	2.6
11	Salina	615	426	421	0.6	4.9
12	Lockport/Rochester/Irondequoit/Rose Hill/Dayton/Reynales	154	440	426	0.15	3.2
				Total	2.8	

Table 10. Present-Day Sample Depth and Formation, Martin No. 1 Well. Modeled temperatures in TQTec were sampled at these points at 10^4 year intervals. See Figs. 31-34 for modeled basin history.

Depth (km)	Unit
0	Allegheny
0.2	Chadakoin
0.75	Bradford
1.1	Brallier
1.35	Brallier
1.6	Rhinestreet
1.85	Hamilton
2.35	Salina
2.6	Salina
2.8	Reynales Dolomite
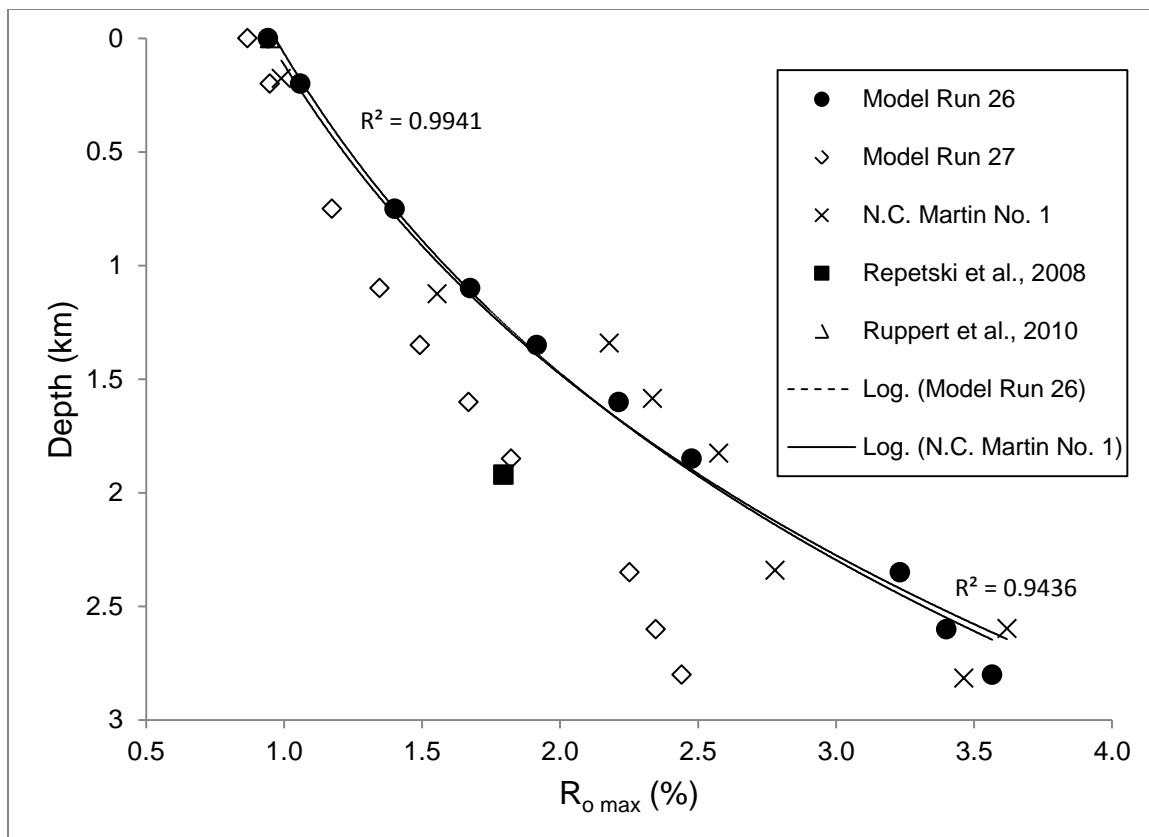
Figure 29. Observed and modeled maximum vitrinite reflectance in the CNX Gas Co. LLC Martin No. 1 Well. "N. C. Martin No. 1" data are observed values from PPSRG database. Model Run 26 of this well model provides best fit to logarithmic regression line of PPSRG data.
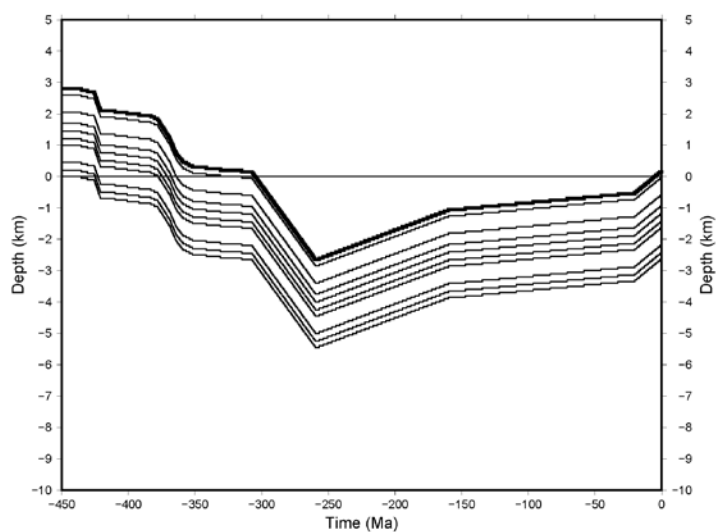
Figure 30. Burial History, Run 26, Martin No. 1 Well. Lines indicate points monitored throughout model simulation, with the bold line indicating the youngest monitored unit. Refer to Table 10 for list of monitored points.
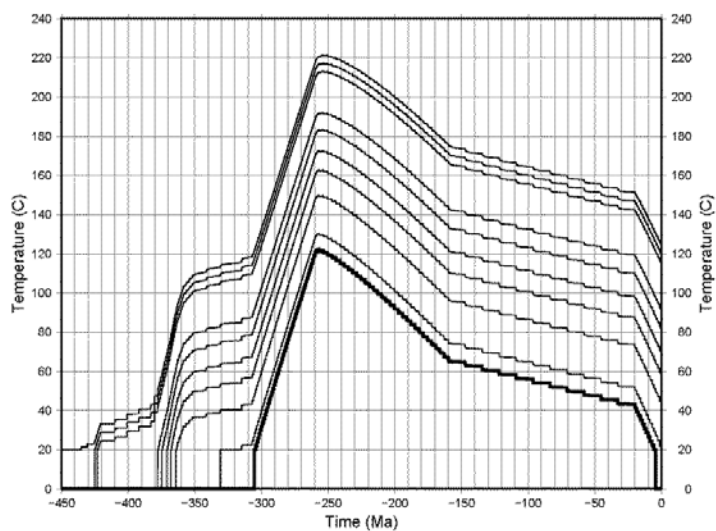
Figure 31. Temperature History, Run 26, Martin No. 1 Well. Lines indicate points monitored throughout model simulation, with the bold line indicating the youngest monitored unit. Refer to Table 10 for list of monitored points.
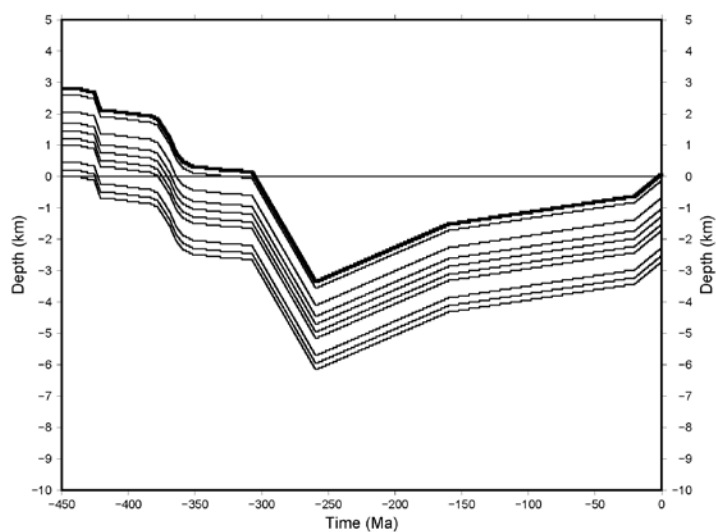
Figure 32. Burial History, Run 27, Martin No. 1 Well. Lines indicate points monitored throughout model simulation, with the bold line indicating the youngest monitored unit. Refer to Table 10 for list of monitored points.
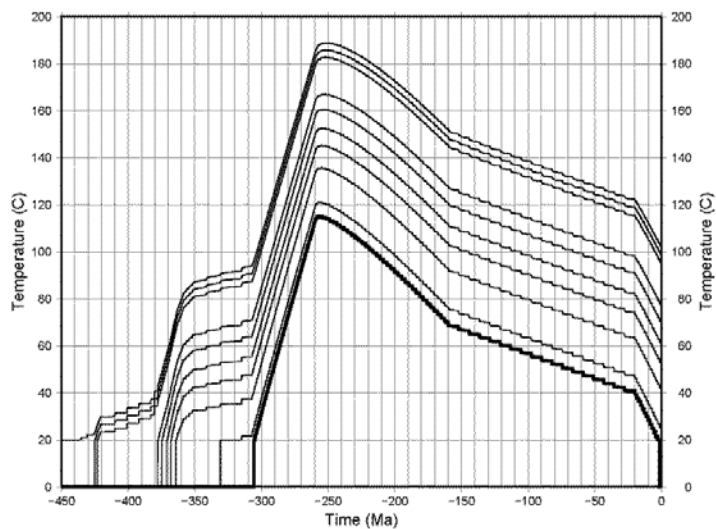
Figure 33. Temperature History, Run 27, Martin No. 1 Well. Lines indicate points monitored throughout model simulation, with the bold line indicating the youngest monitored unit. Refer to Table 10 for list of monitored points.

Table 11. Well Stratigraphy, Svetz No. 1 Well.

Group or Formation	Top (ft)	Top (m)	Thickness (m)
Mauch Chunk	0	0	113
Loyalhanna	370	113	24
Burgoon	448	137	57
Shenango	635	194	69
Cuyahoga	860	262	4
Murrysville	874	266	6
Oswayo	893	272	5
Venango	910	277	175
Chadakoin	1485	453	78
Bradford	1740	530	318
Elk	2784	849	585
Brallier	4703	1433	774
Harrell	7243	2208	108
Burket	7598	2316	27
Hamilton	7685	2342	174
Marcellus	8255	2516	26
Onondaga	8340	2542	6
Huntersville	8360	2548	35
Needmore	8474	2583	9
Ridgeley	8504	2592	12
Shriver	8545	2605	77
Mandata	8798	2682	7
Corriganville	8820	2688	6
Keyser	8840	2694	18
Tonoloway	8900	2713	390
Wills Creek	10178	3102	132
Bloomsburg	10612	3235	12
McKenzie	10652	3247	69
Rochester	10880	3316	12
Keefer	10918	3328	4
Rose Hill	10932	3332	116
Cresaptown SS	11312	3448	57
Tuscarora	11498	3505	112
Juniata	11866	3617	342
Bald Eagle	12988	3959	216
Reedsville	13696	4175	324
Utica	14758	4498	165
Point Pleasant	15300	4663	50
Trenton	15464	4713	104
Black River	15805	4817	146
Loysburg	16284	4963	218
Bellefonte	17000	5182	716
Nittany	19350	5898	213
Larke	20050	6111	148
Mines	20536	6259	94
Upper Sandy	20846	6354	144
Ore Hill	21318	6498	

Table 12. Model Inputs, Svetz No. 1 Well.

Burial #	Burial Units	Thickness (m)	Deposited From (Ma)	Deposited To (Ma)	Burial Depth (km)	Thermal Conductivity, k (W m^{-1} K^{-1})
1	Mauch Chunk/Loyalhanna	137	346	323	0.15	2.636
2	Burgoon	57	353	346	0.05	2.734
3	Shenango/Cuyahoga/Murrysville	79	359	353	0.1	2.734
4	Oswayo/Venango	180	363	359	0.2	2.077
5	Chadakoin	78	365	363	0.05	2.077
6	Bradford/Elk	903	375	365	0.9	2.26
7	Brallier/Harrell/Burket	909	383	375	0.9	1.9
8	Hamilton/Marcellus/Onondaga	206	392	383	0.2	1.752
9	Huntersville/Needmore/Ridgeley	56	408	392	0.05	2
10	Shriver/Mandata/Corriganville	90	418	408	0.1	2.633
11	Keyser/Tonoloway/Wills Creek/Bloomsburg	552	426	418	0.55	4.2287
12	McKenzie/Rochester	81	433	426	0.1	2.1713
				Total	3.35	

Table 13. Present-Day Sample Depth and Formation, Svetz No. 1 Well. Modeled temperatures in TQTec were sampled at these points at 10^4 year intervals. See Figs. 36 and 37 for modeled basin history.

Depth (km)	Unit
-0.1	Allegheny (projected)
0.3	Venango
0.5	Chadakoin
1.2	Elk
1.5	Brallier
1.85	Brallier
2.3	Burket
2.45	Hamilton
2.6	Ridgeley
3.15	Wills Creek
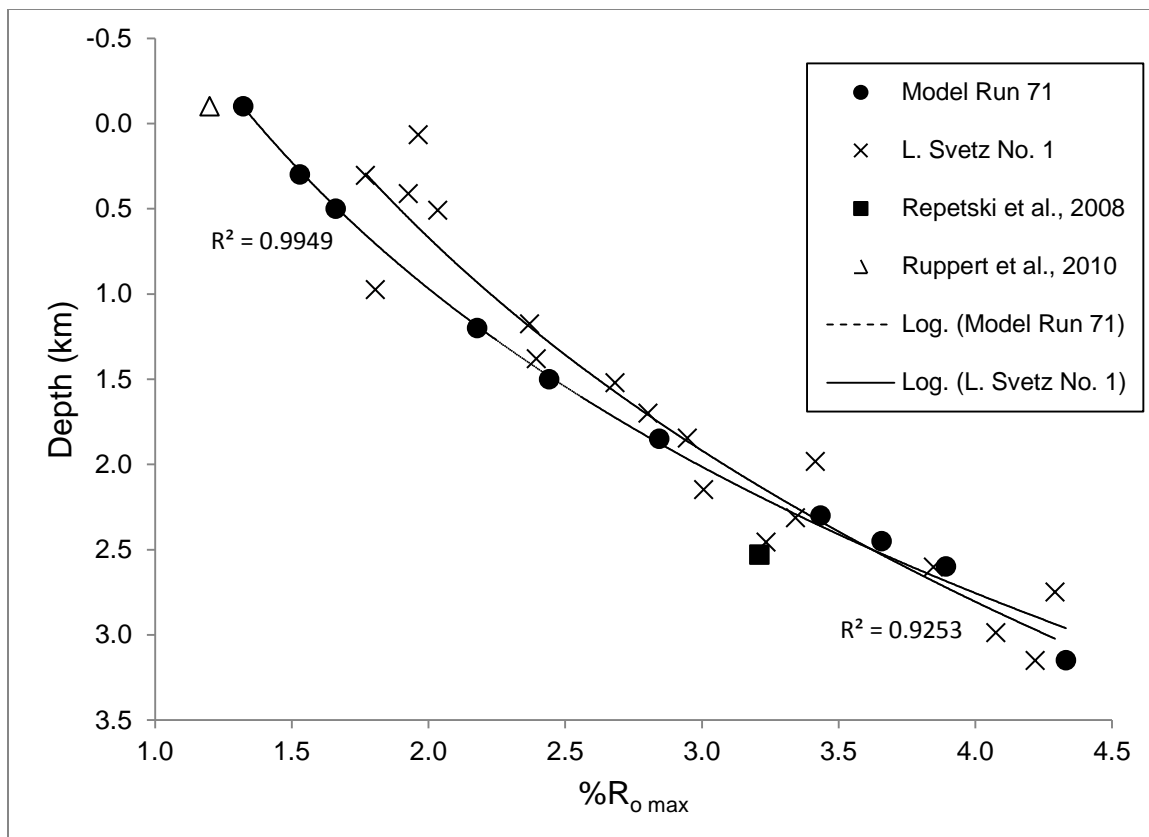
Figure 34. Observed and modeled maximum vitrinite reflectance in the BP Production North America Inc. Svetz No. 1 Well. "L. Svetz No. 1" data are observed values from PPSRG database. Model Run 71 of this well model provides best fit by eye to the data. The shallowest four measurements of "L. Svetz No. 1" are interpreted to be erroneously high.
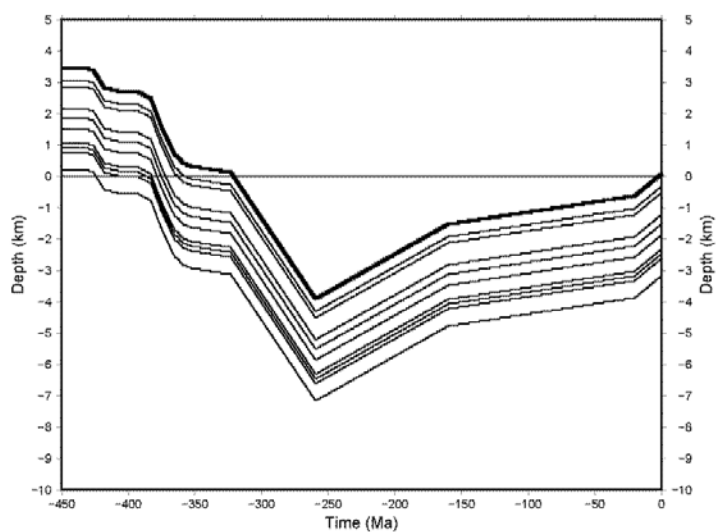
Figure 35. Burial History, Model Run 71, Svetz No. 1 Well. Lines indicate points monitored throughout model simulation, with the bold line indicating the youngest monitored unit. Refer to Table 13 for list of monitored points.
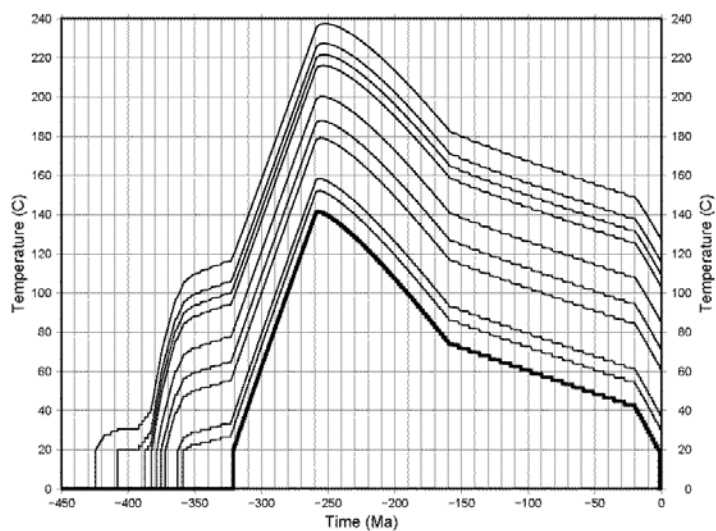
Figure 36. Temperature History, Model Run 71, Svetz No. 1 Well. Lines indicate points monitored throughout model simulation, with the bold line indicating the youngest monitored unit. Refer to Table 13 for list of monitored points.

Table 14. Well Stratigraphy, Conner No. 1 Well.

Group or Formation	Top (ft)	Top (m)	Thickness (m)
Dunkard Group	0	0	67
Waynesburg Coal	220	67	2
Monongahela Gp	226	69	84
Pittsburgh Coal	502	153	2
Conemaugh Gp	510	155	204
Allegheny Gp	1180	360	82
Pottsville Gp	1450	442	43
Mauch Chunk Fm	1590	485	27
Greenbrier Fm	1680	512	30
Burgoon SS	1780	543	58
Shenango Fm	1970	600	40
Cuyahoga Gp	2100	640	85
Oswayo Fm	2380	725	15
Venango Gp	2430	741	120
Chadakoin Fm	2825	861	145
Brallier	3300	1006	960
Rhinestreet	6450	1966	107
Sonyea	6800	2073	70
Genessee West River	7030	2143	37
Geneseo Member	7150	2179	8
Tully LS	7175	2187	8
Hamilton Gp	7200	2195	73
Marcellus	7440	2268	18
Onondaga	7500	2286	73
Oriskany	7740	2359	34
Helderberg	7850	2393	

Table 15. Model Inputs, Conner No. 1 Well.

Burial #	Burial Units	Thickness (m)	Deposited From (Ma)	Deposited To (Ma)	Burial Depth (km)	Thermal Conductivity, k (W m^{-1} K^{-1})
1	Dunkard/Waynesburg	69	300	296	0.05	2.1
2	Monongahela/Pittsburgh	87	304	300	0.1	2.1
3	Conemaugh	204	307	304	0.2	2.1
4	Allegheny/Pottsville	125	323	307	0.1	2
5	Mauch Chunk	58	331	327	0.05	2.6
6	Burgoon/Shenango/Cuyahoga	183	359	349	0.2	2.6
7	Oswayo/Venango	136	363	359	0.15	2.077
8	Chadakoin	145	365	363	0.15	2.077
9	Brallier/Rhinestreet	1067	378	365	1.1	1.9
10	Sonyea/Genesee/Geneseo	114	383	378	0.1	1.8
11	Tully/Hamilton/Marcellus	99	391	383	0.1	1.4
12	Onondaga/Oriskany(Ridgeley)	107	409	391	0.1	2.5
13	Needmore through Rose Hill	800	435	409	0.8	3.69
				Total	3.2	

Table 16. Present-Day Sample Depth and Formation, Conner N271 Well. Modeled temperatures in TQTec were sampled at these points at 10^4 year intervals. See Figs. 40 and 41 for modeled basin history.

Depth (km)	Unit
0	Dunkard
0.15	Pittsburgh Coal
0.4	Allegheny
0.5	Mauch Chunk
0.6	Shenango
1	Brallier
1.4	Brallier
1.8	Brallier
2.3	Marcellus
3	Dolomites
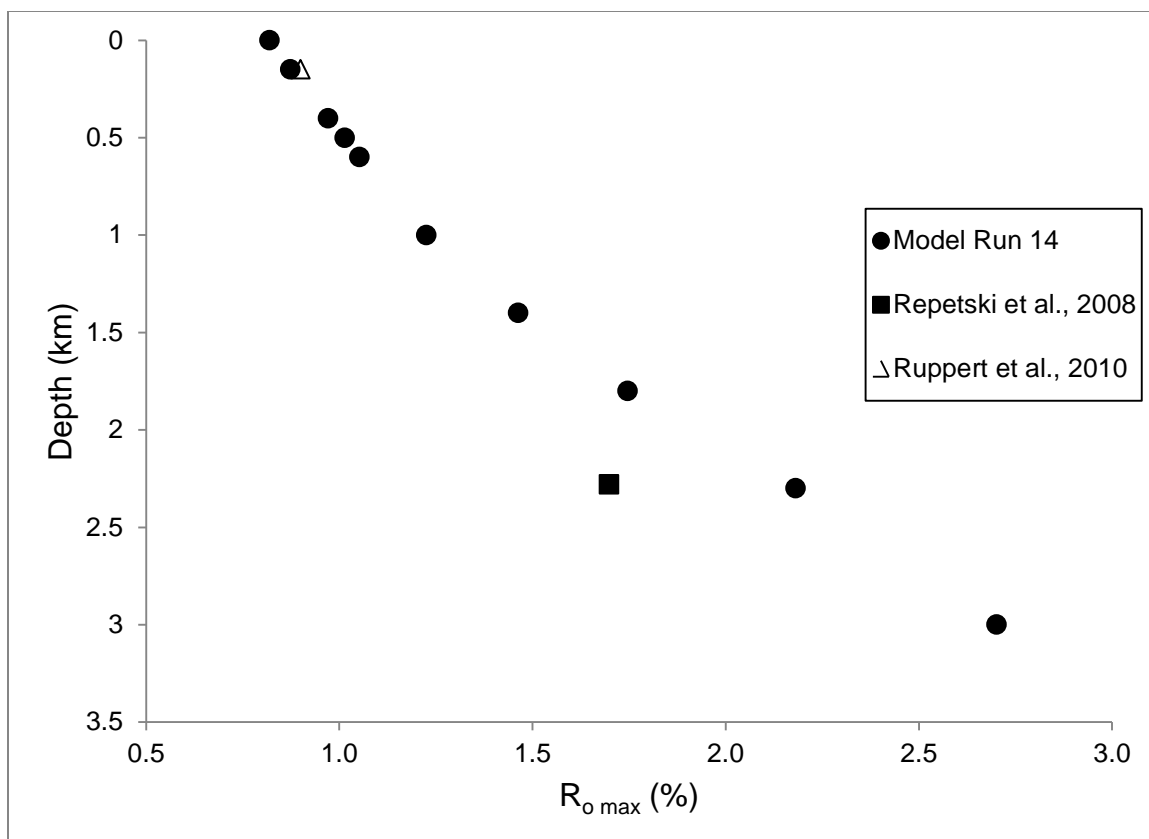
Figure 37. Observed and modeled maximum vitrinite reflectance in the Chevron USA Inc. Conner N271 Well.
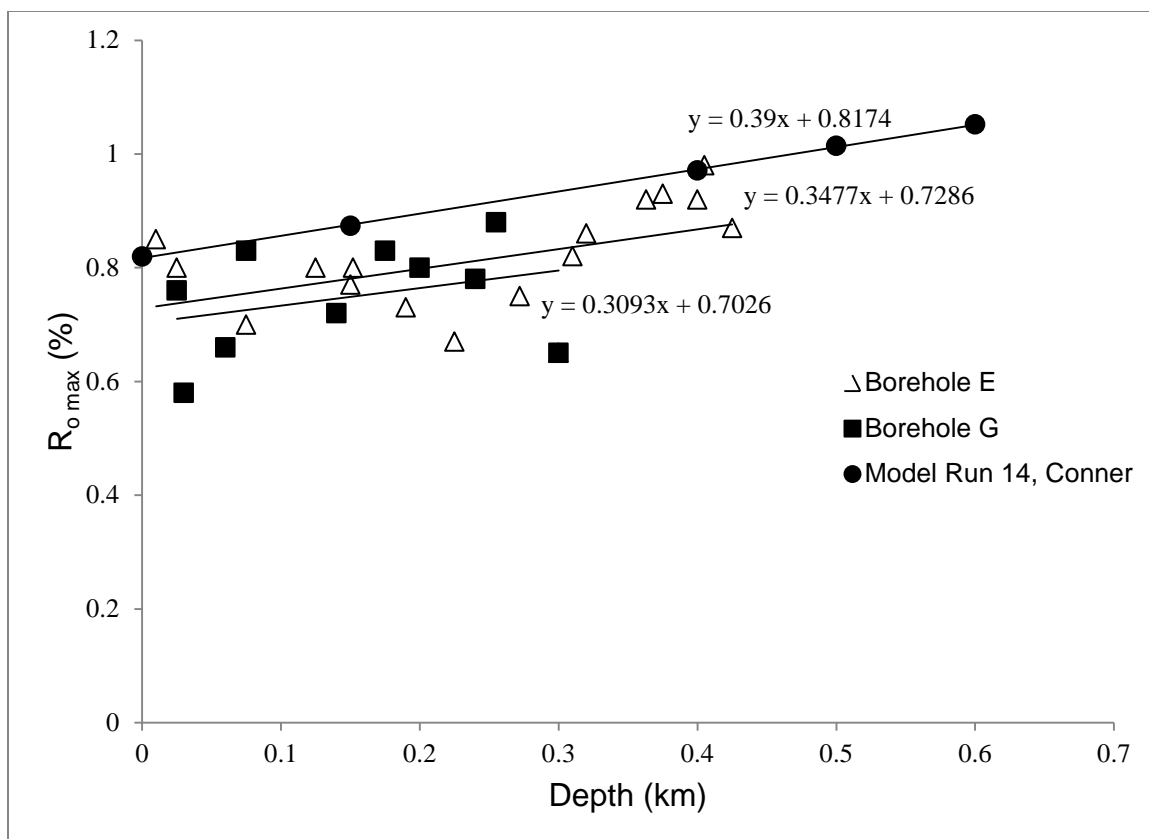
Figure 38. Reflectance Gradients of Boreholes E and G (Zhang and Davis, 1993) and Model Run 14, Conner N271 Well.
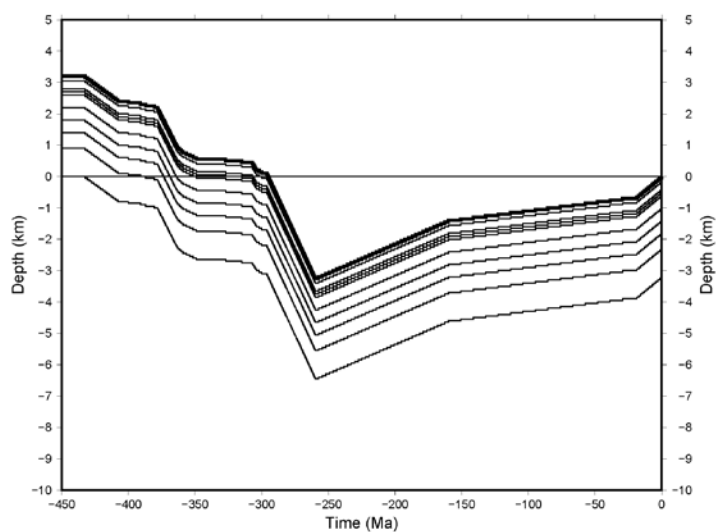
Figure 39. Burial History, Run 14, Conner N271 Well. Lines indicate points monitored throughout model simulation, with the bold line indicating the youngest monitored unit. Refer to Table 16 for list of monitored points.
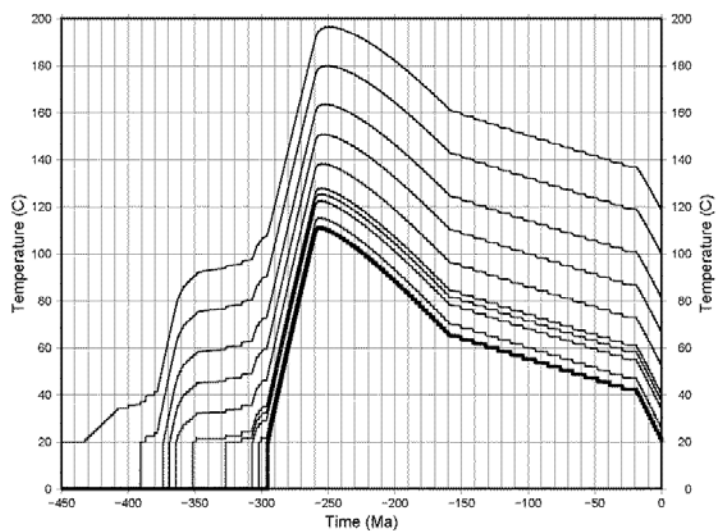
Figure 40. Temperature History, Run 14, Conner N271 Well. Lines indicate points monitored throughout model simulation, with the bold line indicating the youngest monitored unit. Refer to Table 16 for list of monitored points.

Table 17. Well Stratigraphy, Byler No. 24 Well.

Group or Formation	Top (ft)	Top (m)	Thickness (m)
Pottsville	0	0	54
Shenango	176	54	41
Cuyahoga	311	95	63
Berea SS	517	158	7
Bedford Shale	540	165	17
Cussewago SS	597	182	25
Riceville	679	207	17
Venango	734	224	99
Chadakoin	1058	322	188
Ohio Shale	1674	510	278
Huron Shale	2587	789	118
Dunkirk Shale	2974	906	13
Java	3017	920	47
Pipe Creek	3170	966	7
West Falls	3193	973	83
Rhinestreet	3465	1056	111
Sonyea	3830	1167	8
Middlesex	3856	1175	3
Genesee	3867	1179	13
Burket	3910	1192	2
Tully	3918	1194	1
Hamilton	3920	1195	40
Marcellus	4050	1234	5
Onondaga	4066	1239	44
Bois Blanc	4210	1283	8
Helderberg	4235	1291	24
Keyser	4313	1315	21
Bass Islands Dolomite	4383	1336	15
Salina	4431	1351	269
Lockport Dolomite	5315	1620	

Table 18. Model Inputs, Byler No. 24 Well.

Burial #	Burial Units	Thickness (m)	Deposited From (Ma)	Deposited To (Ma)	Burial Depth (km)	Thermal Conductivity, k (W m^{-1} K^{-1})
1	Pottsville	54	322	311	0.05	2.01
2	Shenango/Cuyahoga/Berea/Bedford/Cussewago	153	359	353	0.15	2.6
3	Riceville/Venango	116	365	359	0.1	2.077
4	Chadakoin/Ohio/Huron/Dunkirk	597	372	365	0.6	2.077
5	Java through Burket	275	383	372	0.3	1.9
6	Tully/Hamilton/Marcellus/Onondaga	89	393	383	0.1	1.4
7	Bois Blanc/Helderberg/Keyser	53	398	393	0.05	2.5
8	Bass Islands/Salina	269	426	420	0.25	4.9
				Total	1.6	

Table 19. Present-Day Sample Depth and Formation, Byler No. 24 Well. Modeled temperatures in TQTec were sampled at these points at 10^4 year intervals. See Figs. 44 and 45 for modeled basin history.

Depth (km)	Unit
-0.05	Allegheny (projected)
0	Pottsville
0.15	Cuyahoga
0.3	Venango
0.45	Chadakoin
0.6	Ohio Shale
0.75	Ohio Shale
1	West Falls
1.15	Rhinestreet
1.3	Helderberg
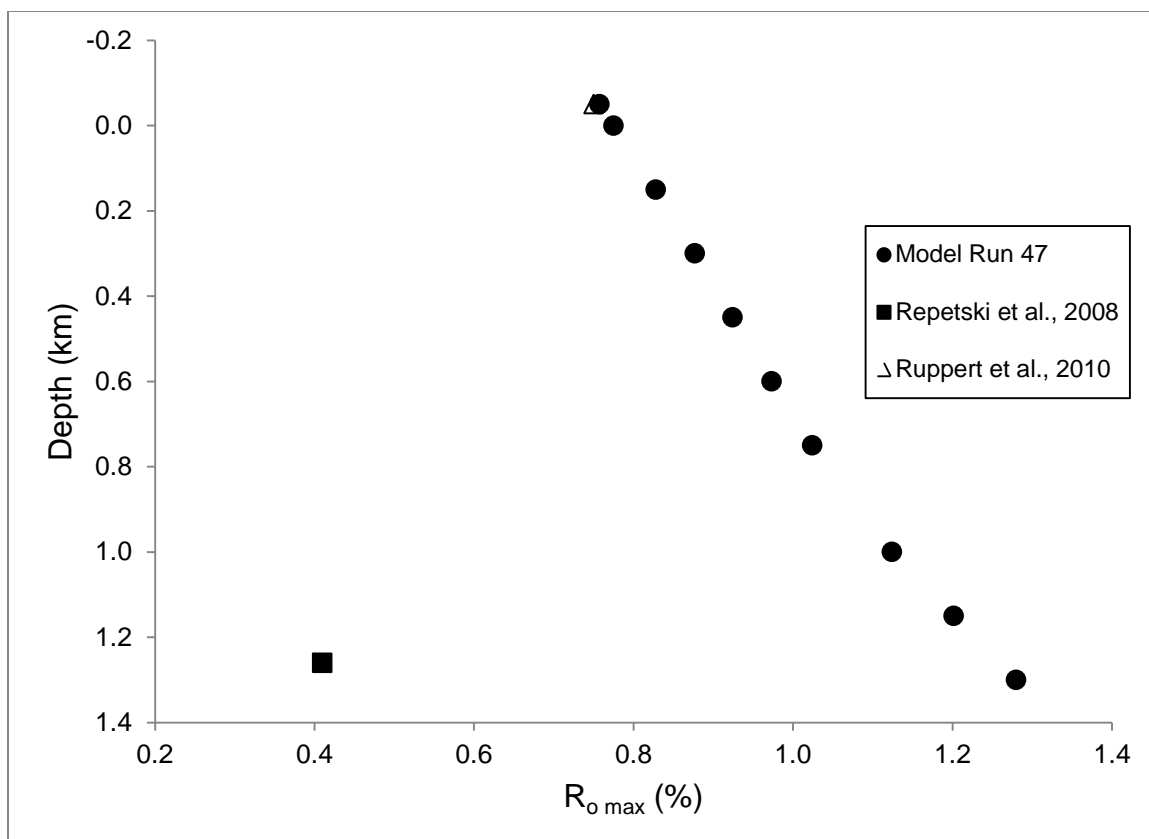
Figure 41. Observed and modeled maximum vitrinite reflectance in the Atlas Resources LLC Byler No. 24 Well.
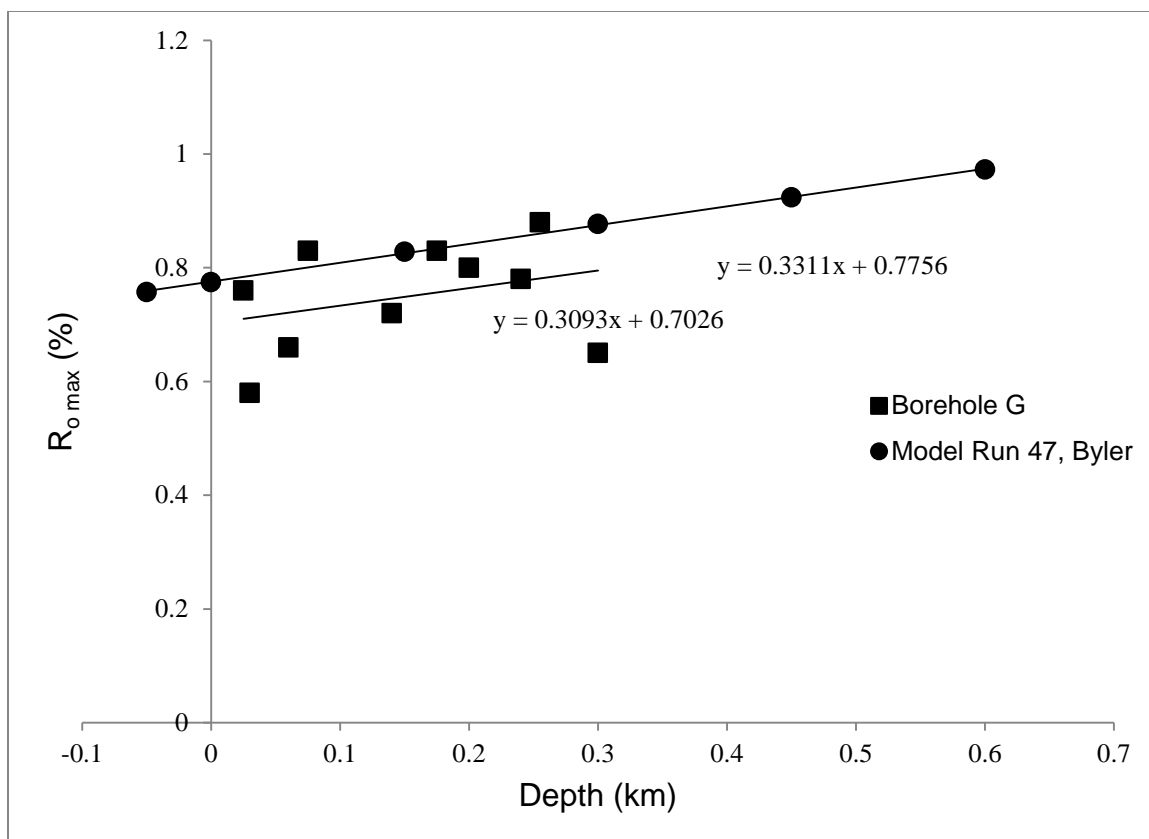
Figure 42. Reflectance Gradients of Borehole G (Zhang and Davis, 1993) and Model Run 47, Byler No. 24 Well.
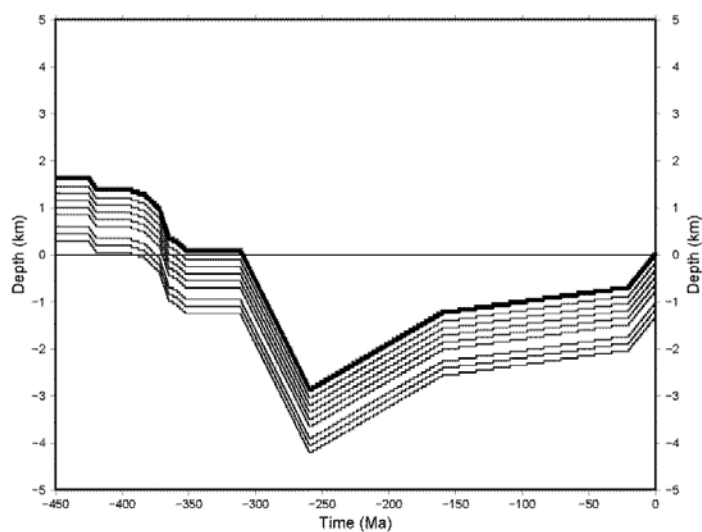
Figure 43. Burial History, Run 47, Byler No. 24 Well. Lines indicate points monitored throughout model simulation, with the bold line indicating the youngest monitored unit. Refer to Table 19 for list of monitored points.
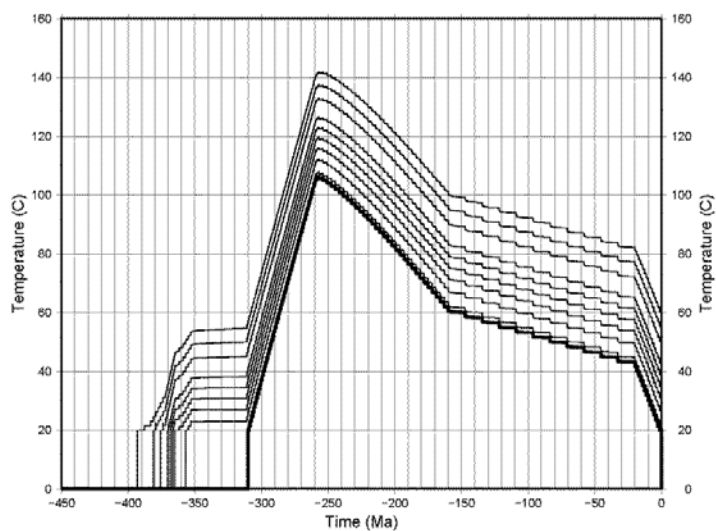
Figure 44. Temperature History, Run 47, Byler No. 24 Well. Lines indicate points monitored throughout model simulation, with the bold line indicating the youngest monitored unit. Refer to Table 19 for list of monitored points.

Table 20. Well Stratigraphy, Henninger No. 1Well.

Group or Formation	Top (ft)	Top (m)	Thickness (m)
Conemaugh	0	0	61
Allegheny	200	61	118
Pottsville	586	179	60
Mauch Chunk	782	238	60
Loyalhanna	978	298	31
Burgoon	1080	329	30
Rockwell	1180	360	130
Catskill	1605	489	553
Foreknobs	3418	1042	91
Scherr	3715	1132	745
Brallier	6158	1877	443
Harrell	7610	2320	61
Burket	7810	2380	13
Tully	7852	2393	2
Hamilton	7857	2395	205
Marcellus	8530	2600	74
Purcell	8772	2674	40
Onondaga	8902	2713	14
Huntersville Chert	8949	2728	41
Needmore Shale	9082	2768	9
Ridgeley	9112	2777	

Table 21. Model Inputs, Henninger No. 1Well.

Burial #	Burial Units	Thickness (m)	Deposited From (Ma)	Deposited To (Ma)	Burial Depth (km)	Thermal Conductivity, k (W m^{-1} K^{-1})
1	Conemaugh	61	310	306	0.05	1.995
2	Allegheny/Pottsville	177	323	310	0.2	2.343
3	Mauch Chunk/Loyalhanna	91	346	323	0.1	2.636
4	Burgoon/Rockwell	160	359	346	0.15	2.734
5	Catskill/Foreknobs	643	372	359	0.65	2.077
6	Scherr	745	376	372	0.75	2.260
7	Brallier	443	380	376	0.45	1.931
8	Harrell/Burket	74	383	380	0.05	1.630
9	Tully/Hamilton/Marcellus/Purcell	320	391	383	0.3	1.391
10	Onondaga/Huntersville/Needmore	64	408	391	0.05	1.314
11	Ridgeley through Rose Hill	800	434	408	0.8	3.69
				Total	3.55	

Table 22. Present-Day Sample Depth and Formation, Henninger No. 1 Well. Modeled temperatures in TQTec were sampled at these points at 10^4 year intervals. See Figs. 48-53 for modeled basin history.

Depth (km)	Unit
0	Conemaugh
0.05	Allegheny
0.1	Allegheny
0.15	Allegheny
0.2	Pottsville
0.55	Catskill
1.2	Scherr
1.9	Brallier
2.38	Burket
2.6	Marcellus
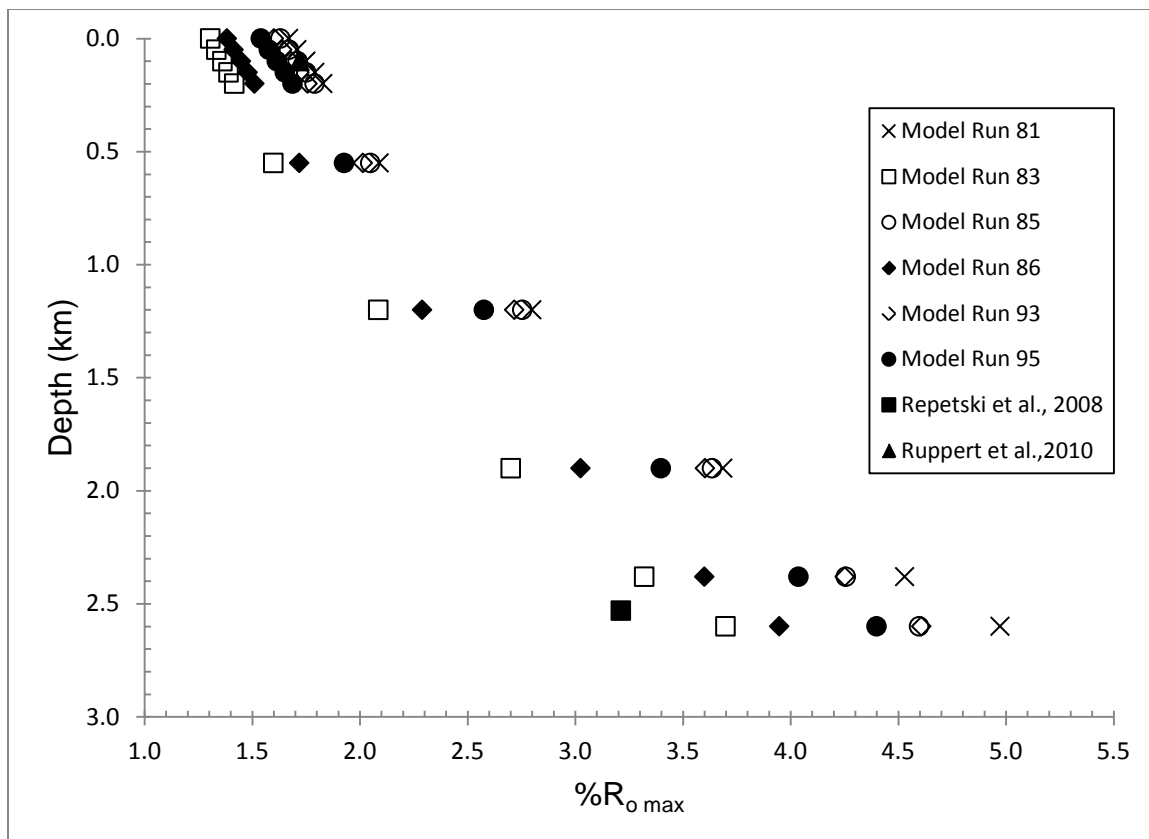
Figure 45. Observed and modeled maximum vitrinite reflectance in the Felmont Oil Corp Henninger No. 1 Well. Runs 85, 86, 93, and 95 model heating by fluid flow associated with the Alleghanian Orogeny.
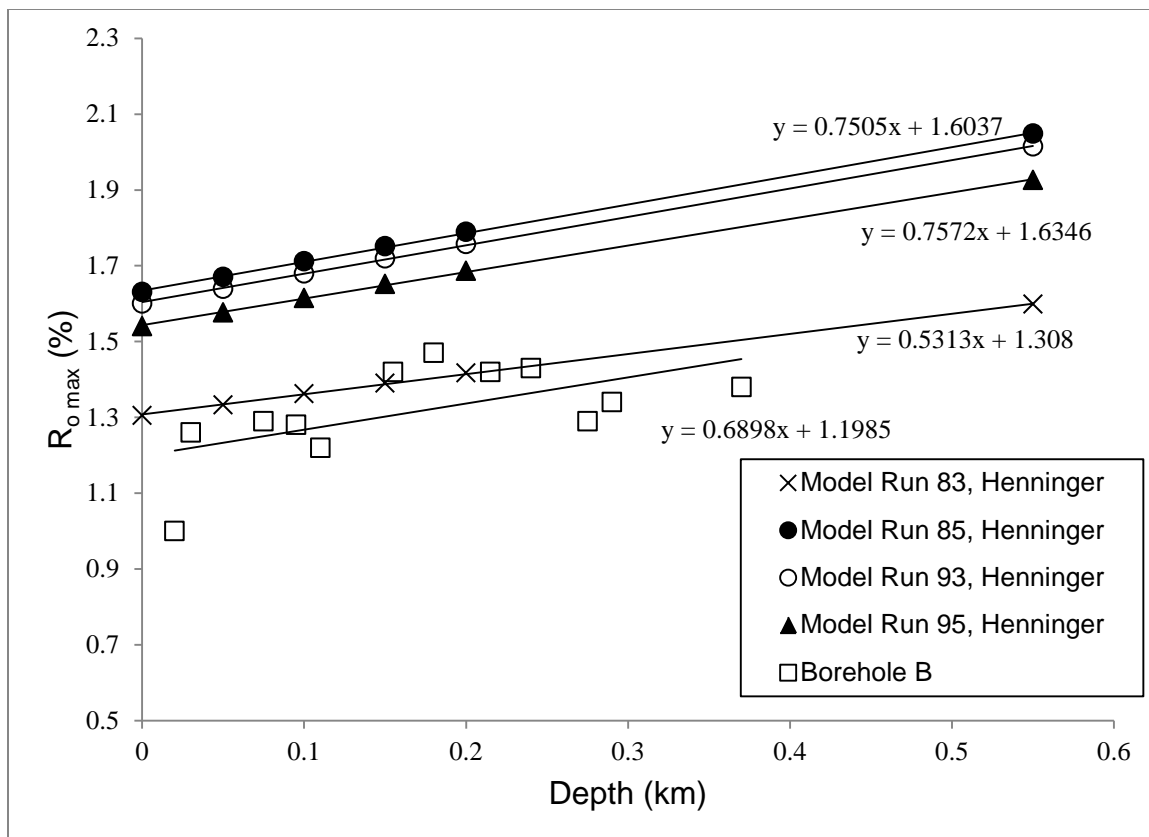
Figure 46. Reflectance Gradients of Boreholes A, B, I (Zhang and Davis, 1993), and Model Run 85, Henninger No. 1 Well.
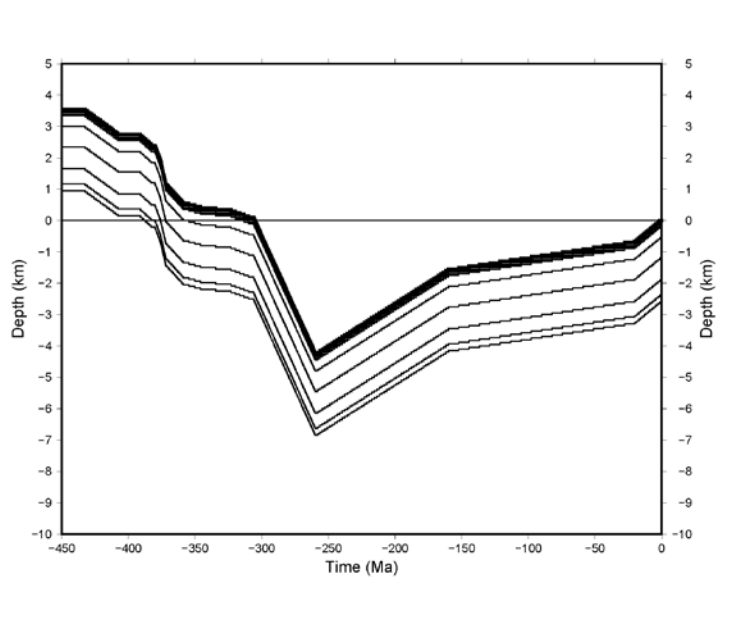
Figure 47. Burial History, Run 81, Henninger No. 1 Well. Lines indicate points monitored throughout model simulation, with the bold line indicating the youngest monitored unit. Refer to Table 22 for list of monitored points.
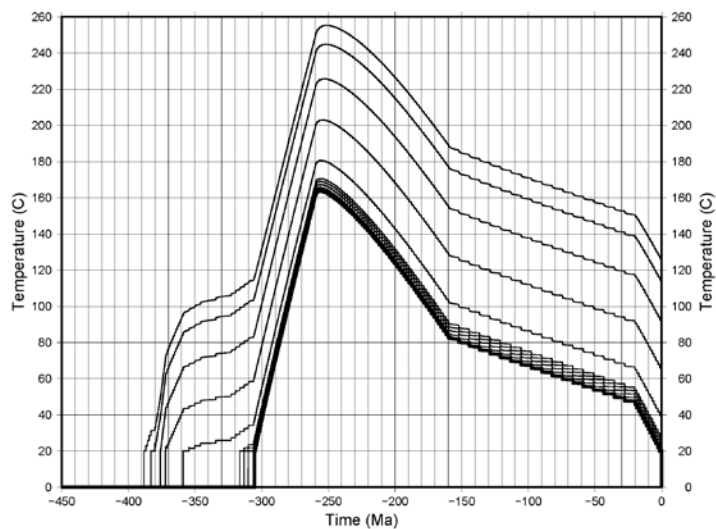
Figure 48. Temperature History, Run 81, Henninger No. 1 Well. Lines indicate points monitored throughout model simulation, with the bold line indicating the youngest monitored unit. Refer to Table 22 for list of monitored points.
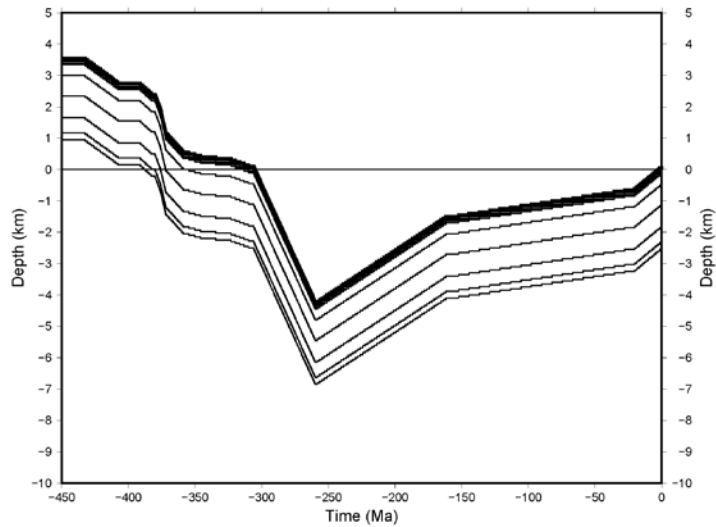
Figure 49. Burial History, Runs 83, 85, 86, Henninger No. 1 Well. Lines indicate points monitored throughout model simulation, with the bold line indicating the youngest monitored unit. Refer to Table 22 for list of monitored points.
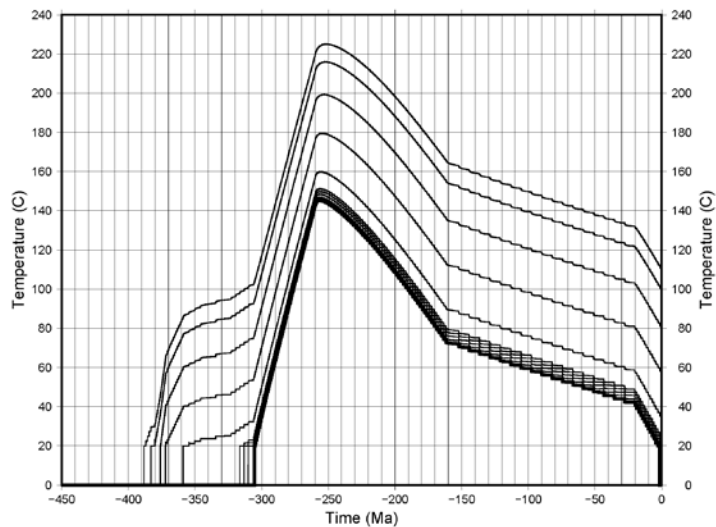
Figure 50. Temperature History, Run 83, Henninger No. 1 Well. Lines indicate points monitored throughout model simulation, with the bold line indicating the youngest monitored unit. Refer to Table 22 for list of monitored points.
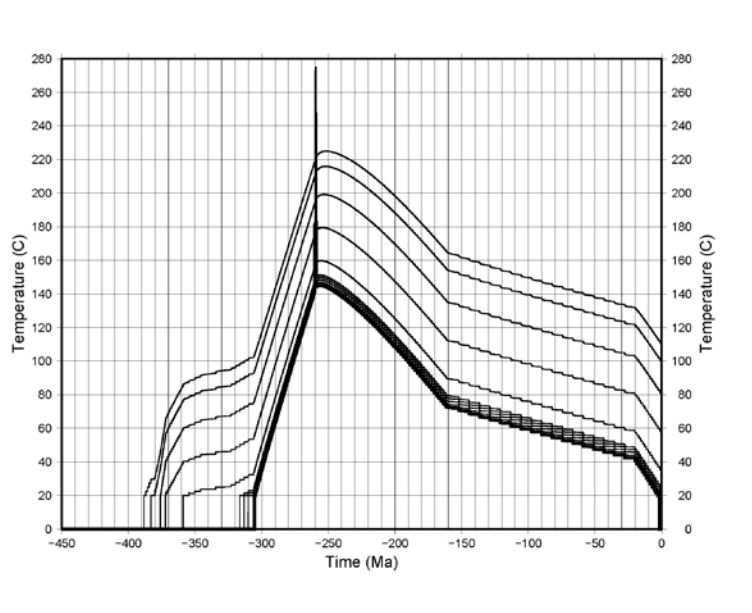
Figure 51. Temperature History, Run 85, Henninger No. 1 Well. Lines indicate points monitored throughout model simulation, with the bold line indicating the youngest monitored unit. Refer to Table 22 for list of monitored points.
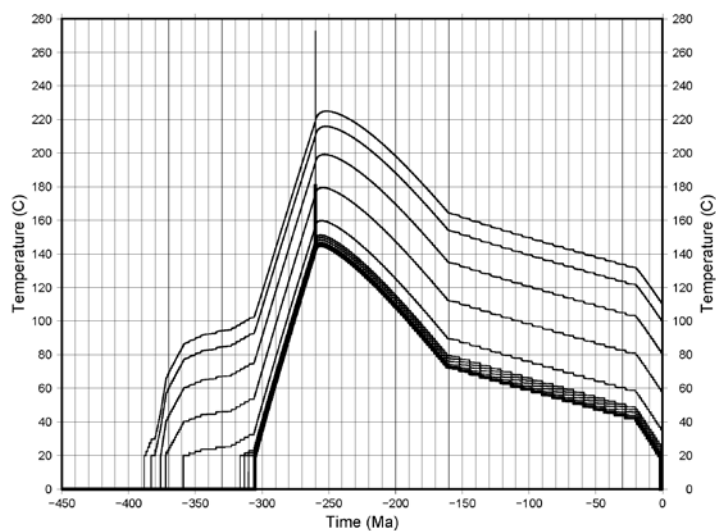
Figure 52. Temperature History, Run 86, Henninger No. 1 Well. Lines indicate points monitored throughout model simulation, with the bold line indicating the youngest monitored unit. Refer to Table 22 for list of monitored points.
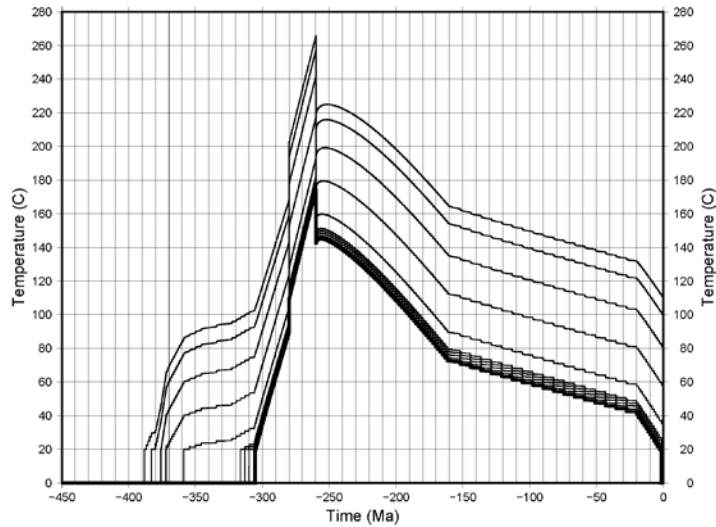
Figure 53. Temperature History, Run 93, Henninger No. 1 Well. Lines indicate points monitored throughout model simulation, with the bold line indicating the youngest monitored unit. Refer to Table 22 for list of monitored points.
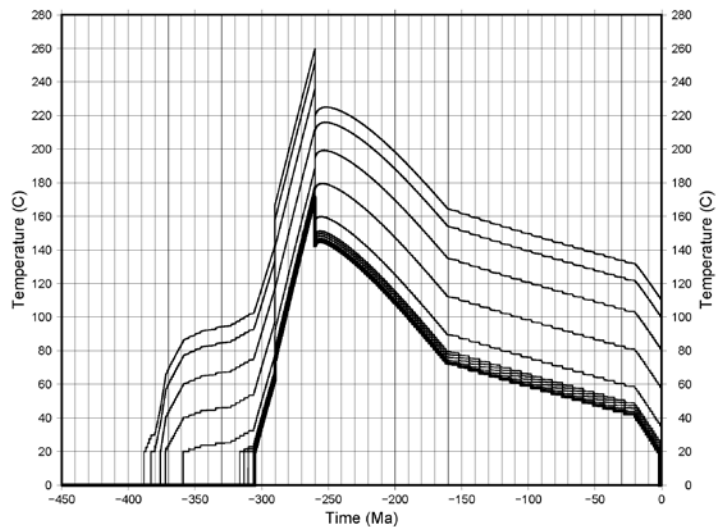
Figure 54. Temperature History, Run 95, Henninger No. 1 Well. Lines indicate points monitored throughout model simulation, with the bold line indicating the youngest monitored unit. Refer to Table 22 for list of monitored points.

Table 23. Well Stratigraphy, Leiden No. 1 Well.

Group or Formation	Top (ft)	Top (m)	Thickness (m)
Allegheny	0	0	89
Pottsville	291	89	47
Pocono	444	135	71
Huntley Mountain	677	206	99
Murrysville	1002	305	16
Devonian	1056	322	101
Catskill	1388	423	215
Chadakoin	2095	639	57
Bradford	2283	696	382
Elk	3535	1077	718
Brallier	5890	1795	201
Harrell	6550	1996	188
Burket	7166	2184	13
Tully	7210	2198	9
Hamilton	7239	2206	207
Marcellus	7918	2413	36
Onondaga	8037	2450	26
Oriskany	8121	2475	

Table 24. Model Inputs, Leiden No. 1 Well.

Burial #	Burial Units	Thickness (m)	Deposited From (Ma)	Deposited To (Ma)	Burial Depth (km)	Thermal Conductivity, k (W m^{-1} K^{-1})
1	Allegheny	89	310	307	0.1	1.8
2	Pottsville	47	323	310	0.05	2
3	Pocono/Huntley Mountain/Murrysville	187	359	347	0.2	2.7
4	Devonian/Catskill	317	363	359	0.3	2.5
5	Chadakoin	57	365	363	0.05	2.07
6	Bradford/Elk	1099	375	365	1.1	2.26
7	Brallier/Harrell/Burket	402	383	375	0.4	1.9
8	Tully/Hamilton/Marcellus/Onondaga	278	393	383	0.3	1.75
9	Ridgeley through Rose Hill	800	434	408	0.8	3.69
				Total	3.3	

Table 25. Present-Day Sample Depth and Formation, Leiden No. 1 Well. Modeled temperatures in TQTec were sampled at these points at 10^4 year intervals. See Figs. 55 and 56 for modeled basin history.

Depth (km)	Unit
0	Allegheny
0.3	Huntley Mountain
0.6	Catskill
0.9	Bradford
1.2	Elk
1.5	Elk
1.8	Brallier
2.1	Harrell
2.4	Marcellus
2.5	Oriskany
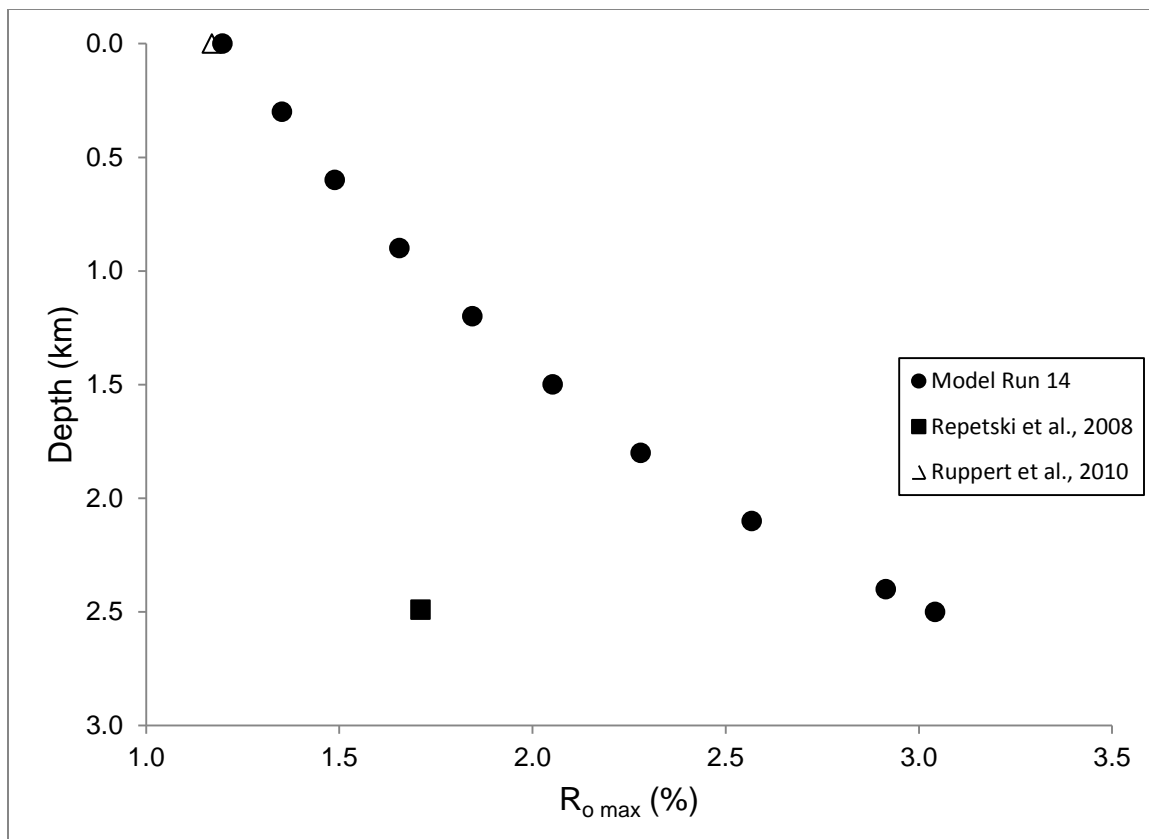
Figure 55. Observed and modeled maximum vitrinite reflectance in the Dorso LP Leiden No. 1 Well.
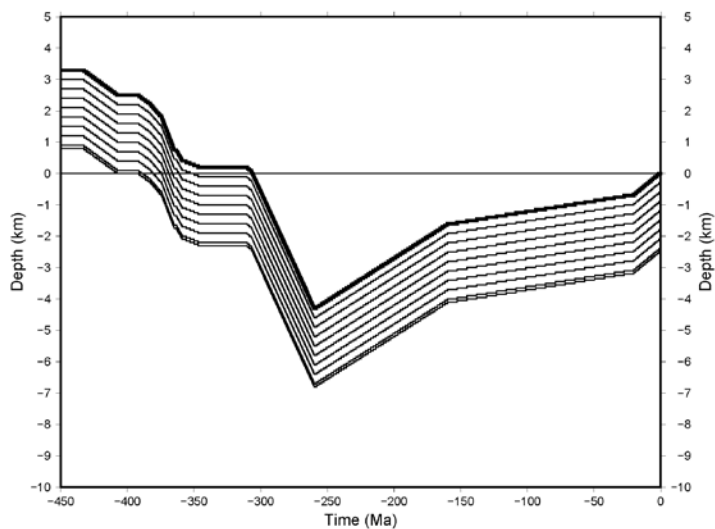
Figure 56. Burial History, Run 14, Leiden No. 1 Well. Lines indicate points monitored throughout model simulation, with the bold line indicating the youngest monitored unit. Refer to Table 25 for list of monitored points.
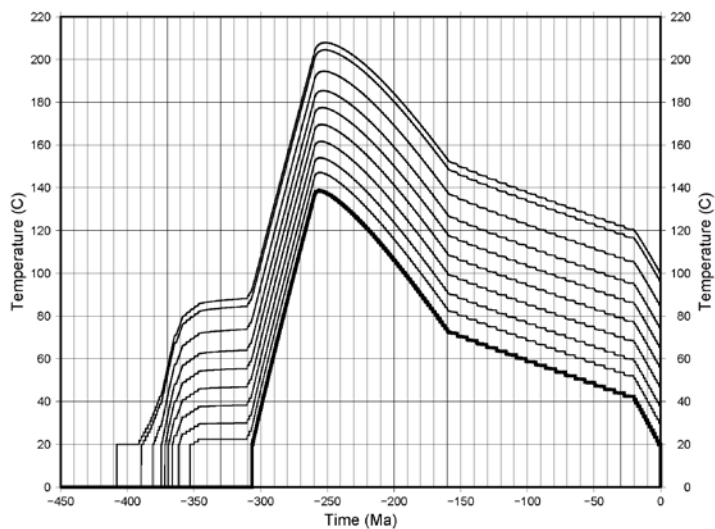
Figure 57. Temperature History, Run 14, Leiden No. 1 Well. Lines indicate points monitored throughout model simulation, with the bold line indicating the youngest monitored unit. Refer to Table 25 for list of monitored points.

Table 26. Well Stratigraphy, Bailey No. 1 Well.

Group or Formation	Top (ft)	Top (m)	Thickness (m)
Pottsville	0	0	138
Patton (Pocono)	454	138	142
Devonian (Conewango)	920	280	76
Catskill	1168	356	230
Chadakoin	1923	586	65
Bradford	2136	651	366
Elk	3338	1017	749
Sonyea	5795	1766	96
Middlesex	6110	1862	66
Genesee	6325	1928	89
Burket	6617	2017	19
Tully	6680	2036	56
Hamilton	6864	2092	158
Marcellus	7383	2250	27
Onondaga	7470	2277	19
Oriskany	7532	2296	

Table 27. Model Inputs, Bailey No. 1 Well.

Burial #	Burial Units	Thickness (m)	Deposited From (Ma)	Deposited To (Ma)	Burial Depth (km)	Thermal Conductivity, k (W m^{-1} K^{-1})
1	Pottsville	138	323	310	0.15	2
2	Pocono	142	359	347	0.15	2.7
3	Devonian/Catskill	306	363	359	0.3	2.5
4	Chadakoin	65	365	363	0.05	2.07
5	Bradford/Elk	1115	378	365	1.1	2.26
6	Sonyea/Middlesex/Genesee/Burket	270	383	378	0.3	1.9
7	Tully/Hamilton/Marcellus/Onondaga	260	393	383	0.25	1.75
8	Ridgeley through Rose Hill	800	434	408	0.8	3.69
				Total	3.1	

Table 28. Present-Day Sample Depth and Formation, COP Tract 285 No. 1 Well. Modeled temperatures in TQTec were sampled at these points at 10^4 year intervals. See Figs. 59 and 60 for modeled basin history.

-0.1	Allegheny (projected)
0.3	Catskill
0.7	Bradford
1.1	Elk
1.5	Elk
1.9	Middlesex
2.3	Oriskany
2.7	Dolomites
3.1	Dolomites
3.55	Dolomites
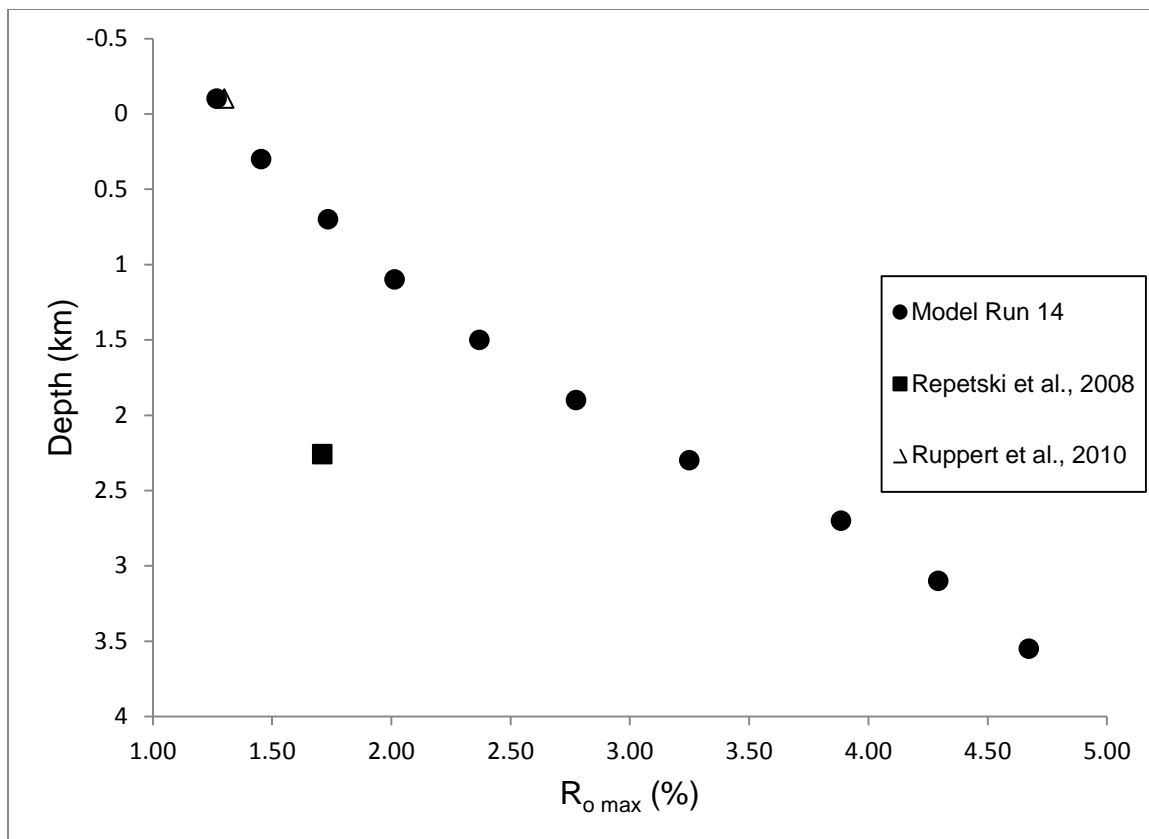
Figure 58. Observed and modeled maximum vitrinite reflectance in the Fairman Drilling Co. Bailey No. 1 Well.
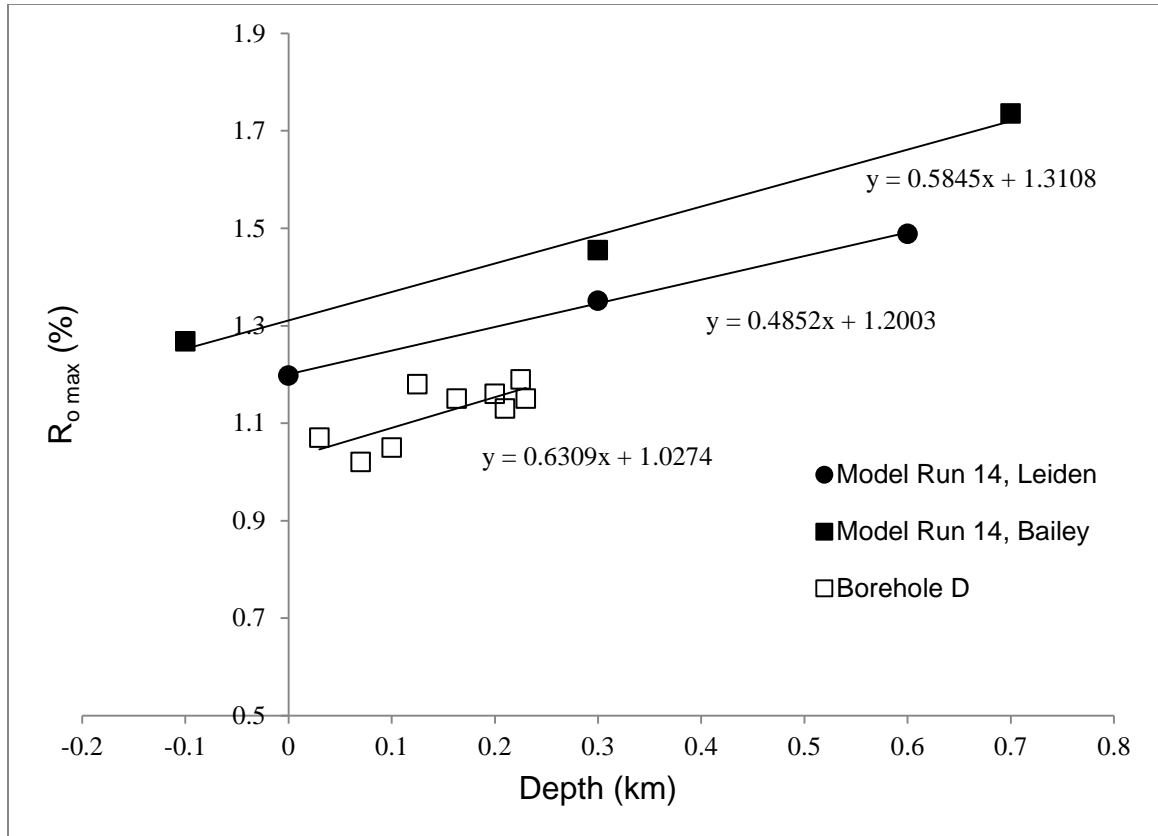
Figure 59. Reflectance Gradients of Borehole D (Zhang and Davis, 1993), Model Run 14, Leiden No. 1, and Model Run 14, Bailey No. 1 Well.
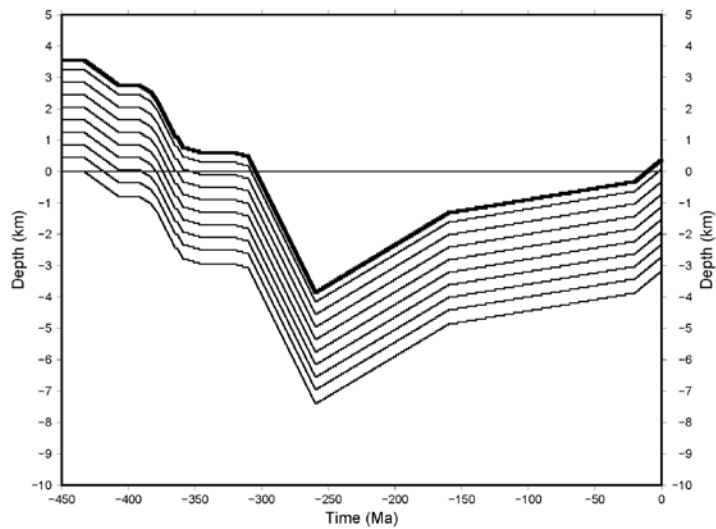
Figure 60. Burial History, Run 14, Bailey No. 1 Well. Lines indicate points monitored throughout model simulation, with the bold line indicating the youngest monitored unit. Refer to Table 28 for list of monitored points.
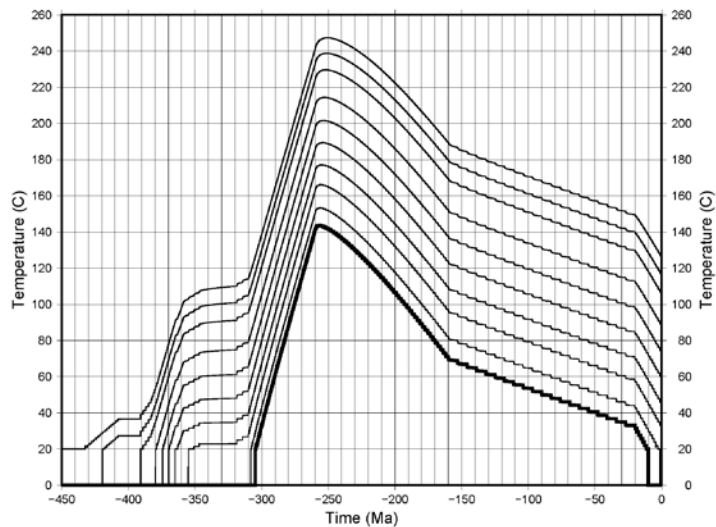
Figure 61. Temperature History, Run 14, Bailey No. 1 Well. Lines indicate points monitored throughout model simulation, with the bold line indicating the youngest monitored unit. Refer to Table 28 for list of monitored points.

MODEL SENSITIVITY

It is useful to examine the sensitivity of the model to various input parameters. Twenty-eight experiments are performed on the Dewey No. 1 (Tioga County) model to assess the effects of five parameters on the model predictions of vitrinite reflectance and apatite fission track ages. The parameters examined for model sensitivity are surface temperature, surface heat flow, overburden (from maximum at the end of the Alleghanian Orogeny to present-day), erosion rate following maximum burial from 260 Ma – 160 Ma, and the thermal conductivity of the Alleghanian overburden. Plots of maximum vitrinite reflectance versus depth and tables of apatite fission track ages are compared for each parameter. Adjusting each parameter affects both reflectance and fission track ages significantly.

Increasing the surface temperature (Fig. 62), increasing the overburden (Fig. 64), and decreasing the erosion rate (Fig. 65) each have the effect of primarily shifting the reflectance gradient to the right. Increasing the heat flow (Fig. 63) and decreasing the thermal conductivity of the overburden (Fig. 66) each have the effect of increasing the reflectance gradient with depth. Changing each of these parameters for the duration of the model simulation also changes the predicted apatite fission track ages (Tables 29 - 33). Each of these parameters is shown to have a significant effect on model predictions of vitrinite reflectance and apatite fission track age. Although reasonable assumptions are made for surface temperature (20 ºC) and thermal conductivity of overburden (2.1 W

m^{-1} K^{-1}), interpreted estimates of Alleghanian overburden and surface heat flow across the basin would change with different assumptions.

Table 29. Effect of changing surface temperature (T$_s$) on apatite fission track age of Catskill, Fm. (present-day surface). Ages decrease with increasing surface temperature.

Surface Temperature, T$_s$ (ºC)	Apatite Fission Track Age, Catskill Fm. (Ma)
10	178.83
15	167.10
20	153.71
25	138.88
30	123.09
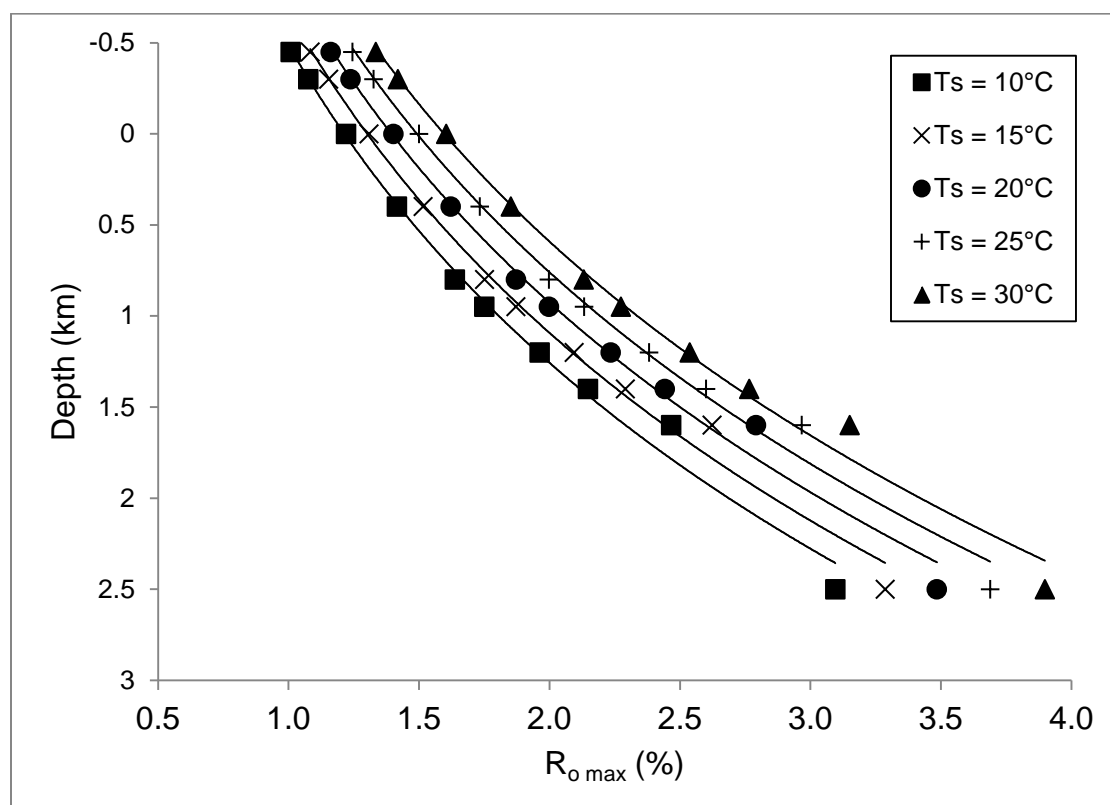
Figure 62. Effect of changing surface temperature (T$_s$) on vitrinite reflectance with depth. The reflectance gradient shifts to the right with increasing surface temperature.

Table 30. Effect of heat flow (q) on apatite fission track age of Catskill, Fm. (present-day surface). Ages decrease with increasing heat flow.

Heat Flow q (mW m^{-2})	Apatite Fission Track Age, Catskill Fm. (Ma)
60	170.50
64	161.72
68	153.71
72	146.17
76	138.74
80	131.55
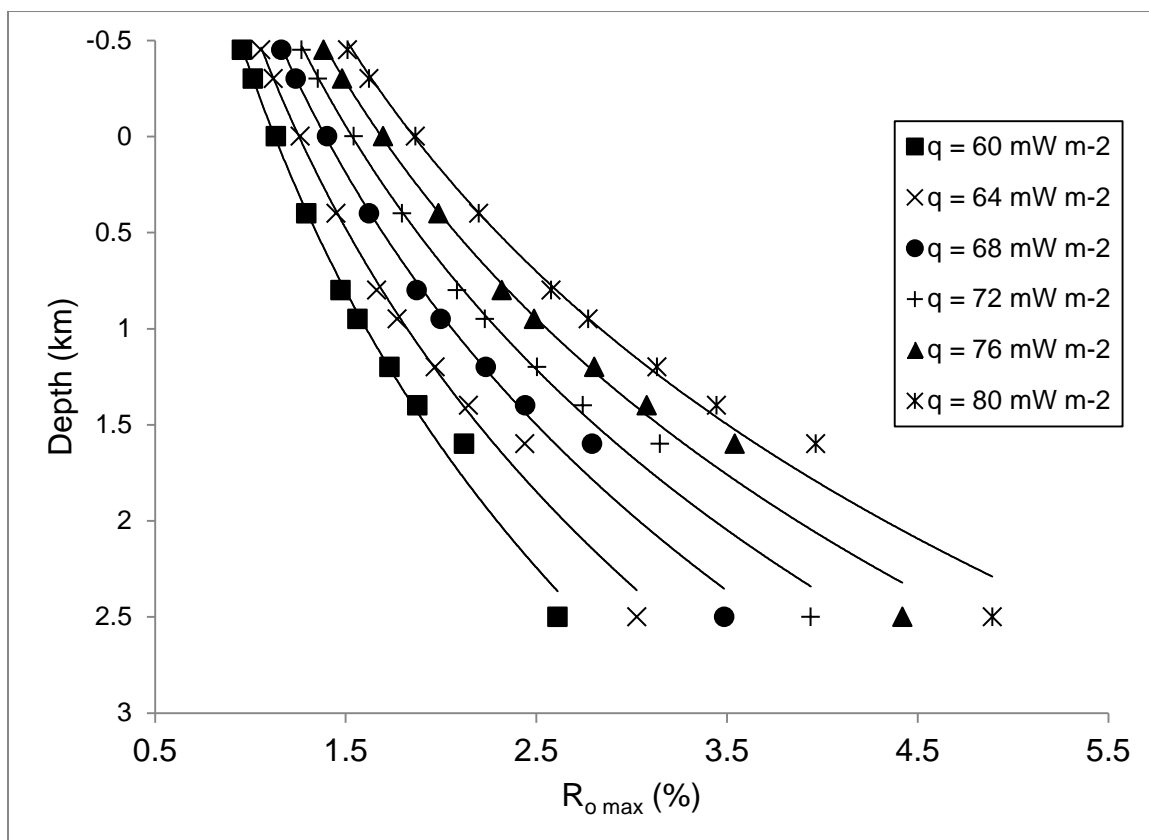
Figure 63. Effect of changing heat flow (q) on vitrinite reflectance with depth. The reflectance gradient increases with increasing heat flow.

Table 31. Effect of changing Alleghanian overburden on apatite fission track age of Catskill, Fm. (present-day surface). Ages decrease with increasing overburden.

Overburden (km)	Apatite Fission Track Age, Catskill Fm. (Ma)
4.0	191.55
4.25	174.66
4.5	153.71
4.75	129.14
5.0	103.28
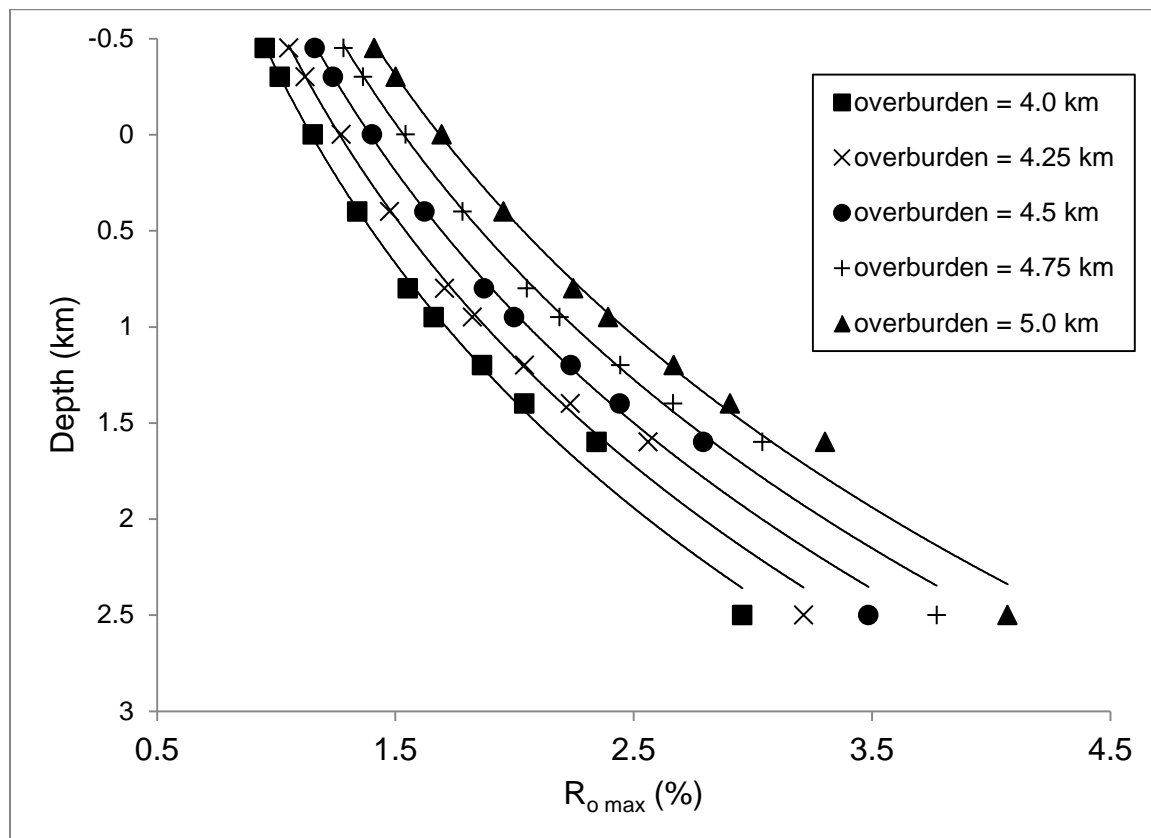
Figure 64. Effect of changing Alleghanian overburden on vitrinite reflectance with depth. The reflectance gradient shifts to the right with increasing overburden.

Table 32. Effect of changing erosion rate from 260 -160 Ma on apatite fission track age of Catskill, Fm. (present-day surface). Ages increase with increasing erosion rate.

Erosion Rate (m myr^{-1})	Apatite Fission Track Age, Catskill Fm. (Ma)
5	48.27
15	82.17
25	138.91
35	194.73
45	221.10
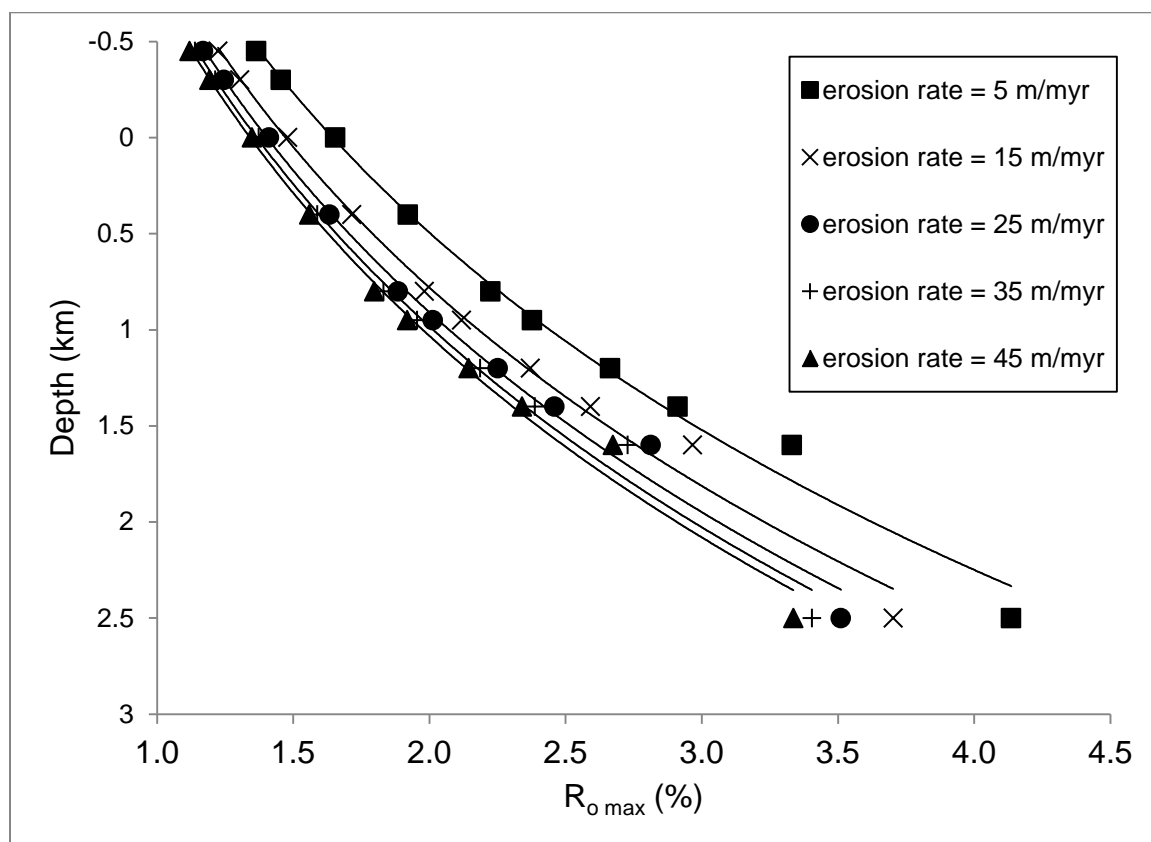
Figure 65. Effect of changing erosion rate from 260 – 160 Ma on vitrinite reflectance with depth. The reflectance gradient decreases with increasing erosion rate.

Table 33. Effect of changing erosion rate from 260 -160 Ma on apatite fission track age of Catskill, Fm. (present-day surface). Ages increase with increasing erosion rate.

Thermal Conductivity, k (W m^{-1} K^{-1})	Apatite Fission Track Age, Catskill Fm. (Ma)
1.4	96.10
1.8	131.38
2.1	153.71
2.4	171.84
2.7	186.88
3.0	200.37
3.3	222.49
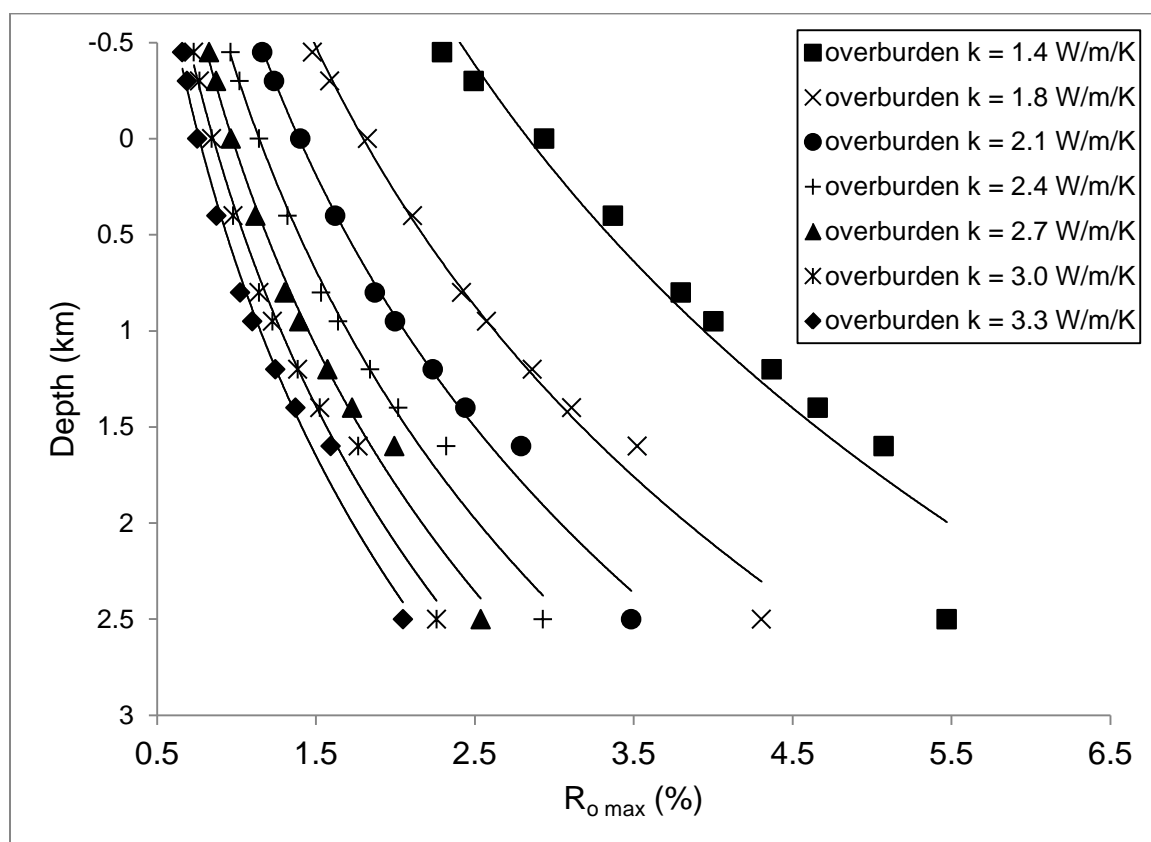
Figure 66. Effect of changing the thermal conductivity of the Alleghanian overburden on vitrinite reflectance with depth. The reflectance gradient increases with decreasing thermal conductivity.

DISCUSSION

Maturity Trends in the Appalachian Plateau

Figures 67 and 68 respectively summarize the maximum Permian burial depths of the Devonian-Carboniferous boundary and the heat flows at each site as estimated by the 1-D thermal modeling. To be consistent with the critically-tapered wedge model the maximum burial depths should decrease monotonically northwestward. This is generally the case (Fig. 67), but there are three anomalously shallow burial predictions for the Conner, Martin, and Byler wells in Washington, Armstrong, and Lawrence Counties, respectively. Although the maximum burial depths can be expected to decline towards the foreland, the model predictions require more than a kilometer of decrease over 75 km horizontally. The heat flows that best fit the thermal maturity data range between 67 and 70 mW m^{-2}, except for two regions (Fig. 68, grey shaded areas). These regions are the areas of higher coal rank (Figs. 2-6) previously noted by other researchers.
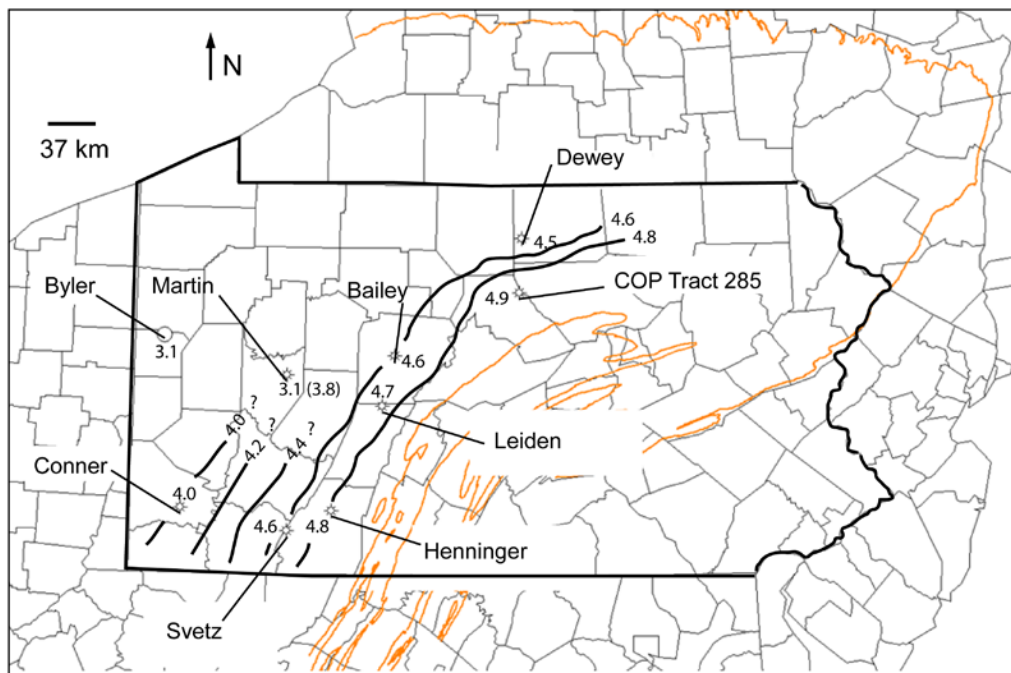
Figure 67. Best-fit Alleghanian burial (Missisippian through Permian) depths predicted by the 1-D thermal models of this study. Burial generally decreases from east to west and supports the theory of the critically tapered wedge, with the exception of the Martin well in Armstrong County.
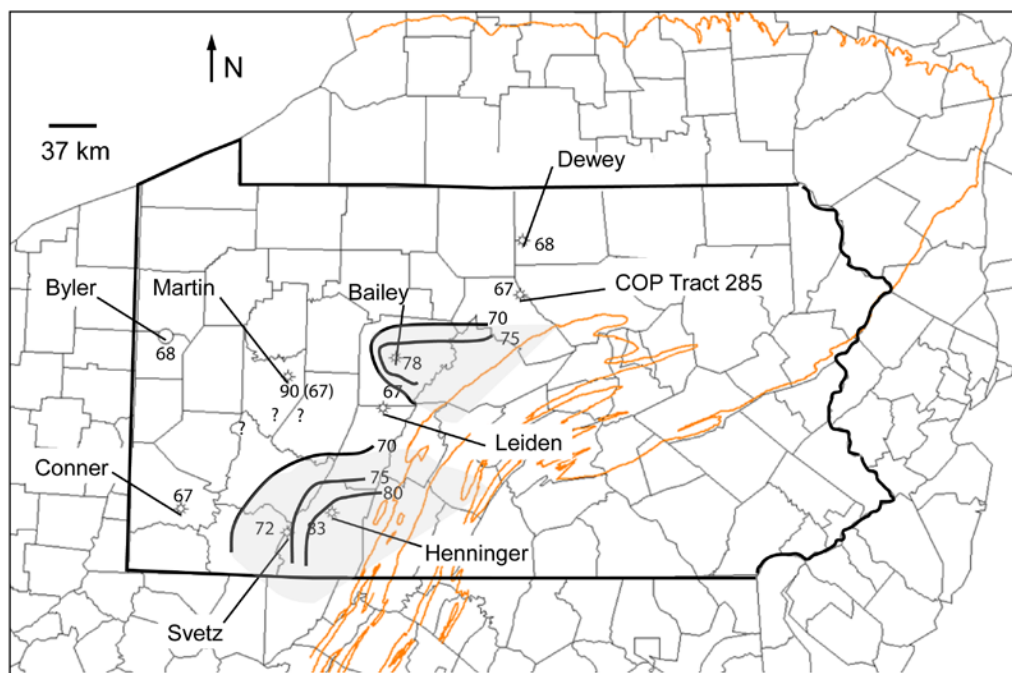
Figure 68. Best-fit burial heat flows from 450 Ma to Present (without modeling of heating by fluids) predicted by the 1-D thermal models of this study. Note the rapid increase of heat flow over the two thermal salients.

The thermal maturity observations in north-central Pennsylvania (Dewey and COP Tract 285) can be matched by a 1-D model assuming a value of maximum burial that is consistent with a critically tapered wedge and assuming a basal heat flow consistent with the flow expected for Grenvillian crust. The four wells to the southwest near the Allegheny structural front (Bailey, Leiden, Henninger, and Svetz) require varying heat flows to match their respective coal maturity data and to match the reflectance gradients of Zhang and Davis (Zhang and Davis, 1993). The westernmost wells (Byler and Conner) match observed data with the same heat flow as the north central wells. The Martin well lies to the west of the area of the basin suspected to have had the most influence of heating by fluid flow. However, this well required the highest heat flow of all the modeled wells to match the observed data. If the reflectance measurements are accurate, a significant heat perturbation would likely be needed to produce the high reflectance gradient in this well.

What is the origin of the two promontories of higher thermal maturity? It is theoretically possible that the two regions were buried more deeply, but the 1-D modeling results presented here do not support this idea (Fig. 67). Model results suggest that the two promontories reflect higher heat flows. These could be higher basal heat flows from the crust, but that is highly unlikely given the localized nature of the promontories. Therefore we test the hypothesis that hot brines originating to the east and deeper in the

basin, flowed westward through localized Upper Devonian sandstone aquifers during and immediately after the Alleghenian Orogeny to provide an additional heat source in the areas of the two promontories.

Heating by Fluids

The distribution of Upper Devonian fluvial systems (Figs. 69 and 70) suggests that the proportion of sandstone varies along strike, with the highest proportion being under or at least near the thermal maturity promontories. Sandier facies resulting from deposition of the Catskill delta could have provided preferred conduits for hot brines flowing from the east.
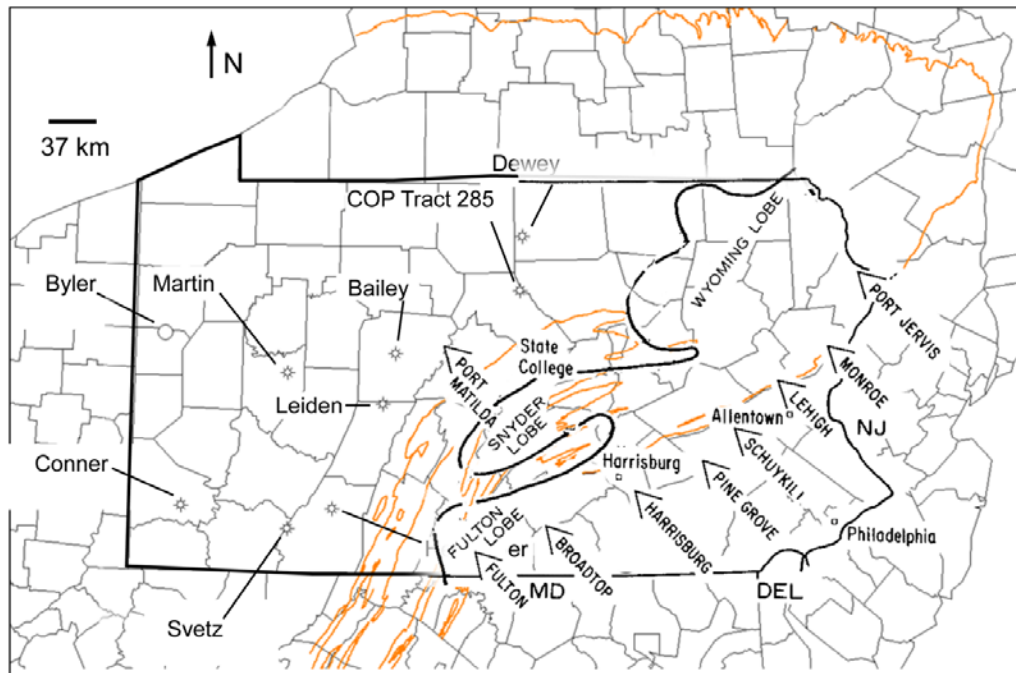
Figure 69. Location of deltas proposed by various authors for the Catskill prograding shoreline. Solid line enclosing the Fulton, Snyder, and Wyoming lobes defined by Willard (1939) based on paleontological data. Arrows denote sediment input centers; eastern arrows indicate earliest Late Devonian fluvial depocenters (Sevon et al. 1978); western arrows denote delta depocenters of Rahmanian (1979).
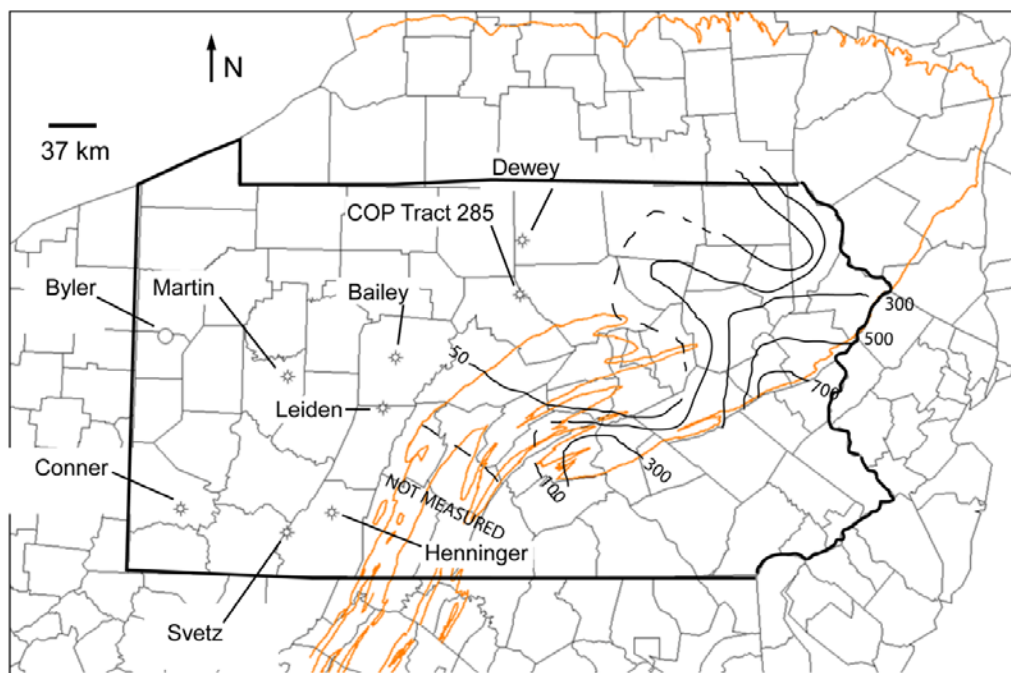
Figure 70. Isopach map of Magnafacies D of the Catskill Formation (in meters) (redrawn from Smith and Rose, 1985). Magnafacies D is defined as repeated fining-upwards fluvial sequences of conglomerate-sandstone-shale or sandstone-shale. Note that the two northern lobes corroborate the Snyder and Wyoming lobes of Willard (1939). The Fulton lobe lies outside the study area of Smith and Rose.

Without modeling the effects of heating by fluid flow, the Henninger No. 1 well in Somerset county requires a higher average heat flow (83 mW m^{-2}) than the Svetz No. 1 well (72 mW m^{-2}) ~ 20 km to the southwest, also in Somerset county. This variation in surface heat flow is likely too high at this scale, unless there is a large variation in crustal heat production in the WPAB. The Henninger well is assumed to have had a slightly

higher burial of 4.8 km of Alleghanian sediments as opposed to the 4.6 km that fits the Svetz well. If the amount of burial were the same as the Svetz well, an even higher heat flow would be needed to fit the data. A greater amount of burial would also fit the coal reflected data, but how much is necessary? An additional 0.2 km of sediment is reasonable over a lateral span of 35 km (based on critically-tapered wedge theory), but an amount of 1 km (required to increase maximum reflectance by 0.5%, based on sensitivity analyses) or greater additional sediment is probably unreasonable given the low-relief depositional environments (alluvial plain, deltaic, lacustrine) in the Permian. Therefore a transient perturbation of higher heat flow is required to bring the Pennsylvanian coals near the Henninger well to their present-day level of maturity. If this transient thermal gradient resulted from lateral fluid flow, is a large difference in maturity over a span of 35 km logical?

A comparison of lateral versus vertical heat flow indicates that these maturity patterns could have been produced by lateral fluid flow. Heat flows from regions of warmer temperatures to regions of cooler temperatures, and it will preferentially flow along higher thermal gradients. According to Fourier's Law, if an average conductivity of rocks in the subsurface at the location of the Svetz and Henninger wells of 2.6 W m^{-1} K^{-1} is assumed, the vertical thermal gradient, dT/dz will be approximately 28 °C km^{-1}. The model predicted difference in temperatures between the Svetz and Henninger wells during the period of fluid flow will be 40 – 50 °C for the Allegheny Gp. through the

Marcellus Fm., and the distance between them is 35 km. Thus the horizontal thermal gradient, dT/dx will be approximately 1.1 °C km^{-1}. It is logical that most of the heat will travel in the vertical direction along the steeper thermal gradient and result in localized anomalies of thermal maturity. What other evidence exists to support the role of fluids in forming these anomalies?

Modeling predicts that fluids could have reached temperatures greater than 250 °C (Figs. 51 - 54). At these temperatures, there should be diagenetic evidence where hot fluids had passed through aquifers in the Upper Devonian. In the Anthracite Basin to the east of the WPAB, heating by fluid flow has also been suggested to have altered the coal rank there (Daniels and Altaner, 1990; Daniels et al., 1990). Authigenic clay reactions formed pyrophyllite and NH_4-rich illite in shales and coals of the Upper Pennsylvanian Llewellyn Fm. (Daniels and Altaner, 1990). These reactions are evidence of temperatures greater than 250 °C in Pennsylvanian rocks in the Anthracite Basin. It is possible that these reactions also occurred in the Upper Devonian in the WPAB.

CONCLUSIONS

The results of modeling in this study have shown that an increase in the thermal gradient in the Henninger well for a period of at least 1 million years from 260 – 259 Ma will reproduce the observed level of maturity at the present day surface. This transient perturbation in the thermal gradient had a significant effect on maturity indicators, because it occurred around the same time as maximum burial of the basin at the end of the Alleghanian Orogeny. If one assumes that the background heat flow was similar to the Svetz well (72 mW m^{-2}), the model predicted temperatures (Figs. 51 – 52) during the increased thermal gradient are 40-50 ºC greater for the units of interest than that expected from normal heat flow by conduction. If one assumes an average thermal gradient of 25 ºC/km, the hot fluids could be produced at a minimum depth of 2 km below the affected Devonian sediments. The Ordovician Bald Eagle Fm. is one possible candidate that could have transmitted hotter fluids along thrust faults to the east into aquifer units in the Upper Devonian. Modeling indicates that increasing the duration of the fluid flow to 20 – 30 myr. allows the increased thermal gradient to be reduced such that maximum temperatures are 35 – 40 ºC (Figs. 53 - 54) above the baseline case (Fig. 50).

The thermal maturity of gas shales in the Devonian in Pennsylvania varies across the basin, generally increasing from west to east. However, these model predictions indicate that maturity may be even higher than some maps indicate (Repetski et al., 2008;

Wrightstone, 2009), particularly in areas that underlie the promontories of high coal maturity in southwest and west-central Pennsylvania. In regions with many recent gas shale wells the wet gas/ dry gas boundary in the WPAB is probably well constrained. The value of these modeling results are to show that this method can be applied to future exploration efforts, and that the model can be used to show why northern Somerset and southern Cambria counties remains mostly undeveloped (Fig. 65). Heating by fluid flow through preferred pathways in Upper Devonian aquifers likely created a region that is over-mature and potentially unproductive. Few wells have been drilled there, and the last well to be drilled was in 2011 (Fig. 71).

Applying this modeling technique to the exploration of future basins where basinal fluid flow is suspected can reduce uncertainty in risk assessments. In the Appalachian basin, these fluids appear to have flowed at or near the time of maximum burial. The fluids had a significant effect on the maturity of the coals and gas shales by increasing maximum temperatures at this critical point in the time-temperature history of the basin. In future basin exploration, it may be possible to identify areas previously thought to be immature as potentially mature if there is any indication that basin-scale fluid flow. In the WPAB, the acquisition of more paleo-temperature data (especially with depth) will shed more light on the processes examined in this study.
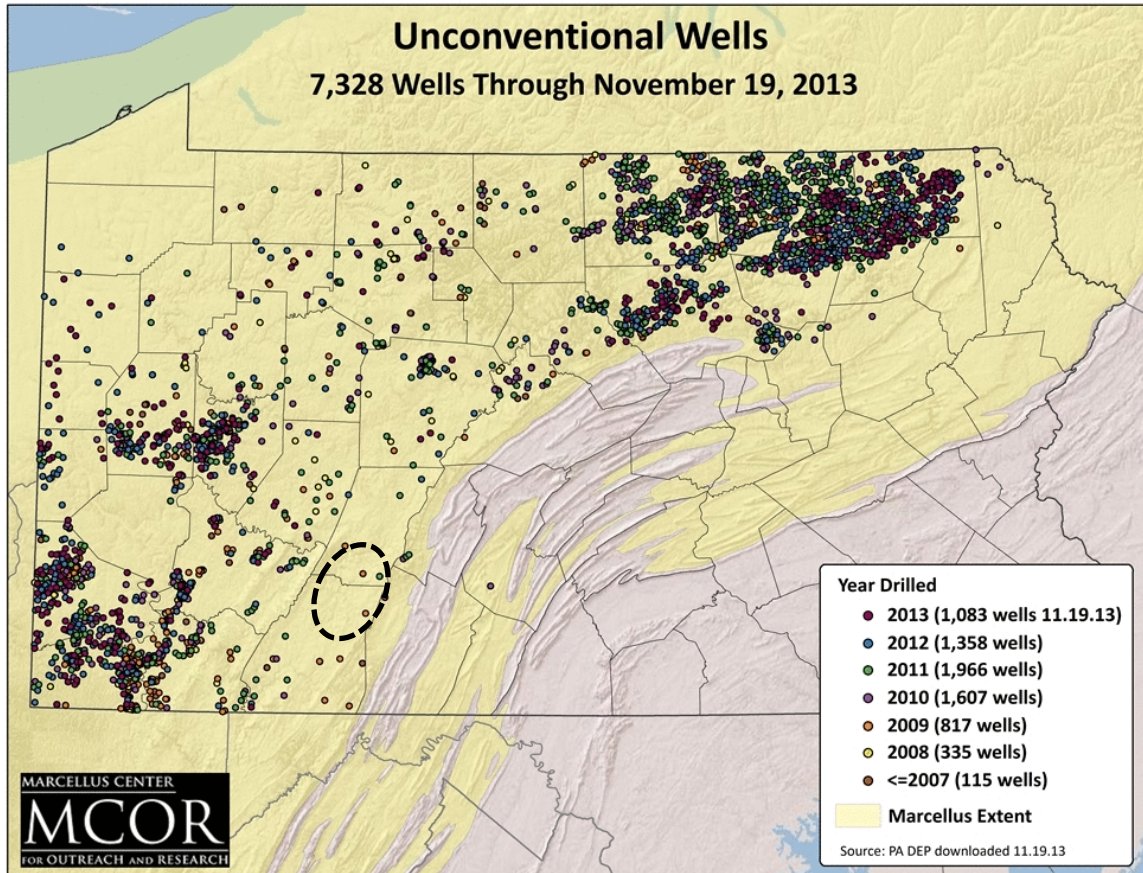
Figure 71. Unconventional wells drilled in Pennsylvania from 2007 – 2013. Relatively few wells have been drilled in the area enclosed by the dashed circle. (MCOR, 2013).

REFERENCES

Araujo, C. V., A. G. Borrego, B. Cardott, R. B. A. das Chagas, D. Flores, P. Gonçalves, P. C. Hackley, J. C. Hower, M. L. Kern, J. Kus, M. Mastalerz, J. G. Mendonça Filho, J. de Oliveira Mendonça, T. R. Menezes, J. Newman, I. Suarez-Ruiz, F. S. da Silva, and I. V. de Souza, 2014, Petrographic maturity parameters of a Devonian shale maturation series, Appalachian Basin, USA. ICCP Thermal Indices Working Group interlaboratory exercise: International Journal of Coal Geology, v. 130, p. 89-101.

Barker, C. E., 2000, A paleolatitude approach to assessing surface temperature history for use in burial heating models: International Journal of Coal Geology, v. 43, p. 121-135.

Beardsmore, G. R., and J. P. Cull, 2001, Crustal heat flow: a guide to measurement and modelling, Cambridge University Press.

Beaumont, C., G. Quinlan, and J. Hamilton, 1987, The Alleghanian Orogeny and its Relationship to the Evolution of the Eastern Interior, North America, *in* C. Beaumont, and A. J. Tankard, eds., Sedimentary Basins and Basin-Forming Mechanisms, v. Memoir 12: Calgary, Alberta, Canadian Society of Petroleum Geologists, p. 425-445.

Beaumont, C., G. Quinlan, and J. Hamilton, 1988, Orogeny and stratigraphy: Numerical models of the Paleozoic in the eastern interior of North America: Tectonics (Washington, D.C.), v. 7, p. 389-416.

Berg, T. M., M. K. McInerney, J. H. Way, and D. B. MacLachlan, 1983, Stratigraphic Correlation Chart of Pennsylvania, Pennsylvania Geological Survey General Geology Report 75.

Blackmer, G. C., G. I. Omar, and D. P. Gold, 1994, Post-Alleghanian unroofing history of the Appalachian Basin, Pennsylvania, from apatite fission track analysis and thermal models: Tectonics (Washington, D.C.), v. 13, p. 1259-1276.

Blackwell, D. D., and M. Richards, 2004, Geothermal Map of North America (1:6,500,000): American Association of Petroleum Geologists.

Blackwell, D. D., M. Richards, Z. Frone, J. Batir, A. Ruzo, R. Dingwall, and M. Williams, 2011, Temperature-At-Depth Maps for the Conterminous U.S. and Geothermal Resource Estimates: Geothermal Resources Council Transactions, v. 35, p. 1545-1550.

Burnham, A. K., and J. J. Sweeney, 1989, A chemical kinetic model of vitrinite maturation and reflectance: Geochimica et Cosmochimica Acta, v. 53, p. 2649-2657.

Carter, K. M., 2007, Subsurface rock correlation diagram, oil and gas producing regions of Pennsylvania, Open-File Report OFOG 07-01.1, Pennsylvania Geological Survey.

Cercone, K. R., D. Deming, and H. N. Pollack, 1996, Insulating effect of coals and black shales in the Appalachian Basin, Western Pennsylvania: Organic Geochemistry, v. 24, p. 243-249.

Chyi, L. L., R. G. Barnett, A. E. Burford, T. J. Quick, and R. J. Gray, 1987, Coalification patterns of the Pittsburgh coal: their origin and bearing on hydrocarbon maturation: International journal of coal geology, v. 7, p. 69-83.

Dahlen, F. A., and J. Suppe, 1988, Mechanics, growth, and erosion of mountain belts: Geological Society of America Special Papers, v. 218, p. 161-178.

Daniels, E. J., and S. P. Altaner, 1990, Clay mineral authigenesis in coal and shale from the Anthracite region, Pennsylvania: The American mineralogist, v. 75, p. 825-839.

Daniels, E. J., S. P. Altaner, S. Marshak, and Eggleston, 1990, Hydrothermal alteration in anthracite from eastern Pennsylvania: Implications for mechanisms of anthracite formation: Geology (Boulder), v. 18, p. 247-250.

Dow, W. G., 1977, Kerogen studies and geological interpretations: Journal of geochemical exploration, v. 7, p. 79-99.

Edmunds, W. E., 2002, Coal in Pennsylvania (2nd ed.), Educational Series 7, Pennsylvania Geological Survey, p. 28.

England, T. D. J., and R. M. Bustin, 1986, Thermal maturation of the western Canadian sedimentary basin south of the Red Deer River; I, Alberta plains: Bulletin of Canadian Petroleum Geology, v. 34, p. 71-90.

Epstein, A. G., J. B. Epstein, and L. D. Harris, 1977, Conodont color alteration: an index to organic metamorphism.

Evans, M. A., 1995, Fluid inclusions in veins from the Middle Devonian shales: A record of deformation conditions and fluid evolution in the Appalachian Plateau: Geological Society of America bulletin, v. 107, p. 0327-339.

Garven, G., 1995, Continental-scale groundwater flow and geologic processes: Annual review of earth and planetary sciences, v. 23, p. 89-117.

Garven, G., and R. A. Freeze, 1984a, Theoretical analysis of the role of groundwater flow in the genesis of stratabound ore deposits; 1. Mathematical and numerical model: American journal of science (1880), v. 284, p. 1085-1124.

Garven, G., and R. A. Freeze, 1984b, Theoretical analysis of the role of groundwater flow in the genesis of stratabound ore deposits; 2. Quantitative results: American Journal of Science, v. 284, p. 1125-1174.

Garven, G., S. Ge, M. A. Person, and D. A. Sverjensky, 1993, Genesis of stratabound ore deposits in the midcontinent basin of North America; 1. The role of regional groundwater flow: American Journal of Science, v. 293, p. 497-568.

Ge, S., and G. Garven, 1992, Hydromechanical modeling of tectonically driven groundwater flow with application to the Arkoma Foreland Basin: Journal of Geophysical Research: Solid Earth, v. 97, p. 9119-9144.

Gerlach, J. B., and K. R. Cercone, 1993, Former Carboniferous overburden in the northern Appalachian Basin - a reconstruction based on vitrinite reflectance: Organic Geochemistry, v. 20, p. 223-232.

Glick, D. C., and A. Davis, 1991, Operation and composition of the Penn State coal sample bank and data base: Organic Geochemistry, v. 17, p. 421-430.

Green, P. F., I. R. Duddy, A. J. W. Gleadow, P. R. Tingate, and G. M. Laslett, 1986, Thermal annealing of fission tracks in apatite: 1. A qualitative description: Chemical Geology: Isotope Geoscience section, v. 59, p. 237-253.

Harris, A. G., L. D. Harris, and J. B. Epstein, 1978, Oil and gas data from Paleozoic rocks in the Appalachian basin; Maps for assessing hydrocarbon potential and thermal maturity (condont color alteration isograds and overburden isopachs): U.S. Geological Survey Miscellaneous Investigations Series Map I-917-E (1:2,500,000).

Harrison, M. J., S. Marshak, and C. M. Onasch, 2004, Stratigraphic control of hot fluids on anthracitization, Lackawanna synclinorium, Pennsylvania: Tectonophysics, v. 378, p. 85-103.

Hoover, D. S., and A. Davis, 1980, Development and evaluation of an automated reflectance microscope system for the petrographic characterization of bituminous coals, p. Medium: ED; Size: Pages: 275.

Huang, W.-L., 1996, Experimental study of vitrinite maturation: effects of temperature, time, pressure, water, and hydrogen index: Organic Geochemistry, v. 24, p. 233-241.

Hulver, M. L., 1997, Post-Orogenic Evolution of the Appalachian Mountain System and its Foreland: Ph.D. thesis, The University of Chicago, Chicago, Illinois.

Johnsson, M. J., 1986, Distribution of maximum burial temperatures across northern Appalachian Basin and implications for Carboniferous sedimentation patterns: Geology (Boulder), v. 14, p. 384-387.

Klitgord, K. D., and H. Schouten, 1986, Plate kinematics of the central Atlantic, *in* P. R. Vogt, and B. E. Tucholke, eds., The Geology of North America: The Western North Atlantic Region, v. M: Boulder, Colorado, Geological Society of America, p. 351-377.

Koch, J., and M. Günther, 1995, Relationship between random and maximum vitrinite reflectance: Fuel, v. 74, p. 1687-1691.

Laughrey, C. D., J. Kostelnik, J. A. Harper, and K. M. Carter, n.d., The Pennsylvania Petroleum Source Rock Geochemistry Database.

Legg, M. J., 2010, The Tectonic and Thermal Evolution of Hawke's Bay Basin, New Zealand: Master's thesis, The Pennsylvania State University.

Levine, J. R., and A. Davis, 1989, Reflectance anisotropy of Upper Carboniferous coals in the Appalachian foreland basin, Pennsylvania, U.S.A: International Journal of Coal Geology, v. 13, p. 341-373.

Lopatin, N., 1971, Temperature and geological time as factors of carbonification: Akad. Nauk SSSR Izv. Ser. Geol., v. 3, p. 95-106.

Manspeizer, W., and H. L. Cousminer, 1988, Late Triassic-Early Jurassic synrift basins of the U.S. Atlantic margin, *in* R. E. Sheridan, and J. A. Grow, eds., The Atlantic Continental Margin, v. The Geology of North America: Boulder, Colorado, Geological Society of America, p. 197-216.

Milici, R. C., and C. Swezey, 2006, Assessment of appalachian basin oil and gas resources: Devonian shale-middle and upper paleozoic total petroleum system, US Department of the Interior, US Geological Survey.

Miller, J. D., and D. V. Kent, 1988, Regional trends in the timing of Alleghanian remagnetization in the Appalachians: Geology (Boulder), v. 16, p. 588-591.

O'Hara, K., J. C. Hower, and S. M. Rimmer, 1990, Constraints on the Emplacement and Uplift History of the Pine Mountain Thrust Sheet, Eastern Kentucky: Evidence from Coal Rank Trends: The Journal of Geology, v. 98, p. 43-51.

Oliver, J., 1986, Fluids expelled tectonically from orogenic belts: Their role in hydrocarbon migration and other geologic phenomena: Geology, v. 14, p. 99-102.

Orkan, N., and B. Voight, 1985, Regional Joint Evolution in the Valley and Ridge Province of Pennsylvania in Relation to the Alleghany Orogeny, Guidebook of the 50th Annual Field Conference of Pennsylvania Geologists: Harrisburg, Pennsylvania, Bureau of Topographic and Geological Survey, p. 144-164.

Osborn, S. G., J. C. McIntosh, J. S. Hanor, and D. Biddulph, 2012, Iodine-129, 87Sr/86Sr, and trace elemental geochemistry of northern Appalachian Basin brines: Evidence for basinal-scale fluid migration and clay mineral diagenesis: American journal of science (1880), v. 312, p. 263-287.

Poag, C. W., and W. D. Sevon, 1989, A record of Appalachian denudation in postrift Mesozoic and Cenozoic sedimentary deposits of the U.S. Middle Atlantic continental margin: Geomorphology, v. 2, p. 119-157.

Pollack, H. N., S. J. Hurter, and J. R. Johnson, 1993, Heat flow from the Earth's interior: Analysis of the global data set: Reviews of Geophysics, v. 31, p. 267-280.

Portenga, E. W., and P. R. Bierman, 2011, Understanding Earth's eroding surface with 10 Be: GSA Today, v. 21, p. 4-10.

Quinlan, G. M., and C. Beaumont, 1984, Appalachian thrusting, lithospheric flexure, and the Paleozoic stratigraphy of the eastern interior of North America: Canadian Journal of Earth Sciences, v. 21, p. 973-996.

Reed, J. S., J. A. Spotila, K. A. Eriksson, and R. J. Bodnar, 2005, Burial and exhumation history of Pennsylvanian strata, central Appalachian basin: an integrated study: Basin research, v. 17, p. 259-268.

Repetski, J. E., R. T. Ryder, J. A. Harper, and M. H. Trippi, 2002, Thermal maturity patterns (CAI and %Ro) in the Ordovician and Devonian rocks of the Appalachian basin in Pennsylvania: Open-File Report, Reston, Virginia, U.S. Geological Survey, p. 57.

Repetski, J. E., R. T. Ryder, D. J. Weary, A. G. Harris, and M. H. Trippi, 2008, Thermal Maturity Patterns (CAI and% Ro) in Upper Ordovician and Devonian Rocks of the Appalachian Basin: A Major Revision of USGS Map I-917-E Using New Subsurface Collections, Reston, Virginia, U.S. Geological Survey, p. 25.

Roden, M. K., and D. S. Miller, 1989, Apatite fission-track thermochronology of the Pennsylvania Appalachian Basin: Geomorphology, v. 2, p. 39-51.

Roedder, E., 1984, Fluid inclusions: Reviews in Mineralogy, v. 12, p. 1-&.

Rowan, E. L., 2006, Burial and Thermal History of the Central Appalachian Basin, Based on Three 2-D Models of Ohio, Pennsylvania, and West Virginia: Open-File Report, Reston, Virginia, U.S. Geological Survey, p. 35.

Rowan, E. L., R. T. Ryder, J. E. Repetski, M. H. Trippi, and L. F. Ruppert, 2004, Initial Results of a 2D Burial/Thermal History Model, Central Appalachian Basin, Ohio and West Virginia, U.S. Geological Survey Open File Report, Reston, VA, U.S. Geological Survey, p. 38.

Ruppert, L. F., J. C. Hower, R. T. Ryder, J. R. Levine, M. H. Trippi, and W. C. Grady, 2010, Geologic controls on thermal maturity patterns in Pennsylvanian coal-bearing rocks in the Appalachian basin: International Journal of Coal Geology, v. 81, p. 169-181.

Ryder, R. T., P. C. Hackley, H. Alimi, and M. H. Trippi, 2013, Evaluation of Thermal Maturity in the Low Maturity Devonian Shales of the Northern Appalachian Basin.

Ryder, R. T., M. H. Trippi, C. S. Swezey, R. D. Crangle, Jr., R. S. Hope, E. L. Rowan, and E. E. Lentz, 2012, Geologic cross section C-C' through the Appalachian basin from Erie County, north-central Ohio, to the Valley and Ridge province, Bedford County, south-central Pennsylvania.

Slingerland, R., K. P. Furlong, T. W. Gardner, and W. D. Sevon, 1989, Geodynamic and geomorphic evolution of the Permo-Triassic Appalachian Mountains: Geomorphology, v. 2, p. 23-37.

Smith, A. T., 1983, Geology of Redbed Cu-U Occurrences in the Upper Devonian Catskill Fm., Pennsylvania: Ph.D. thesis, The Pennsylvania State University, 214 p.

Suzuki, N., H. Matsubayashi, and D. W. Waples, 1993, A simpler kinetic model of vitrinite reflectance: AAPG bulletin, v. 77, p. 1502-1508.

Sweeney, J. J., and A. K. Burnham, 1990, Evaluation of a simple model of vitrinite reflectance based on chemical kinetics: AAPG bulletin, v. 74, p. 1559-1570.

Ting, F. T., 1978, Petrographic techniques in coal analysis, Analytical methods for coal and coal products, v. 1: Orlando, Florida, Academic Press, p. 3-26.

Tissot, B. P., R. Pelet, and P. Ungerer, 1987, Thermal history of sedimentary basins, maturation indexes, and kinetics of oil and gas generation: Aapg Bulletin-American Association of Petroleum Geologists, v. 71, p. 1445-1466.

Traverse, A., 1987, Pollen and spores date origin of rift basins from Texas to nova scotia as early late triassic: Science (New York, N.Y.), v. 236, p. 1469-1472.

Turcotte, D. L., and G. Schubert, 2002, Geodynamics, Cambridge University Press.

Walker, J. D., J. W. Geissman, S. A. Bowring, and L. E. Babcock, 2013, The Geological Society of America Geologic Time Scale: Geological Society of America Bulletin, v. 125, p. 259-272.

Waples, D. W., 1980, Time and temperature in petroleum formation: Application of Lopatin's method to petroleum exploration: AAPG bulletin, v. 64, p. 916-926.

Wrightstone, G., 2009, Marcellus Shale - Geologic Controls on Production: AAPG Annual Convention, p. 10.

Wygrala, B. P., 1989, Integrated study of an oil field in the southern Po basin, northern Italy: Ph.D. thesis, Univ Köln, Berichte Kernforschungsanlage Jülich 217 p.

Zhang, E., and A. Davis, 1993, Coalification patterns of the Pennsylvanian coal measures in the Appalachian foreland basin, western and south-central Pennsylvania: Geological Society of America bulletin, v. 105, p. 162-174.

APPENDIX

Selected model input parameters, output results, and model source codes not included in

the main body of the thesis are available at Penn State

ScholarSphere: https://scholarsphere.psu.edu/collections/x346d771v